Thermoeconomic analysis of geothermal power cycles for IDDP-1 chloride mitigation

Alberto Mereto

Thesis of 60 ECTS

Master of Science (M.Sc.) in Sustainable Energy Science

January 2016

Thermoeconomic analysis of geothermal power cycles for IDDP-1 chloride mitigation

Alberto Mereto

Thesis of 60 ECTS credits submitted to the School of Science and Engineering at Reykjavík University in partial fulfilment of the requirements for the degree of
Master of Science (M.Sc.) in Sustainable Energy Science

January 2016

Student:

_____
Alberto Mereto

Supervisors:

_____
María Sigríður Guðjónsdóttir

_____
Vijay Chauhan

Examiner:

_____
Páll Valdimarsson

The undersigned hereby grants permission to the Reykjavík University Library to reproduce single copies of this Thesis entitled **Thermoeconomic analysis of geothermal power cycles for IDDP-1 chloride mitigation** and to lend or sell such copies for private, scholarly or scientific research purposes only.

The author reserves all other publication and other rights in association with the copyright in the Thesis, and except as herein before provided, neither the Thesis nor any substantial portion thereof may be printed or otherwise reproduced in any material form whatsoever without the author's prior written permission.

_____

Date

_____

Alberto Mereto
Master of Science

Thermoeconomic analysis of geothermal power cycles for IDDP-1 chloride mitigation

Alberto Mereto

January 2016

Abstract

This thesis deals with the thermoeconomic analysis of four geothermal power cycles proposed for utilization of superheated steam from IDDP-1. These cycles mainly consider mitigation techniques applied for the removal of the chloride present in the fluid. Through executing a comparative thermoeconomic analysis, this research highlights the importance of the correlation between exergetic efficiency, exergy costing and capital costs. Exergy analysis and cost estimation were performed for each component and for the cycles as a whole. The cycles were proposed in literature and are designed to process efficient chloride-induced corrosion mitigation techniques to be applied to the world's first magma-EGS well, IDDP-1. The work compares four cycles, three of them apply wet scrubbing technique while the fourth is a binary cycle. The base case cycle considered in this study is a single flash cycle where the superheat of the fluid is quenched before the turbine. A cycle with an additional turbine together with a cycle with heat recovery are the two alternative cycles utilizing wet scrubbing. The cycle with heat recovery performs best under every aspect as it is the one with the highest power output and the lowest unit cost of exergy of all cycles. Design and economic limitations of the other cycles also confirm the heat recovery cycle as being the most realistic one. On the contrary, the binary cycle resulted as the most expensive in unit cost of exergy and the base case cycle performed the worst in power output. In total, this work provides an idea of the path to follow in designing a geothermal power plant by accomplishing a component by component thermoeconomic analysis and combining the factors used to obtain the optimal cycle design.

Varmahagfræði greining á jarðvarma vinnsluferlum fyrir IDDP-1 klóríð ráðstafarnir

Alberto Mereto

Janúar 2016

Útdráttur

Lokaverkefni þetta skoðar varmahagfræði fjögurra tillagna að vinnsluhringjum fyrir yfirhitaða gufu úr IDDP-1. Vinnsluhringirnir nýta aðalega aðferðir sem ætlaðar eru til að fjarlægja klóríð úr vökvanum. Með því að framkvæma sambærilega varmahagfræði greiningu, undirstrikar rannsókn þessi mikilvægi fylgni á milli skilvirkni aðgengilegrar orku, kostnaðar aðgengilegrar orku og fjármagnskostnaðar. Greining á aðgengilegri orku og kostnaðaráætlun voru framkvæmdar fyrir hvern lið og fyrir vinnsluhringina í heild. Upplýsingar um vinnsluhringina voru teknar úr bókum og eru þeir hannaðir til að stemma stigu við tæringu vegna klóríðs í fyrstu kvikuholu í heiminum, IDDP-1. Verkefnið skoðar fjóra ferla, þrír þeirra notast við vothreinsun, á meðan sá fjórði notast við varmaskiptatækni. Viðmiðunar hringurinn sem notaður er hér er einnar hvellsuðu ferill þar sem yfirhitaða gufan er kæld fyrir hverfilinn. Ferill með auka hverfil ásamt varmaföngunar ferli eru tveir af skoðunar ferlunum sem nýta vothreinsun. Ferilinn með varmaföngunar ferlinu kemur best út í öllum liðum þar sem hann gefur af sér mesta aflið og lægsta einingakostnað aðgengenilegrar orku af öllum ferlunum. Hönnunar og efnahagslegar hömlur hinna ferlanna staðfesta einnig að varmaföngunar ferillinn er raunhæfasti kosturinn. Hinsvegar, ferillinn sem nýtti varmaskiptatækni var með hæsta einingakostnað aðgengilegrar orku og viðmiðunarferillinn gaf frá sér minnsta aflið. Verkefni þetta gefur hugmynd um í hvaða átt á að halda í hönnun á jarðvarmavirkjunum með því að búa til lið fyrir lið varmahagfræði greiningu og sameina hana með þáttum sem notaðir eru til að hanna sem bestan feril.

Acknowledgements

I wish to express my sincere gratitude to Mr. Vijay Chauhan, advisor and co-supervisor. His collaboration and support throughout the entire duration of the work have been essential to the achievement of this thesis. Mr. Chauhan not only actively participated to the proceedings and provided Matlab codes but also represented a guide and source of inspiration at every stage of the process.

In like manner, I am extremely grateful to my supervisor, Doctor María Sigríður Guðjónsdóttir, for offering a support of fundamental importance as well as guidelines and encouragement; her collaboration, presence and help have been of immeasurable value to the development of this work.

I would like to express my deep sense of gratitude to Landsvirkjun, the Icelandic energy company that allowed me to access their confidential data regarding the costs of components of their geothermal power plant. The access to their data has been a turning point into the proceedings of this thesis. In particular, but not only, I thank Mr. Gunnar Guðni Tómasson and Mr. Bjarni Pálsson from Landsvirkjun.

I also owe many thanks to Mr. Kristinn Ingason, from Mannvit, for letting me meet him and gain precious information to use in my work, included informing me of the existence of Landsvirkjun's project planning report.

My sincere gratitude also goes to Doctor Guðrún Arnbjörg Sævarsdóttir, the dean of the School of Science and Engineering, for her assistance, presence and valuable advice.

I thank also Doctor William Harvey for his advice in the early developing of the thesis that have been applicable throughout the entire work.

I would like to give a big thanks to my brother Federico, for drawing for me most of the power cycles illustrated in my thesis.

I am grateful also to my family, who believed in me, and to my friends, on whom I can always count.

Finally, I would like to thank all the people who assisted and supported me, by being physically or morally present, who gave me motivation and hope.

Table of Contents

Abstract iv
Útdráttur v
Acknowledgements vi
Table of Contents vii
List of Figures ix
List of Tables x
Nomenclature xi
1 Background 1
1.1 Introduction 1
1.1.1 Geothermal activity 1
1.1.2 Iceland Deep Drilling Project, IDDP-1 3
1.2 Case study description 4
1.2.1 Chloride induced corrosion 4
1.2.2 Corrosion mitigation techniques 5
1.2.3 Power cycles description 6
1.2.3.1 Single flash with wet scrubbing 7
1.2.3.2 Single flash cycle with wet scrubbing and heat recovery 8
1.2.3.3 Single flash cycle with wet scrubbing and an additional turbine 9
1.2.3.4 Binary cycle 9
2 Methods 11
2.1 Exergy analysis component-by-component 11
2.1.1 Definition of exergy 11
2.1.2 Component-specific exergy study 12
2.2 Thermoeconomic analysis applied to components 12
2.2.1 Thermoeconomics 12
2.2.2 Single component analysis 13
2.2.3 Thermoeconomic optimization 14
2.2.4 Cost rates and evaluations 16
2.3 Cost estimations 18
2.3.1 Cost estimation of purchased equipment 18
2.3.2 Component by component cost estimation 18
2.3.3 Cost indices 21
2.3.4 Time value of money 22
2.3.5 Not included costs 22
2.4 Components sizing 23
2.4.1 Separator 23
2.4.2 Turbine 25
2.4.3 Cooling tower 25
2.4.4 Condenser 26
2.4.5 Heat Exchanger 26
2.4.6 Other components 27
2.4.7 Chemicals for wet scrubbing 27
2.5 Use of Matlab 28
3 Application 29
3.1 State-by-state cycle thermoeconomic balance 29
3.1.1 Single flash cycle with wet scrubbing 29
3.1.2 Single flash cycle with wet scrubbing and heat recovery 35

3.1.3 Single flash cycle with wet scrubbing and additional turbine 37
3.1.4 Binary Cycle 39
3.2 Application criteria 42
4 Analysis and results 44
4.1 Thermoeconomic analysis of cycles 44
4.1.1 Single flash with wet scrubbing 44
4.1.2 Wet scrubbing and heat recuperator 48
4.1.3 Wet scrubbing and additional turbine 51
4.1.4 Binary cycle 54
4.1.5 Cycles comparison 57
4.2 Optimization through scenarios 59
4.2.1 Well cost 59
4.2.2 Pumps efficiencies variation 59
4.2.3 Price of chemicals' influence 60
4.2.4 Life time of plant 61
4.2.5 Interest rate variation 61
4.2.6 O&M costs 63
4.2.7 Scenario combinations 63
5 Conclusions 65
Bibliography 67
Appendix A 72
Appendix B 75
Appendix C 77

List of Figures

Figure 1: Location of Krafla in Iceland (source: Google Maps) 2
Figure 2: Pressure-enthalpy diagram for pure H_2O with selected isotherms ((Friðleifsson et al., 2014).....4
Figure 3: Dry and wet turbine expansion processes for superheated inlet steam (source: DiPippo, 2012).....7
Figure 4: Schematic diagram of a single flash cycle with wet scrubbing.....8
Figure 5: Schematic diagram of a single flash cycle with wet scrubbing and heat recovery.....8
Figure 6: Schematic diagram of a single flash cycle with wet scrubbing and an additional turbine 9
Figure 7: Schematic diagram of a binary cycle 10
Figure 8: Schematic exergy flow of a component (Source:(Valdimarsson, 2015)) 13
Figure 9: Productivity curve of IDDP-1 43
Figure 10: Enthalpy evaluated from temperature and pressure measurements (source: (Einarsson et al., 2015) 43
Figure 11: Exergy rates in the single flash wet scrubbing cycle.....45
Figure 12: Total cost flow rate for single flash cycle 46
Figure 13: Unit cost of work for single flash cycle 46
Figure 14: Cost flow rates of components of the single flash cycle with wet scrubbing 47
Figure 15: Exergy rates in the heat recovery cycle.....49
Figure 16: Unit cost of work of the heat recovery cycle.....50
Figure 17: Heat exchanger cost rate and comparison of unit cost of exergy entering the turbine between SF and HR 51
Figure 18: Exergy rates in the additional turbine cycle 52
Figure 19: Unit cost of work of the additional turbine cycle.....53
Figure 20: Turbines investment rates comparison.....54
Figure 21: Exergy rates of binary cycle.....55
Figure 22: Unit cost of work of the binary cycle.....56
Figure 23: Investment rates of heat exchangers.....57
Figure 24: Net work output and unit cost of exergy of studied cycles 58
Figure 25: Investment cost of cooling water pump (left) and drain pump (right) according to efficiency.....60
Figure 26: Multi-criteria scenario combination of heat recovery cycle.....64

List of Tables

Table 1: Cost per unit of kWh produced by single flash cycle 48
Table 2: Cost per unit of kWh produced by heat recovery cycle 51
Table 3: Cost per unit of kWh produced by additional turbine cycle 54
Table 4: Cost per unit of kWh produced by binary cycle 57
Table 5: Effects of a cheaper well 59
Table 6: Effects of more efficient pumps 60
Table 7: Effects of a higher cost for chemicals 61
Table 8: Effects of a longer lifetime of plant 61
Table 9: Effects of a higher interest rate (8%) 62
Table 10: Effects of a higher interest rate (12%) 62
Table 11: Effects of higher O&M costs 63

Nomenclature

Latin letters

A	area [m^2]
b	molal concentration [mol/kg]
c	cost per unit of exergy [$/kJ]
C	concentration [g/kg]
$\dot{C}$	cost rate [$/s]
D	diameter [m]
e	exergy [kJ]
$\dot{E}$	exergy rate [kJ/s]
h	enthalpy [kJ/kg]
i	interest rate
I	investment cost [$]
L	length [m]
M	molar mass [g/mol]
$\dot{m}$	mass flow [kg/s]
$\dot{Q}$	heat transfer rate [kJ/s]
s	entropy [kJ/kgK]
T	temperature [K]
U	heat transfer coefficient [$W/m^2°C$]
v	velocity [m/s]
V	volume [m^3]
$\dot{Z}$	investment cost rate [$/s]

Greek letters

α	cost scaling factor
ε	exergetic efficiency
φ	O&M expense factor
η	specific efficiency
ρ	density [kg/m^3]
τ	operation time per year [s]

Subscripts

k, n	number of component/state
0	dead state condition
cw	cooling water
D	destruction
e, out	exit/outlet
F	fuel
H	working fluid
HX	heat exchanger
i, in	inlet
is	isentropic
l	liquid
L	loss
P	product
Q	heat transfer
v	vapour
W	work
wb	wet bulb

Superscripts

CI	Capital investment
OM	Operation and maintenance
n	useful lifetime [years]

Acronyms

CPI	Consumer Price index
CRF	Capital Recovery Factor
LMTD	Logarithmic mean temperature difference
SF	Single flash cycle
BC	Binary cycle
AT	Additional turbine cycle
HR	Heat Recovery cycle

1 Background

1.1 Introduction

Iceland produces 100% of its electricity from renewable sources, geothermal energy's share is 28.9% of the electric power generation totalling 5239GWh in 2014 (Orkustofnun (National Energy Authority), 2015). While harnessing geothermal energy for electricity generation, hot geothermal fluid present beneath the surface is extracted and sent to power plants. Most of the time, geothermal fluid extracted is not pure steam. Depending on the location and below surface characteristics, it contains various other elements, most of which are undesirable for power plants' components. Such undesirable impurities include non condensable gases and various minerals. Often, the combination of those contaminants creates major problems in the plant by causing severe corrosion and damage to the components.

Geothermal plants strive to mitigate these impurities, but too often they use steam depuration systems that are not always best for their specific case, both in terms of thermodynamic efficiency and costs. On the one hand, when the reservoir is a source of superheated steam, utilizing mitigation techniques for impurities that lower the temperature, such as wet scrubbing, causes loss of power output due to quenching of superheat present in the fluid. On the other hand, by not intervening on the steam to depurate it, the components would undergo high corrosion and have short life duration that would generate either high costs of maintenance or high costs of purchasing due to the highly resistant materials they have to be made of, or even both. Hence, it is important to study these issues in order to obtain an economical solution.

Solutions to tackle the problem of efficient mitigation systems can be found in literature (Hjartarson et al., 2014; Simonson & Palmer, 1994),(Hirtz, Buck, & Kunzman, 1991).The major focus of this thesis derives from the study made by Hjartarson et al. (2014) in the article on the first well of the Iceland Deep Drilling Project (IDDP-1) in Krafla geothermal area. The study shows the presence of high chloride content in the geothermal fluid, supported by other studies on the chemistry of IDDP-1 (Ármannsson et al., 2014)(Stefánsson, 2014). Hjartarson et al. have brought the analysis of various mitigation systems to be considered as alternatives in order to reduce the risk of corrosion by chloride and yet keep as high as possible the energy content of the steam. The current work looks into the thermoeconomic aspects of various mitigation systems in different cycle configurations and seeks the best mitigation system in terms of both thermodynamic and economic efficiencies.

1.1.1 Geothermal activity

Iceland is an island that was formed 24 million years ago as a consequence of the widespread volcanism along the mid-Atlantic ridge between European and north American tectonic plates, it is one of the few portions of land that rose to the surface along the ridge (Saemundsson, 1979). This mid-ocean ridge is a divergent plate boundary where the plates spread from each other at a rate of around 2cm/year (Árnadóttir, Geirsson, & Jiang, 2008). The geological profile of the country is also characterised by active volcanic areas, with central volcanoes and fissure swarms crossing the territory diagonally from southwest to northeast. All of this results today in various geothermal areas and reservoirs in Iceland.

Conventionally, there are two types of reservoirs ranked in terms of temperature. The low-temperature reservoirs are geothermal systems having temperature not exceeding 150°C while high-temperature reservoirs have temperature of 200°C and well above.
Reservoirs are also characterised by the phase of the geothermal fluid it contains at equilibrium conditions and therefore are referred to as either liquid-dominated or vapour-dominated reservoir. A two-phase geothermal reservoir is where vapour and water coexist. The phase of the fluid is directly correlated with the pressure of the reservoir. It can happen that human intervention by drilling may alter the pressure of a reservoir causing a drop in pressure that can allow boiling in water reservoirs therefore earning a steam phase.
Krafla is the geothermal field that is considered in this study. It is located in the active volcanic zone in northeast of Iceland (Figure 1) and characterised by dilute geothermal solutions. The geothermal field takes its name from the volcanic system of 100km long fissure swarm named after its homonymous central volcano Krafla. Last activity of Krafla volcanic zone occurred between 1975 and 1984 when lava erupted and dykes were injected along the fissure zone (Saemundsson, 1991). The caldera of Krafla has been identified to be of an approximate size of 8x10km and was probably formed during the last inter-glacial period, about 0.1 million years ago during an explosive eruption of acidic rocks and the formation of rhyolite and dacite ridges (Saemundsson, 1991).
Active volcanic zones represent high temperature areas and therefore high potential for harnessing hot geothermal fluid. Krafla geothermal field is the object of IDDP-1, the first deep drilling well in Iceland.

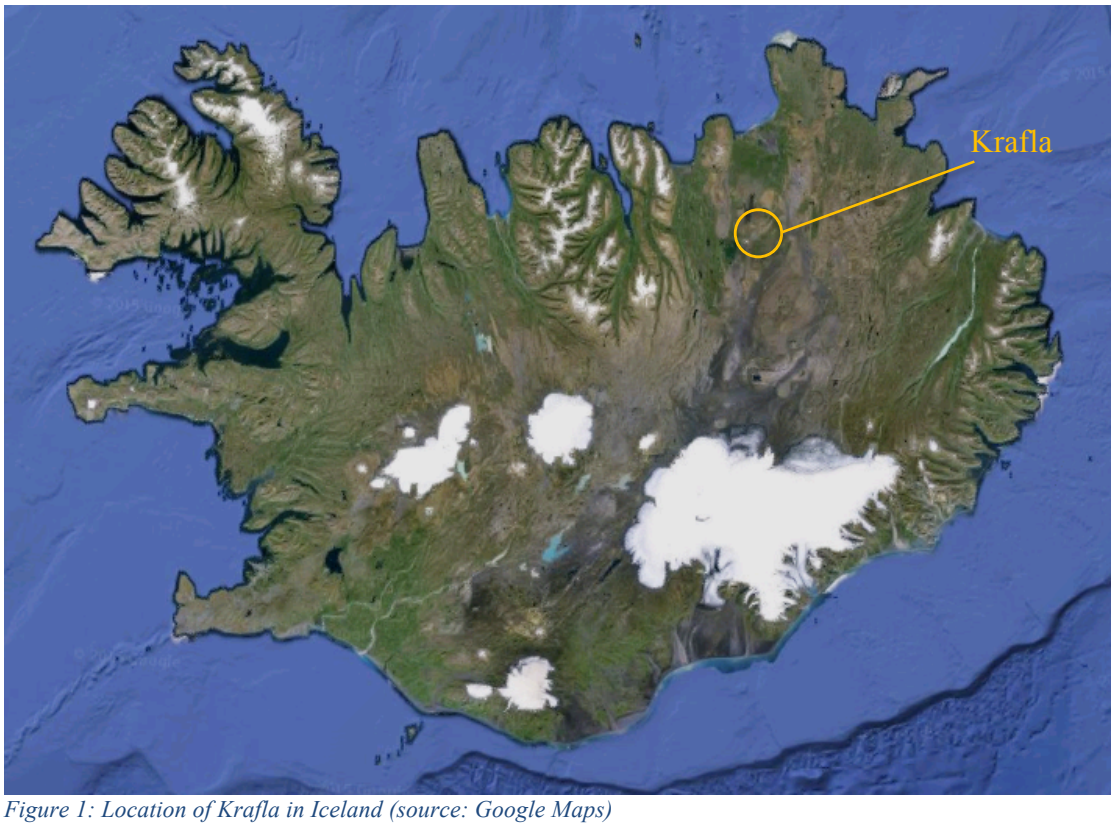

Figure 1: Location of Krafla in Iceland (source: Google Maps)

1.1.2 Iceland Deep Drilling Project, IDDP-1

The Iceland Deep Drilling Project is a research and development project that looks into drilling production wells at a depth around 4-5km in order to obtain high-enthalpy superheated steam having high specific work output. The aim of extracting energy out of hydrothermal systems at supercritical conditions is to produce higher work output by drilling less wells and therefore reducing the relative cost of drilling for the overall project. The IDDP was founded in 2000 by a consortium of three Icelandic energy companies and the national energy authority of Iceland.

In 2009, the drilling of IDDP-1 reached a depth of 2.1km and entered magma with a temperature above 900°C. The drilling of the well encountered countless problems. Some of the incidents are for example major circulation losses with subsequent switch from drilling mud to water, repeated damaging of the drill bits specially designed for this type of drilling, and also the need of cementing in various points became essential. The drilling operators judged right the decision to put a sacrificial casing down to a depth of 1950m inside a production casing in order to be able to produce from a >500°C contact area. In the various attempts and obstacles, IDDP-1 well resulted in entering magma three times with 1m depth difference between each attempt but always being able to exit it safely. The IDDP-1 well had to be cooled down rather abruptly in 2012 due to valve failure and the pilot studies and flow test terminated. (G. Ó. Fridleifsson et al., 2015).

The results of the IDDP-1 well are nevertheless extremely positive and represent a success because it became, after 2 years of flow test, the world's highest temperature producing geothermal well, with a wellhead temperature of 450°C and pressure of the dry superheated steam between 40 and 140 bar. At such a temperature, with wellhead pressure between 40-80bar, the fluid was able to flow at 40-50kg/s with an enthalpy of 3200kJ/kg (Einarsson, Sveinsson, Ingason, Kristjansson, & Holmgeirsson, 2015). Furthermore, the fact of using cold water as a drilling fluid induced fracking that produced high permeability making IDDP-1 the world's first magma-EGS (enhanced geothermal system) (G. Ó. Fridleifsson et al., 2015). The success of this drilling and research was very rewarding, and might in the near future lead to a revolution in exploitable energy efficiency of high-temperature fields around the world.

Figure 2 below shows a pressure-enthalpy diagram for pure H_2O that can be representative of the conditions in IDDP-1. The shaded area showing the conditions under which steam and liquid water co-exist is bounded on the left by the boiling point curve and to the right by the dew point curve. The arrows show various different cooling paths of ascending fluids. The concept behind the Iceland Deep Drilling Project is to produce supercritical fluid to the surface in such a way that it transitions directly to superheated steam along a path like F-G in Figure 2, resulting in a much greater power output than from a typical geothermal well. (Friðleifsson, Elders, & Albertsson, 2014).

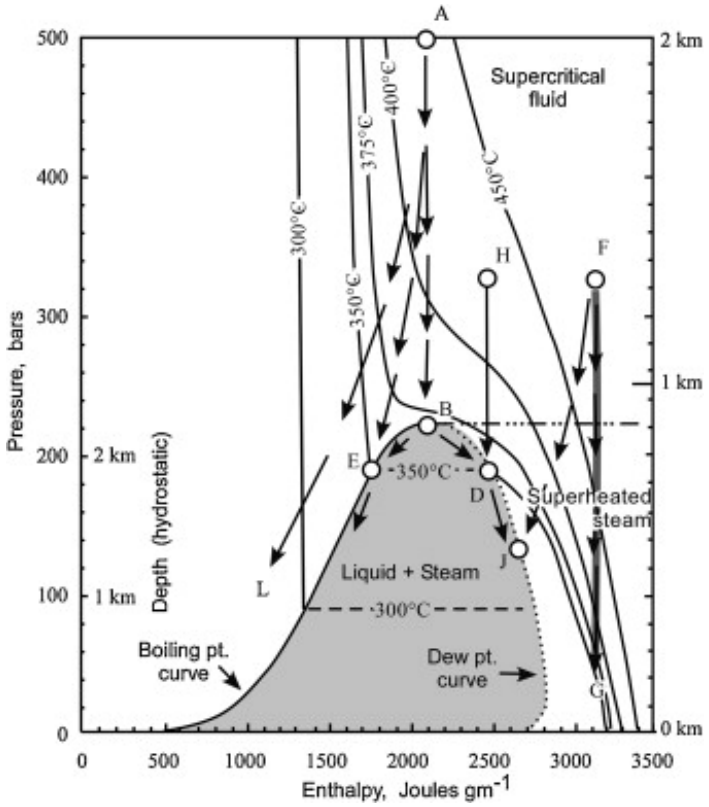

Figure 2: Pressure-enthalpy diagram for pure H_2O with selected isotherms (source:(Friðleifsson et al., 2014))

1.2 Case study description

1.2.1 Chloride induced corrosion

Hydrogen chloride (HCl) is a known component of some volcanic gases and some volcanic-related hydrothermal systems. The main factors responsible for the formation of HCl are pH value, temperature and Cl concentration. Lower pH, higher temperature and higher chlorinity allow more HCl to be volatilized with steam. HCl is a compound that is very hazardous when it dissolves into water because it parts into hydrogen and chloride ions. In these circumstances HCl is very likely to cause stress corrosion, cracking of stainless steel components, as well as inner crystalline corrosion and severe pitting corrosion. If the steam temperature is above dew point, HCl does not represent a big threat, but once the steam cools enough for droplets to form the compound becomes extremely hazardous and is able to corrode steel. The specificity of HCl is that by dissolving into small droplets it forms hydrochloric acid that in high concentrations causes pitting corrosion. On the other hand if there is sufficient amount of water, when HCl dissolves into it, hydrogen chloride results being less concentrated and is therefore no longer of any concern (Hjartarson et al., 2014).

The corrosion of the steel elements happens because of a combination of various factors. The surfaces of the steel components are covered with a magnetite film (Fe_3O_4) to protect them from many chemicals. The free chloride ion is not directly a corrosive element to steel but it is the one responsible for breaking the protective film. Once damaged, the magnetite film leaves the steel exposed to direct contact with hydrogen ions that are those actually corroding the metal. The chloride ions can migrate beneath scale deposits and react with the metals present. The corrosion can even lead to hydrolysis of the ions when the metals in the components react with hydrogen and

therefore generate more HCl (Hjartarson et al., 2014). The chemical reactions representing these interactions may be written as follows (Hjartarson et al., 2014):

Reaction of HCl with magnetite film on the steel surface breaking the film:

$$Fe_3O_4 + 8HCl \rightarrow FeCl + 2FeCl_3 + 4H_2O \quad (1)$$

Electrochemical reaction representing the actual corrosion:

$$Fe + 2H^+ \rightarrow Fe^{2+} + H_2 \quad (2)$$

Hydrolysis and chloride induced electrical balance generating HCl:

$$FeCl_2 + 2H_2 \rightarrow Fe(OH)_2 + 2HCl \quad (3)$$

It should be noted that these chemical reactions are not the only reactions occurring and that they may vary depending on other chemicals present in the steam.
These specific characteristics and the behaviour of HCl make it essential to remove both the chloride and the acid hydrogen ions from the fluid. The fact that they are present simultaneously is the real threat.

1.2.2 Corrosion mitigation techniques

The following mitigation techniques described are based on the paper by Hjartarson et al. (2014).
The first mitigation technique, the traditional one used in geothermal superheated steam cycles to remove chloride, and the most recurrent in the examples of this work, is the wet scrubbing method. Wet scrubbing is widely used in industries dealing with gases containing harmful substances that must be eliminated, as for example in the case of exhaust gases. This technique relies on using a reactant, such as sodium hydroxide, NaOH, dissolved in water and injecting it into the superheated steam. The injection of water cools down the steam to its saturation point allowing the formation of a liquid phase in the stream dissolving the HCl. The steam has to be cooled until it reaches a quality equal to 98% in order for the wet scrubbing to be applied (Hjartarson et al., 2014). The presence of NaOH will allow the dissolved HCl to bond and be neutralized according to the following chemical reaction:

$$NaOH + HCl \rightarrow NaCl + H_2O \quad (4)$$

Following this reaction, the dissolved NaCl in the liquid composes the contaminated water phase that gets separated from the newly depurated steam flow in a separator.
Wet scrubbing is very efficient in terms of neutralizing HCl in the superheated geothermal steam but causes total loss of superheat present in the fluid. The wet scrubbing technique applied directly to the superheated steam without any means of utilizing the superheat to produce work is unfortunately an enormous waste of exergy. If no alternative is considered, the utilization of superheated steam becomes useless when wet scrubbing is applied as it only exploits 98% saturated steam losing the exergy contained in the superheat.

Another corrosion mitigation technique studied in this work is the application of binary cycle. The design of cycle does not really eliminate the corrosion but limits it to heat exchangers. The binary cycle was considered mainly because the heat exchangers are

stationary components and have more margin of selection in the material they are made of. The corrosion in the heat exchanger would occur only in the tubes containing the contaminated geothermal fluid. The heat exchanger can tolerate the same rate of corrosion longer than the turbine as the turbine is a moving part with more limited choice of construction material. The turbine is subject to faster breakdown due to corrosion fatigue, accelerated by the high radial forces affecting the component. The aim of the binary cycle application is to save the turbine from corrosion at the cost of heat exchangers.

The last mitigation technique described in the work by Hjartarson et al. (2014) is dry scrubbing. In dry scrubbing, solid or liquid material is injected into the stream; after the mixing, the flow is driven through an electrostatic precipitator or a bag house filter where the contaminants and chemicals are filtered out. There are two similar ways to implement dry scrubbing: absorption and adsorption. In the case of absorption, a chemical reaction occurs between the contaminants and the injected material (absorbent). In the case of adsorption, the chemical attaches to the surface of the adsorbate without a direct chemical reaction (Hjartarson et al., 2014).
The positive aspect about dry scrubbing is that it does not require to cool down the steam and therefore preserves the superheat. Unfortunately, even though it is a method that looks promising it is still under development. The results brought in its analysis is only laboratory data and the true nature of the components is still not clearly defined. A problem seems to arise immediately nevertheless; it is that there will be the presence of particles in the turbine making this cycle delicate or even impossible to realise as the turbine would be destroyed in a very short period of time. Due to the early development stage and consequent lack of data, regarding both the costs of components and the real applicability, the thermoeconomic study of the dry scrubbing cycle will not be part of this work.

1.2.3 Power cycles description

The design of the various cycles, for which thermoeconomic analysis was performed in this thesis, are from the work of Hjartarson et al. (2014). The work proposes different options of cycle structures to avoid hydrogen chloride induced corrosion. Three cycle configurations utilize wet scrubbing technology while one cycle is a binary cycle, the cycles are listed here:

- Single flash with wet scrubbing
- Single flash cycle with wet scrubbing and heat recovery
- Single flash cycle with wet scrubbing and an additional turbine
- Binary cycle

In a cycle, when the turbine inlet stream is saturated steam, the expansion process inside the turbine is wet. When the inlet stream is superheated steam the expansion is dry only if the outlet is also superheated (back pressure turbine). The expansion is both dry and wet if the entering stream is superheated and reaches the wet region inside the turbine. A temperature-entropy diagram is represented by Figure 3 to illustrate the dry and wet expansion processes.

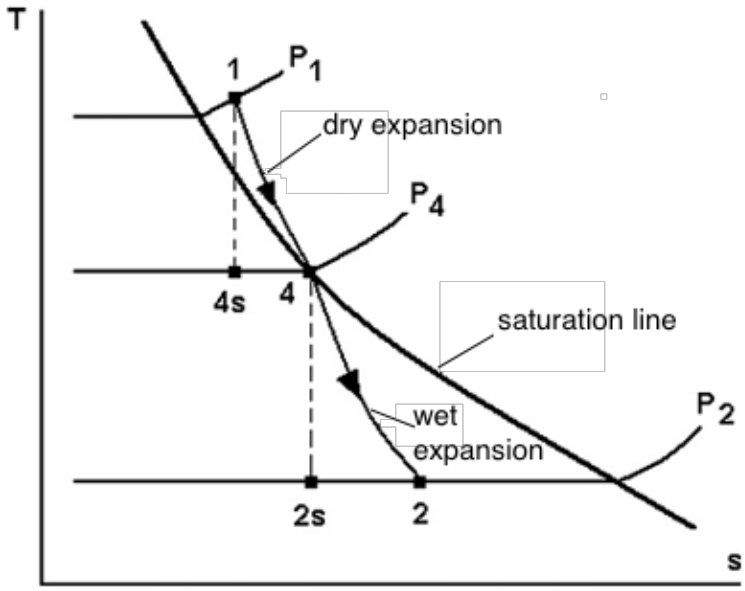

Figure 3: Dry and wet turbine expansion processes for superheated inlet steam (source: DiPippo, 2012)

In the figure above, P_1 is the isobar curve representing the inlet pressure of the turbine at state point 1, P_2 is the condenser pressure (state point 2) and P_4 is the pressure at which the expansion enters the wet region (state point 4). In the case of saturated steam, state point 4 is the inlet stream and state point 2 remains the outlet stream, therefore the expansion is only wet. The state points 4s and 2s both represent state points of isentropic expansions, respectively dry and wet. In the case of superheated steam and a condensing turbine, the expansion is from state 1 to state 2, therefore passing by state 4. This shows that the expansion is both dry and wet. In the case of a back pressure turbine, the expansion would start at state point 1 and the exiting stream would be before reaching state point 4 at P_4, making the expansion solely dry.
In this thesis, the Baumann rule was used throughout all the cycles analyses and therefore affects the power outputs of all cycles with wet expansions. According to DiPippo (2012), the higher the amount of moisture present during the expansion process, the lower the isentropic efficiency. This effect is measured by the Baumann rule that states that to every 1% average moisture present, corresponds roughly a 1% drop in turbine efficiency. Therefore, there is a degradation in performance taken into account for the turbines operating in the wet region (DiPippo, 2012). However, the Baumann rule will not apply to a turbine that is designed for wet operation; the efficiency given for such a turbine is the real efficiency, i.e. the efficiency in wet operation.

1.2.3.1 Single flash with wet scrubbing

The first cycle shown in Figure 4 is a single flash cycle with wet scrubbing. The flow at state 7 consists of water with diluted NaOH that is injected into the superheated steam coming from the well from state 1. Thanks to the addition of cool water, fluid at state 2 becomes saturated up to 98% dryness fraction where the wet scrubbing process occurs before separation. The steam at state 3 is not superheated and therefore the turbine expansion process is wet. After expansion, the fluid is condensed through a condenser and finally reinjected in the ground at state 9.

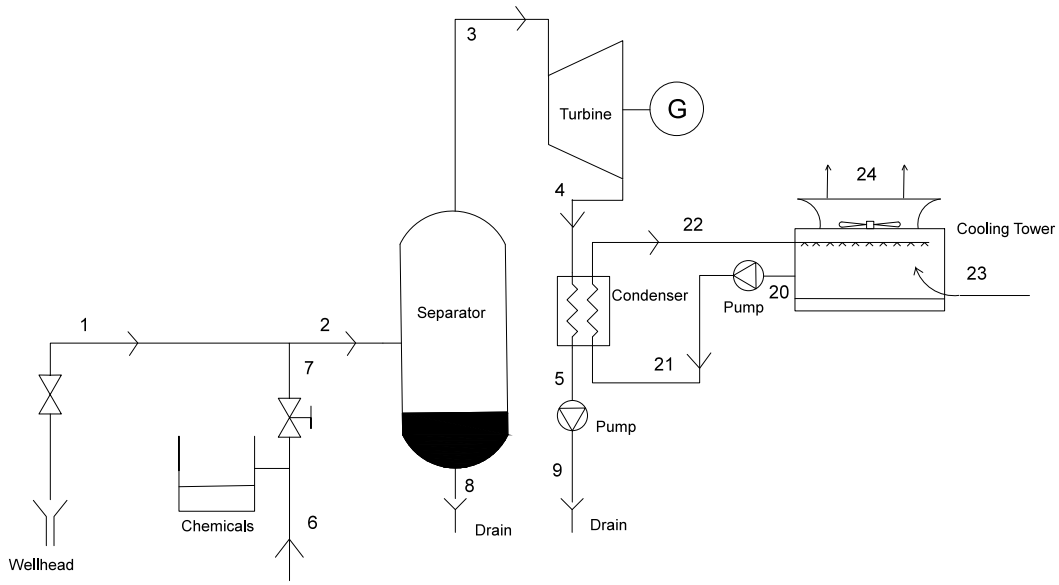

Figure 4: Schematic diagram of a single flash cycle with wet scrubbing

1.2.3.2 Single flash cycle with wet scrubbing and heat recovery

The second cycle is the single flash cycle with wet scrubbing and heat recovery. The schematic diagram of the cycle is shown in Figure 5. The superheated steam at state 1 passes through a heat exchanger before wet scrubbing. The cooled steam at the heat exchanger exit is kept superheated (ca. 20°C of superheat) to avoid any condensing and therefore any corrosion. The fluid subsequently undergoes wet scrubbing by mixing with stream coming from state 9. The process of separation occurs then and the clean steam exiting the separator in state 4 passes through the same heat exchanger reaching again the superheated condition in state 5. The turbine expansion is then both wet and dry; the fluid, as in the previous cycle, is condensed and reinjected.

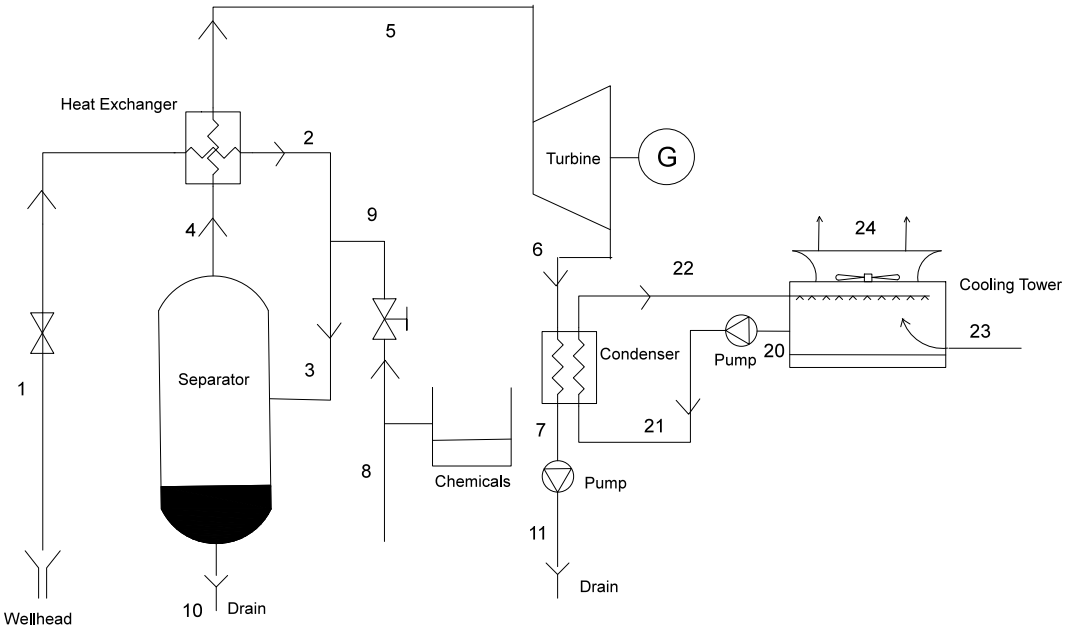

Figure 5: Schematic diagram of a single flash cycle with wet scrubbing and heat recovery

1.2.3.3 Single flash cycle with wet scrubbing and an additional turbine

The third cycle considered is a single flash unit with wet scrubbing and an additional turbine. Figure 6 shows the schematic diagram of the cycle. The superheated steam from the well goes through a turbine for a dry expansion where the outlet steam maintains 20°C of superheat to avoid condensation. After the first expansion, the steam undergoes the same process of wet scrubbing explained for the previous cycles with subsequent wet expansion and then the condensation followed by the reinjection.

It is important to note, in this case, that the presence of the first turbine in the cycle design is only applicable for the chloride mitigation process. In reality, there are various other elements, solid particles, present in the geofluid that would make the first turbine impossible to be installed there as it would suffer extremely high corrosion and almost immediate breakdown because of these particles.

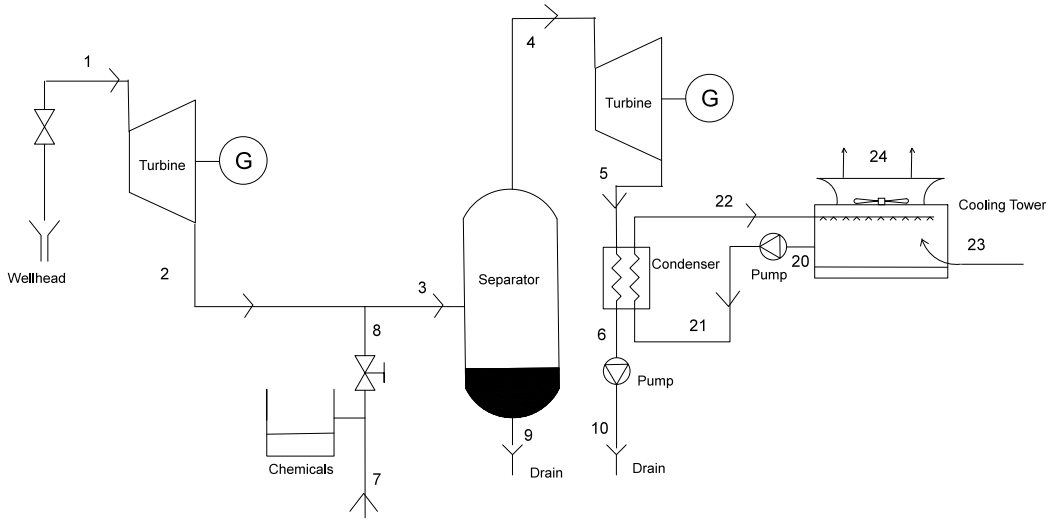

Figure 6: Schematic diagram of a single flash cycle with wet scrubbing and an additional turbine

1.2.3.4 Binary cycle

The fourth cycle and the only configuration of cycle that uses a different working fluid and no chemical treatment is the binary cycle. This cycle, represented by Figure 7, uses water as a working fluid that gets heated and vaporised up to superheated condition. Water was selected as a working fluid because it is the closest to an ideal working fluid; models using ammonia, isobutane and isopentane showed worse power outputs by a factor of 2 (Hjartarson et al., 2014). The working fluid flows in opposite direction of the geofluid. At state point b, the water enters a preheater (PH) where it is heated by the geofluid that already released most of its heat. Then, the water enters an evaporator (EV) after state point c where it changes state thanks to a hotter geofluid. Finally, the working fluid passes through a superheater (SH), exchanging heat with superheated geofluid, in order to gain the superheated condition. Once superheated, the fluid expands in a turbine and is pumped back to a higher pressure after condensing. The geofluid is reinjected at the outlet of the preheater. The vaporizer pressure is around 10bar lower than the wellhead pressure in most cases.

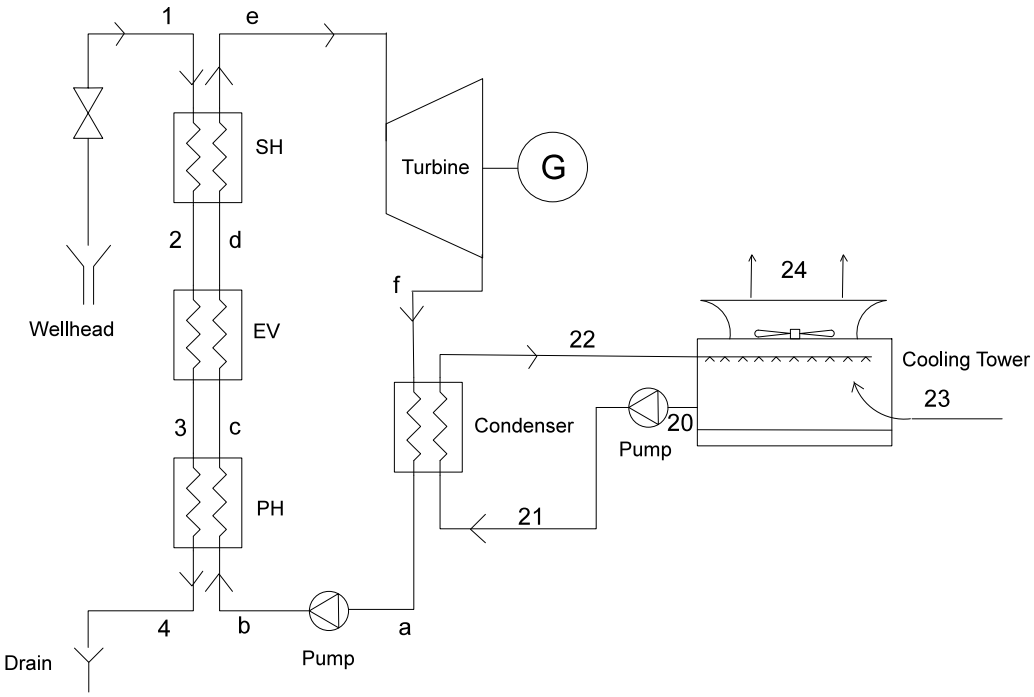

Figure 7: Schematic diagram of a binary cycle

2 Methods

2.1 Exergy analysis component-by-component

2.1.1 Definition of exergy

According to Bejan et al. (1996), who give a clear definition of exergy, it is of fundamental importance to design and develop thermal systems that are able to effectively use energy resources (Bejan & Tsatsaronis, 1996). In order to define the effective use, both the first and second laws of thermodynamics must be used. According to the first law of thermodynamics, energy can neither be created nor be destroyed but can be transformed from one state to another. In this case, the concept of energy is limited because it would be useful to idealise something that can be destroyed in the analysis of thermal systems. Exergy is the property to which destruction can apply, and therefore only follows the second law of thermodynamics. This law implies the existence of entropy and is stated by Kelvin-Planck as: "It is impossible for any system to operate in a thermodynamic cycle and deliver a net amount of energy by work to its surroundings while receiving energy by heat transfer from a single thermal reservoir" (Bejan & Tsatsaronis, 1996). Exergy is the availability, but also, unlike energy, exergy properly sizes the quality of energy. For example, it allows comparison between 1kJ of electricity produced in a power plant and 1kJ of energy contained in the cooling water of the plant. Clearly, electricity has the greater quality and therefore the greater economic value.

The method of exergy analysis aims at utilizing energy resources more effectively because it enables to identify the cause, location and actual magnitude of waste and loss (Dincer & Rosen, 2012). Today the emphasis on exergy aspects regarding systems and processes is much greater. The exergetic emphasis tends towards system analysis and thermodynamic optimization, involving also the sectors of physics, biology, economics and management besides the engineering branch. "*As a result of these recent changes and advances, exergy became a new distinct discipline because of its interdisciplinary character as the confluence of energy, environment and sustainable development*" (Ahmadi & Dincer, 2011).

In thermodynamics, when two systems at different states are placed into communication, an opportunity of doing useful work appears due to the fact that the systems will interact to reach equilibrium. When one of the systems is idealised as the environment, and the other is the system of interest, exergy represents the maximum theoretical useful work obtainable as the two systems interact to equilibrium.

Exergy is an extensive property that can be destroyed, lost, and transferred between systems, all related by the exergy balance of the system under consideration. Physical exergy is associated with the temperature and pressure of a stream of matter. In this study, where the stream is geothermal fluid and the chemical reactions characterising the scrubbing are too little to be of concern, chemical, kinetic and potential exergies are neglected. Therefore, the total exergy e associated with a stream of matter can be expressed, on a unit-of-mass basis (specific exergy), as follows:

$$e = (h - h_0) - T_0(s - s_0) \tag{5}$$

Where h and s are respectively the specific enthalpy and entropy of the stream, while the subscript 0 represents the same properties at the dead state (environment) and T_0 is the environment temperature.

When introducing the mass flow $\dot{m}$ of the stream, we obtain the total exergy flow rate of the stream according to the following relation:

$$\dot{E} = \dot{m}e \tag{6}$$

2.1.2 Component-specific exergy study

When the exergetic analysis comes to the examination of components individually, it is possible to relate the exergy balance with the following relation:

$$\dot{E}_{i,n} = \dot{E}_{e,n} + \dot{E}_{D,n} + \dot{E}_{L,n} \tag{7}$$

Where $\dot{E}_{i,n}$ represents the exergy rate entering component n while $\dot{E}_{e,n}$ represents the exergy rate exiting the same component. The two exergetic elements remaining with subscripts D and L respectively show the exergy destruction and loss for the given component. Whether the exergy is lost or destroyed only depends on the choice of the boundary of the system, but the sum $\dot{E}_{D,n} + \dot{E}_{L,n}$ will be constant if both $\dot{E}_{i,n}$ and $\dot{E}_{e,n}$ stay constant.

The exergetic efficiency, ε, is expressed as the ratio between the exiting exergy stream(s) of interest and the inlet exergy stream(s):

$$\varepsilon = \frac{\dot{E}_e}{\dot{E}_i} = 1 - \frac{\dot{E}_D + \dot{E}_L}{\dot{E}_i} \tag{8}$$

The exergetic efficiency shows how much of the fuel exergy is converted into the product exergy, and consequently, the percentage fuel exergy wasted in exergy loss and destruction is directly expressed by $100\% - \varepsilon$ (in percentage). Because a single component can have various feeds and products, in order to elaborate a correct exergetic analysis, it is essential to correctly identify inlets and outlets for every single component.

2.2 Thermoeconomic analysis applied to components

2.2.1 Thermoeconomics

Thermoeconomics is the application of economic principles to thermodynamics. It is safe to affirm that for every thermodynamic system in real life application there is a concrete economic value to it. Thermoeconomics is the concept able to seek for the best performance of thermodynamic cycles in relation with their costs. Bejan et al (1996) define thermoeconomics as "*the branch of engineering that combines exergy analysis and economic principles to provide the system designer or operator with information not available through conventional energy analysis and economic evaluations but crucial to the design and operation of a cost-effective system*" (Bejan & Tsatsaronis, 1996). Thermoeconomics is also known as exergoeconomics as the thermodynamic aspects are exergy analysis.

Thermoeconomics is a useful tool when it comes to identify mechanisms that degrade energy and resources, it serves as a systematic tool in developing and optimizing energy systems. The main characteristic of exergoeconomics is that it recognizes exergy and not energy as the commodity that has value in a system and therefore costs and/or prices are assigned to exergy related variables.

Thermodynamic inefficiencies of any thermal system are clearly shown by the exergy analysis for any process both quantitatively and qualitatively. Engineers try to reduce inefficiencies and improve the performance of the systems. Each unit of energy adds to cost, and, in such a competitive market a major attention is given by engineers on how much these inefficiencies cost. Correct cost flow evaluations allow improving the cost effectiveness of the system and also help in governing the final cost. The thermoeconomic analysis is based on the practical assumption that the economic cost of the system increases with the increasing capacity and increasing efficiency of the system. For this reason, it is very useful to be able to link costs of components directly to their efficiency.

2.2.2 Single component analysis

The total exergy given to a component as inlet (fuel or feed) exergy is transformed into exit exergy (product) while some part goes as exergy destruction and some as exergy loss, according to the boundary choice, as shown in Figure 8 below.

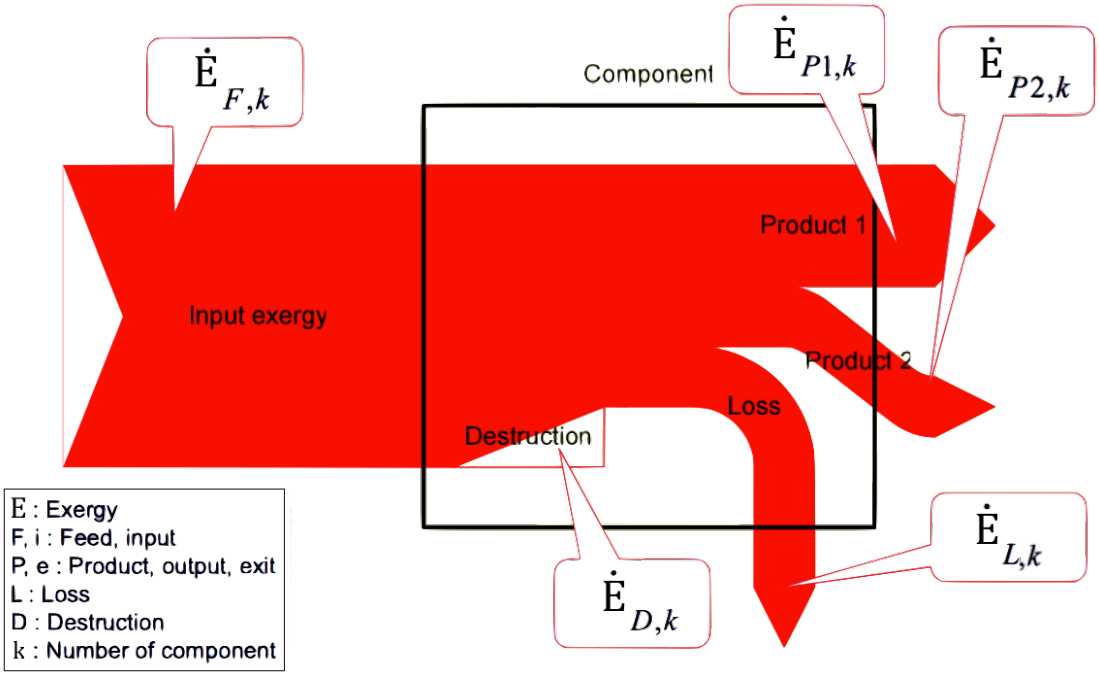

Figure 8: Schematic exergy flow of a component (Source:(Valdimarsson, 2015))

The total cost of product exergy varies directly with the fuel, the destructed exergy and the lost exergy. When increasing the efficiency of the system or component, both the exergy losses and exergy input to the system decrease for a fixed value of output. Hence the cost of product is lowered. In order to increase the efficiency of the system, changes in design and geometric parameters have to be made that generally add to the total cost of the system or component. The purpose of the thermoeconomic analysis is to obtain the optimum values of design and geometric parameters that are also practically feasible to attain, which give the lowest product cost.

The thermoeconomic analysis requires economic costs and provides the natural trade-off between efficiency, capital and operation and maintenance costs. When possible, cost balance is formulated for each component individually in order to have the most precise results as possible. In exergy costing, a cost is associated with each exergy stream according to the following relation for any stream n:

$$\dot{C}_n = c_n \dot{E}_n \tag{9}$$

Here, c_n represents the average cost per unit of exergy (e.g. in \$/kJ) and therefore $\dot{C}_n$ is the cost rate of the nth stream.
In a general economic analysis of an industry, product cost is defined according to the fuel cost, capital expenditure and other operation and maintenance costs required for production or services. This relation forms a general basis for controlling the total expenditure for producing the product or services. The relation also helps to find out the parameters required to control the product cost. The general equation is given as:

$$\dot{C}_e = \dot{C}_i + \dot{Z}^{CI} + \dot{Z}^{OM} \tag{10}$$

The equation means that the total cost associated with the product $\dot{C}_e$ is the sum of the fuel cost $\dot{C}_i$, capital investment $\dot{Z}^{CI}$ and the other costs related to operation and maintenance $\dot{Z}^{OM}$ of the system generating the product.
A true thermodynamic analysis involves the exergy analysis of the system. The value of particular thermodynamic fluid flow is recognized by the value of exergy the fluid contains, which defines the ability of the flowing fluid to produce work. The exergoeconomic analysis is based on the principle of assigning cost to every flow stream entering and exiting a system. The cost of the particular flow will be proportional to the amount of exergy it contains and hence the amount of work it can produce (Chauhan, 2014).
In a specific kth component analysis, where more than one exergy stream enters and/or exits, the sum of the cost rates of exiting exergy streams is equal to the sum of all cost rates of entering streams plus the circumstantial capital investment and operating and maintenance costs. The sum of the last two terms in Eq. (10) is denoted by $\dot{Z}_k$. Accordingly, for a component k that receives heat transfer q and generates power W, one can write:

$$\sum_e \dot{C}_{e,k} + \dot{C}_{W,k} = \dot{C}_{q,k} + \sum_i \dot{C}_{i,k} + \dot{Z}_k \tag{11}$$

Where $\sum_e \dot{C}_{e,k}$ is the sum of the cost rates of the streams exiting component k, $\dot{C}_{W,k}$ is the cost rate of the work generated by component k, $\dot{C}_{q,k}$ is the cost rate of the heat transfer received by component k and $\sum_i \dot{C}_{i,k}$ is the sum of the cost rates of the streams entering component k.
It is simple to note that this equation tells that the total cost of the exiting exergy streams is equal to the sum of all the costs to obtain them, that is the entering exergy streams costs and the various components costs.

2.2.3 Thermoeconomic optimization

Many of the thermodynamic systems existing today involve high complexities such that it is very difficult or sometimes impossible to obtain parameters that lead to their optimum performance. It is therefore preferred to obtain parameters that give a near optimum or improved performance of the system. The first step in designing a system is to produce a workable system so that the system is able to perform the required task and meet all the specifications required. The optimum design is the one that, among all workable designs, performs best in terms of the requirements. It may be found by the best combination of parameters. A near optimal design is generally preferred for complex systems where getting an optimum design is time consuming and therefore adding to cost. Hence, in engineering applications, the optimum design is the one that

performs better than other design specifications taking into consideration all the boundary conditions related to available resources and constraints such as environmental, safety, operability and maintainability of the system (Chauhan, 2014).
It is usually not achievable to optimize a complex system as a single entity. The most challenging task for doing the optimization of a system is to formulate the objective function for optimization. It is therefore preferable to consider a complex system as a combination of subsystems; where every subsystem's optimization should preferably be studied individually and then incorporated into the system. It is necessary to define the system boundaries before the optimization is done (Bejan & Tsatsaronis, 1996). The criteria for optimizing the system or improving its performance is then the objective function chosen; it can be of various natures such as economic, thermodynamic, technological and environmental. When seeking the optimization of a subsystem the complexity comes with the fact that reaching the optimal performance of a single criteria has to leave unviolated all the other criteria. For doing optimization, the designer has to formulate objective functions in some mathematical form. Depending on the objective function, one can decide the variables, dependent variables and parameters related to the chosen subsystem in order to achieve the most complete optimization study. The objective of the optimization process is to increase the efficiency of the system through increasing the efficiency of its subsystems. According to Eq. (8), increasing the efficiency leads to a decrease in exergy loss and destruction, which are the factors contributing to the inefficiencies. It is general observation that increasing thermodynamic efficiencies can only be attained by increasing system's efficiency which automatically adds to the total cost. This is due to the fact that the objective of increasing thermodynamic efficiency does not take fuel and other investment cost into consideration (El-Sayed & Tribus, 1983).
On the other hand, thermoeconomic optimization aims at minimizing the cost of product taking both thermodynamic and economic aspects into account. Therefore, in order to tackle the problem of optimization and formulate it correctly, one needs to have complete information of both thermodynamic and economic aspects. The thermodynamic information helps to build up a complete thermodynamic model of the system. Thermodynamic model is prepared using energy, mass and other conservation laws, only to be completed with exergy calculations. This model can be simulated for a given set of parameters of the system and hence shows the effects of each decision variable on other dependent variables and system as a whole. The cost model built using the economic information of the system helps to calculate cost values for a given set of thermodynamic values of parameters (see section 2.3 Cost estimations). The objective of the thermoeconomic optimization is to minimize the cost of product for a given period. This product cost is expressed as the function of dependent and independent variables.
The mathematical model of the objective function, for a fixed output quantity, is written as:

$$Minimize\ \dot{C}_{e,tot} = \dot{C}_{i,tot} + \dot{Z}_{tot}^{CI} + \dot{Z}_{tot}^{OM} \quad \text{, for a fixed output} \tag{12}$$

where the terms defined in the above equation are expressed as the functions of the decision variables (Valero, Lozano, Serra, & Torres, 1994). For developing appropriate boundary conditions required for the system to run in actual conditions, various equality and inequality constraint equations need to be formulated. This is done using the thermodynamic and economic model and other balance equations. Various methods are available for solving the optimization problem, this thesis uses, among other

approaches, some of fundamental importance proposed by Bejan and Tsatsaronis in 1996 (Bejan & Tsatsaronis, 1996), as well as works by Frangopoulos in 1991 (Frangopoulos, 1991) to which many other papers refer to. The next section discusses the methodologies applied.

2.2.4 Cost rates and evaluations

A complete thermoeconomic analysis comes with giving cost to each exergy stream flowing into and out of every component of a system. For a system with *k* components and having *s* number of total exergy streams such that number of components are less than number of streams, we need to have *s* number of cost balance equations in order to calculate the cost flow rates of all streams. Since one equation can be obtained from every component as defined earlier, the remaining equations can be obtained from general principles as given by Bejan et al (2008), also discussed earlier.

For a component with single exergy stream defined as product, the cost rate balance is solvable for the cost per unit of exergy of that exiting stream with no additional relation needed. Auxiliary relations may be formulated in the case of other exiting streams not considered as products.

In the case of a component involving *n* exiting streams defined as products, *n-1* auxiliary relations have to be formulated. For a component for which the production cost of each of *n* streams is not known, it is assumed to have the same average cost per unit of exergy supplied to each product stream.

The average cost per unit of exergy remains constant for the stream if no exergy is supplied to the stream such that entering and exiting states of stream contain same matter. This happens when the fuel is defined as the difference between entering and exiting states of the same stream of matter. The cost changes only when the exergy is supplied to the stream.

The cost of inlet (fuel) and outlet (product) for each component can be defined once the cost rates associated with each stream is found. This is done by replacing the exergy terms in the exergetic inlet and exit relationships.

After the cost flow rates of both exit streams and inlet streams are defined, certain quantities known as thermoeconomic variables need to be evaluated. These variables play an important role in thermoeconomic analysis. These variables include:

- average unit cost of inlet ($c_{i,i}$)
- average unit cost of outlet (exiting stream) ($c_{e,i}$)
- cost rate of exergy loss ($c_{L,i}$)

The average cost per exergy unit of inlet and outlet can be calculated from values of costs and inlet and outlet exergy for each component given for the k^{th} component as (Tsatsaronis & Pisa, 1994),(Tsatsaronis & Winhold, 1985):

Unit cost of inlet:

$$c_{i,k} = \frac{\dot{C}_{i,k}}{\dot{E}_{i,k}} \tag{13}$$

Unit cost of outlet:

$$c_{e,k} = \frac{\dot{C}_{e,k}}{\dot{E}_{e,k}} \tag{14}$$

The costs associated with exergy loss (exergy rejected to the environment) are hidden costs since there is no cost term directly associated with exergy loss and are revealed through thermodynamic analysis. When one wants to understand the cost formation process and cost flow in the system, all exergy loss streams are costed as if they were

to be processed further. In order to give it an economic magnitude, a good way is to assume that the exergy loss is compensated by additional supply of fuel, therefore, the exergy loss cost rate is by definition expressed as:

$$\dot{C}_{L,k} = c_{i,k}\dot{E}_{L,k} \tag{15}$$

The relations for the k[th] component can then be expressed as:

$$\dot{C}_{e,k} = \dot{C}_{i,k} - \dot{C}_{L,k} + \dot{Z}_k \tag{16}$$

Nevertheless, the simplest approach to estimate the cost of a stream of exergy loss associated with the k[th] component is to set:

$$\dot{C}_{L,k} = 0 \tag{17}$$

In this way, the unit cost of the product $c_{e,k}$ bears the full burden of the costs associated with the k[th] component as can be seen when combining Eq. (16) and Eq. (17). Eq. (17) should be applied only in the case of streams finally released to the environment (Bejan & Tsatsaronis, 1996; Frangopoulos, 1987).
On the other hand, when there is an exiting stream that needs real further processing such as disposal, or like in the case of this thesis a reinjection, the costs of the further process have to be somehow added to the costs of the previous streams in order to be accounted in the total process. Then, a simple relation is added and the unit cost of the exiting stream c_e is estimated in relation to the capital cost rate of the processing components $\dot{Z}_{process}$ and its exergy rate $\dot{E}_e$ as follows:

$$c_e = -\frac{\dot{Z}_{process}}{\dot{E}_e} \tag{18}$$

In this case, the exiting exergy flow is not labelled as exergy loss but as an exiting flow with further processing, even though that exergy is no longer of any use in the system and cannot be exploited.

The above defined variables are applied to thermoeconomic evaluation using methodology suggested by Bejan et al. (2008) in many ways. Firstly, the components with the higher values of $\dot{Z}_k$ and $\dot{C}_{L,k}$ are the ones for which design changes are suggested. Secondly, among theses components, the ones with high value of relative cost difference get the most attention. Thirdly, components with low value of thermoeconomic factor can have their efficiency increased generating savings in the entire system even if the investment costs may increase because the increase in efficiency reduces exergy loss and destruction, decreasing the product cost. Then, with the same logic, components with high value of thermoeconomic factor may see their efficiency decreased so that the cost of the entire system decreases even though performance decreases too. This is because a higher value of thermoeconomic factor implies a greater contribution to the product cost from the component's cost. Finally, components with low exergetic efficiency and high exergy destruction and loss need improvements in the exergetic efficiency.
The optimization of these variables for one component helps the optimization of the system as a whole.

The variables mentioned are calculated while making changes to one variable and keeping the others constant so that the effects of the changes can be studied individually. If any change is noticed in a desired way, then the changed value becomes a candidate for the next iteration, if not, the variable is kept unchanged.

2.3 Cost estimations

2.3.1 Cost estimation of purchased equipment

The section of cost estimation is one of the most delicate and definitely challenging. Estimating the cost of purchased equipment, including spare parts and components, is the first step in any detailed cost estimation. As seen previously, in order to execute a proper thermoeconomic analysis, it is best to focus on every single component individually to later bring them together for the overall system. In order to have a realistic result of this thesis, with a concrete applicability to the real world and specifically to the case of IDDP-1 in Iceland, it was essential to have real life, up to date costs of components and clear conditions about the site.

Since this work is for academic purpose, obtaining bids and detailed prices for real life situations from manufacturing companies was extremely unlikely, and hence gave limited results. The difficulty in retrieving real world information led to a heterogeneous cost estimation process; prices of components have been estimated using different techniques depending on the component itself, the availability of prices and formulas. A few price estimations have been evaluated by using cost estimation formulas found in the literature, while others have been retrieved by scaling real existing values using a simple scaling approach. Some assumptions had to be made, as realistic as possible, but still remain educated guesses. All these price estimation processes are explained in the following section.

2.3.2 Component by component cost estimation

During the project planning in a real life situation, components are sized and quantified according to the requirements; the accuracy of cost estimations substantially depends on the quality of the information available and the budget available. In the case of this current study, costs have been estimated mainly from literature available and also thanks to the collaboration of Landsvirkjun, an energy company in Iceland owning geothermal power plants.

When vendor quotations are lacking, or when cost to prepare cost estimates is too high, cost estimating charts and mathematical formulas can come extremely useful. These charts and formulas are obtained through the correlation of a large amount of information regarding the design and cost of various components. The charts strongly depend on equipment features defined by parameters like design type, material, temperature and pressure. The accuracy of estimating charts is often relatively poor, but a number to start with, especially in a comparative analysis is already a fundamental starting point.

In a given capacity range of component, when knowing the size and all the costs related to the component, the data correlation results in a straight line. The simplest way for estimating a product cost is using the exponential law that defines the product cost as an exponential function of the size of the component. The scaling exponent α defines the steepness of the line, and represents an essential cost estimating parameter as shown by the relation:

$$C_{PE,Y} = C_{PE,W}\left(\frac{X_Y}{X_W}\right)^{\alpha} \tag{19}$$

Here, one can calculate the purchase cost $C_{PE,Y}$ of an equipment item Y at a capacity or size expressed by X_Y when the cost and capacity or size of equipment W are known, being respectively $C_{PE,W}$ and X_W. Depending on the type of equipment item, X may vary in physical quantity as it represents the primary design variable or combination of variables that characterises the capacity or size of the piece of equipment. In order to define the scaling exponent α, various tables are available in the literature and give the size range where this scaling exponent can apply. If no information is available, the six-tenth rule may be applied, giving an arbitral value of 0.6 to the scaling exponent α in the case of thermal processes (Bejan & Tsatsaronis, 1996). Several values of the scaling exponent α may be found according to the reference year and the varying size for the same equipment item, for this thesis two sources have been used. The first used comes from Bejan and Tsatsaronis in 1996 (Bejan & Tsatsaronis, 1996) while the second is Perry's Chemical Engineers Handbook of 2008 (Green & Perry, 2008).
When using the scaling relation shown by Eq. (19), the more the factors and parameters the components have in common, the more precise and realistic the results will become. For the purpose of this work, Landsvirkjun, the previously cited Icelandic energy company, authorized the access to one of their project planning reports containing detailed costs, sizes and parameters of the totality of a geothermal power plant that the company is currently building. The power plant in question, Theistareykir, is located very close to the site of IDDP-1, the size of the sections of Theistareykir, of 45MWe, are very similar in rated capacity to the expected power generation from IDDP-1; therefore, IDDP-1 is comparable to Theistareykir by an important number of elements ('Þeistareykir', 2015). These factors make the comparison simpler and have been of crucial importance in the developing of this thesis. Such detailed information allows the use of the exponential scaling relation in various cases, with virtually little margin of error, even considering the costs such as transportation, installation and others on components that apply to the case in a very similar or even equal way as IDDP-1. As Theistareykir installation and building is still in progress at the moment this study is being done, the information contained in their report is of high confidentiality. For understandable professional reasons Landsvirkjun expressed the will that the information in their project planning report shall not be disclosed to the public, and in respect of their will, none of the sensitive numbers will be shown in this study. Nevertheless, the precious information from Theistareykir has been used and integrated into the calculations, therefore the results were considered accurate enough for the purpose of this work.
The components whose costs have been obtained through scaling from the data from Landsvirkjun's Theistareykir project planning report are:

- Steam system:
    - Steam separator
    - Reinjection well
    - Steam gathering and pipes
- Power generation:
    - Generator
    - Automatic Voltage Regulator
    - Spare parts
- Cooling system:
    - Cooling tower
    - Cooling water pipes

- Facility:
    - Electricity system
    - Control rooms
    - Transformers
    - Fire protection
    - Others…

Other components such as the turbine, the condenser, and pumps were also referred to from the data of Landsvirkjun but were only used as a reference point as they were priced using mathematical formulas explained further.
The heat exchangers cost estimations were not possible to be retrieved from real data as for example they are not part of the design of Theistareykir plant. In order to estimate the cost of the various heat exchangers used in the different cycles analysed in this thesis, the scaling technique illustrated by Eq. (19) has been used. The reference component comes from Green and Perry (2008). The cost is then adapted according to the material chosen and the design of the heat exchanger estimated using engineering design data by Coulson and Richardson (2006); for the heat exchanger design choice and sizing see further section 2.4 Components sizing.
According to Green and Perry (2008), an approximate cost for a shell and tube heat exchanger is 21700$ (USD 1999) for a 93m^2 heat exchange area. An approximate value for other heat exchangers can be estimated from this using the exponential scaling formula, with a scaling exponent α equal to 0.59; this formula can apply with such a factor only in the range between 1.9 and 1860 m^2 for heat exchange area (Green & Perry, 2008).
Furthermore, the remaining components of the cycles were estimated using mathematical formulas, also found in the literature. A positive aspect of these formulas is that they gave results that differed by an acceptably low percentage margin from the results obtained by using the exponential scaling from the data of Theistareykir. The margin is not explicitly stated in respect of the non-disclosure agreement.
The formulas in question initially come from El-Sayed and Frangopoulos (1991), but were re-elaborated and updated various times until the versions used here by Xiong et al. (2012), Roosen et al. (2003) and Uhlenbruck and Lucas (2003).

For the turbine:

$$C_{turb} = 3880.5\left[1 + 5e^{\left(\frac{T_{in}-866}{10.42}\right)}\right]\left[1 + \left(\frac{1-0.85}{1-\eta_{T,i}}\right)^3\right]W_T^{0.7} \tag{20}$$

Where T_{in} is the inlet temperature in Kelvin, $\eta_{T,i}$ is the isentropic efficiency of the turbine, and W_T is the work output of the turbine. The result is in 2006 USD.

For the condenser:

$$C_{cond} = 280.74\,\frac{\dot{Q}_{cond}}{U_{cond}\,LMTD} + 746\,\dot{m}_{CW} + 70.5\,\dot{Q}_{cond}\,(-06936\ln(T_{CW} - T_{WB}) + 2.1898) \tag{21}$$

Where $\dot{Q}_{cond}$ is the heat transfer, LMTD is the logarithmic mean temperature difference, $\dot{m}_{CW}$ is the mass flow rate of the cooling water, and T_{CW} and T_{WB} are respectively the temperatures of the cooling water and the wet bulb. U_{cond} is the heat rate of transfer (used 2200W/m^{2}K (Coulson, Richardson, & Sinnot, 2006)). The result is in 2006 USD.

For a pump:

$$C_{pump} = 378\left[1 + \left(\frac{1 - 0.808}{1 - \eta_{p,is}}\right)^3\right]\dot{E}_{out}^{0.71} \quad (22)$$

Where $\eta_{p,is}$ is the isentropic efficiency of the pump (used 0.75 in this work unless otherwise specified) and $\dot{E}_{out}$ is the exergy rate of the product of the pump. The result is in 2006 USD.

The chemicals used in the scrubbing process have to be priced too. While, for simplicity reasons, the fresh water is assumed to come at no cost, NaOH is costed by obtaining a quotation online as for example Alibaba, to give an indicative cost estimation, the price is therefore 0.33$/kg in 2015 ('Sodium Hydroxide Naoh Alkali Price', 2015). To have the price usable during the entire lifespan of the plant it has to take into consideration the capital recovery factor, CRF (see section 2.3.4 Time value of money).
Then, the cost equation for NaOH (in 2015):

$$\dot{Cost}_{NaOH} = 0.33\,\dot{m}_{NaOH} \quad (23)$$

From this equation, the cost rate is directly obtained as the dimension is [$/s]. Therefore:

$$\dot{C}_{NaOH} = Cost_{NaOH}\,CRF \quad (24)$$

Finally, the last item but surely not the least important estimated is the production well. The production well is believed to cost around 20 million USD by HS Orka, one of the Icelandic energy companies participating in the IDDP. Such a cost is extremely high for a production well, but as explained in the previous chapter, it has encountered magma three times nevertheless (G. ó. Fridleifsson, Elders, & Bignall, 2013).

2.3.3 Cost indices

An important element to take into consideration when doing cost estimations is that costs, formulas and estimations might be based on reference years prior to the current. Many economic factors influence the course of currencies by modifying its face value to a different real value over time. For this, and in order to keep a sense to the numbers expressed in plain currency, it is fundamental to bring the prices all to the same reference year. For an easier understanding and a quicker realisation of the values it is preferable to bring costs to their equivalent in present value, usually the last completed year is the closest reference to the present. Therefore, prices in this study are all brought

to 2014 USD. The general relation for converting values between years is a simple relation that can be illustrated as follows:

$$reference\ year\ cost = base\ year\ cost\ \frac{reference\ year\ CPI}{base\ year\ CPI} \qquad (25)$$

Where CPI stands for Consumer Price Index; it is possible to find various price indices according to who the consumer is. Many sources can provide cost indices for plant costing such as Marshall & Swift cost index (Marshall and Swift, 2015) or CEPCI (chemical engineering plant cost index) ('Economic Indicators', 2015).

2.3.4 Time value of money

The life of a power plant is limited, and so it is for its components. In order to be able to achieve a proper thermoeconomic analysis, and to give a cost to every unit of exergy produced in a certain period, a good consideration of the investments has to be made. The best way, and simplest, to evenly distribute the initial capital investment over the useful life of the plant is to use the capital recovery factor (CRF). It consists in breaking the initial investment into annuities, that are equal-amount money flows occurring at equal time intervals. The factors that compose the CRF are the useful life of the plant n and the interest rate, i (comprehensive of the total risk), over this time. The equation is as follows:

$$CRF = \frac{i(1+i)^n}{(1+i)^n - 1} \qquad (26)$$

In the case of a power plant, a factor φ can be added to the CRF to account for ordinary O&M expenses over the years, occurring at a constant rate every year. Also, electricity generation plants traditionally and for practical reasons express their numbers in much shorter periods of time than the year. Therefore, this thesis dealing with exergy rates and power, represented by joules per second (watts), the main unit of time is the second. Therefore, the capital cost rate $\dot{Z}_n$ of a component n can be expressed as:

$$\dot{Z}_n = \frac{CRF\ I_n\ \varphi}{\tau} \qquad (27)$$

$\dot{Z}_n$ is the capital investment per unit of operation time in a year, in this case the operation time in a year is τ, in seconds. I_n is therefore the capital investment of component n and φ must be expressed as 1 + O&M percentage rate in pure number (e.g. φ = 1.05 for 5% O&M costs per year). Logically, this concept also applies to the entire power plant as a whole when considering all plant costs in I_n and $\dot{Z}_n$ as the total capital cost rate.

2.3.5 Not included costs

In order to avoid revealing sensitive data about Theistareykir report, about the real costs of electricity and about every price paid in the power plant, many costs are not being included in this analysis. These costs represent minor components as well as buildings, salaries, roads and all the non cited elements in this major section. Nevertheless, their sum is not negligible in a real plant price estimation; therefore, the final cost of electricity cannot be considered as a real condition, but a low, approximate estimation.

2.4 Components sizing

Designing a power cycle or even a power plant is also a matter of choosing the right type and size of components to install. Selecting the size is an effect of efficiency preferences and necessities but also a cause of cost definition as these three elements are intrinsically correlated. The aim of this sizing work is to be able to apply the cost calculations explained in the previous section. For some components the question may be easily solved but others may have various type and design alternatives. Such a precise analysis of design is usually achieved by teams of engineers with consistent budget and of course resources and experience. In this thesis, as it is only a part of the objective, the choice of design is limited to a broader approach, in the limits of time and resources available. Not every component is being studied in the detail of the design, and the ones studied are analysed in an indicative way rather than a ready-to-build design. It is also important to note that, this project being a comparative analysis of various cycles, by using the same criteria of sizing in every cycle, whether it is precise or a bit broader, the comparison is still applicable. This section explains the choices of design where applicable and the extent of the analysis that has been made on every component.

In this thesis, the first component of every cycle is the IDDP-1 well and it is assumed to be the only production well. It is a very specific case as the well has unique characteristics as stated in the introductory sections. Furthermore, there is no sizing in the well, the only adjustable parameter is the wellhead pressure upon which depends the mass flow rate of the fluid extracted. Adjusting and deciding these parameters will define sizes of components of the cycles and therefore their costs, this analysis will come in the next chapter. For any other geothermal power plant, it is common to estimate the number of production wells to be drilled with their respective location, distance and various characteristics.

For the components following the production well, a more detailed analysis is explained in the following subsections.

2.4.1 Separator

Most of the time, there is a liquid phase in every geothermal reservoir, even in steam dominated reservoirs the presence of a minor liquid phase is possible. The separator is an essential component of geothermal power plants as it is important to have a steam with the best quality possible in order to have pure steam entering the turbine. In the case of superheated steam, a separator would not be necessary but in the cycle configurations where the steam is processed and condensation occurs it is required to separate the liquid phase from the vapour phase.

The type of separator chosen is the same type of separator that is used in the previously cited report of the plant of Theistareykir, the characteristics of the plant, of the location and of the fluid were similar enough to assume that the same type of separator would be an acceptable choice. The horizontal separator is widely used in Iceland in a general habit (Zarrouk & Purnanto, 2015). This type of separator is a horizontal knitted wire mesh separator that allows high enthalpy geothermal fluids to be processed and has a better separation efficiency than for example a grid bucket type vertical (Ingvarsson, 2015). Some other advantages of this horizontal separator are that it is at right angle with the steam flow making the separation more efficient, and it is easier to access the horizontal separator for measuring, equipment, and maintenance. (Moghaddam, 2006).

In order to size the separator, the Souders-Brown equation was applied. This equation allows to calculate the steam velocity v_v in [m/s] through the separator and depends

upon densities and the Souders-Brown constant k_f, it is written as follows (Souders & Brown, 1934):

$$v_v = k_f \sqrt{\frac{\rho_l - \rho_v}{\rho_v}} \tag{28}$$

Where ρ_l and ρ_v are respectively the density of liquid and vapour (steam) phases. k_f is defined according to the type of separator and gauge pressure, it is expressed in [m/s], the value used is 0.2m/s from Ingvarsson (2015).
Once the velocity defined, the area of the cross section of the separator A_S can be calculated with the following equation:

$$A_S = \frac{\dot{V}_v}{v_v} \tag{29}$$

Here, A_S is the area in [m^2] while $\dot{V}_v$ is the steam volume flow rate in [m^3/s].
The characterizing size of the separator when using scaling factors for costing, represented by Eq. (19), is the volume of the separator. Therefore, one needs to define the length of the separator in order to be able to calculate the total volume. Furthermore, according to Zarrouk and Purnanto (2015), a characteristic element in designing separators is the L/D ratio, that is the length and diameter ratio, decided according to various parameters. Some of these defining parameters are for example steam- and water-retention times, the flow rates of water and steam and the fraction filled by liquid. Because the separator chosen is the same type as in Theistareykir, and that the L/D ratio of the separator in use in Theistareykir is known, for this study the same ratio has been used.
Now, with simple geometric relation it is possible to calculate the diameter D of the separator from the area A_S illustrated here:

$$D = \sqrt{\frac{4A_S}{\pi}} \tag{30}$$

Then, with the known L/D ratio, the length of the analysed separator is calculated with:

$$L = D \left({}^{L}/_{D}\right)_{Theistareykir} \tag{31}$$

And finally the volume of the separator to be installed is calculated with another basic geometric relation:

$$V = 2\pi \left(\frac{D}{2}\right)^2 L \tag{32}$$

The size of the separator is then calculated and it is possible to use the volume to evaluate its cost with Eq. (19).

2.4.2 Turbine

The aim of the turbine is to produce work output by expansion of the steam. In every cycle configuration studied in this work, there is a condensing turbine; nevertheless, the cycle illustrated in Figure 6 has an additional back pressure turbine. The cost of the turbine, according to Eq. (20), depends upon inlet temperature, efficiency and work output. These factors will vary in relation to the configuration of the cycle analysed and also to the wellhead pressure. The work output of the turbine can be calculated by using the following equation (Harvey, 2015):

$$\dot{W}_T = \dot{m}_{in}(h_{in} - h_{out}) \tag{33}$$

Where $\dot{m}_{in}$ is the mass flow rate of the steam entering the turbine and $h_{in} - h_{out}$ is the difference of the enthalpies at the inlet and outlet of the turbine.

Since the mass flow rate depends on the wellhead pressure, it is obvious from this equation that the work output depends on the wellhead pressure. By definition, the isentropic efficiency, η_T, of the turbine can be expressed using the isentropic enthalpy of the exiting stream, $h_{out,isen}$, by:

$$\eta_T = \frac{h_{in} - h_{out}}{h_{in} - h_{out,isen}} \tag{34}$$

And its exergetic efficiency is $\varepsilon_T = \frac{\dot{W}_T}{\dot{E}_{in} - \dot{E}_{out}}$.

Finally, the temperature depends on the cycle configuration and on the processing of the fluid.

2.4.3 Cooling tower

The cooling tower is the component responsible of cooling the water which gains heat in the condenser from the working fluid. The type of cooling tower assumed in the current study is a cross flow cooling tower. The cooling tower calculations are directly linked to the condenser's characteristics. The characterizing dimension of the cooling tower is its cooling water mass flow rate. The amount of heat removed from the working fluid by the cooling tower is given as:

$$\dot{Q}_{cond} = \dot{m}_{steam}(h_{in} - h_{out}) \tag{35}$$

Where $\dot{Q}_{cond}$ is the heat quantity that has to be removed, $\dot{m}_{steam}$ is the mass flow rate of the steam at the exit of the turbine. $h_{in} - h_{out}$ is the difference in enthalpy of the working fluid between inlet and outlet of the condenser.

In the same way, one can calculate the heat transfer occurring on the cooling water side by stating:

$$\dot{Q}_{cw} = \dot{m}_{cw}\, c_p \left(T_{cw,out} - T_{cw,in}\right) \tag{36}$$

Where $\dot{Q}_{cw}$ is the quantity of heat that the cooling water will absorb by going from initial temperature $T_{cw,in}$ to final temperature $T_{cw,out}$. Then, $\dot{m}_{cw}$ is the cooling water mass flow rate and c_p is the specific heat of water.

The heat released by the working fluid is equal to the heat absorbed by the cooling water; therefore, by using Eq. (35) and Eq. (36), the mass flow rate of the cooling water can be found as:

$$\dot{m}_{cw} = \frac{\dot{m}_{steam}(h_{in} - h_{out})}{c_p \ (T_{cw,out} - T_{cw,in})} \tag{37}$$

For costing purposes, as the cooling tower cost is being evaluated by exponential scaling, sizing the cooling water flow rate is sufficient. There are further calculations related to the cooling tower that are included in the application process explained in next chapter. Eq. (37) shows the required mass flow rate to pass through the condenser, sufficient for the costing scope, but the total fluid flow rates inside the tower also account for water losses due to evaporation and are included in the next chapter (Cengel & Design, 2005)(Muangnoi, Asvapoositkul, & Wongwises, 2007).

2.4.4 Condenser

The condenser is the component placed next after the turbine to bring the expanded steam to a liquid phase. The design of the condenser is a shell and tube type condenser where the working fluid flows through the tubes and the cooling water in the shell.
As shown by Eq. (21), the cost of the condenser considers as cost-determining factors the heat transfer rate, the cooling water mass flow rate and the logarithmic mean temperature difference (LMTD). The pinch point used for the condenser design and heat rate analysis is a pinch point of 5K.
Both the heat transfer rate of the condenser $\dot{Q}_{cond}$ and the cooling water mass flow rate $\dot{m}_{cw}$ were expressed respectively in Eq. (35) and Eq. (37) in the sizing of the cooling tower. The LMTD can be calculated by combining the temperatures of the inlets and outlets of the condenser as follows (Coulson et al., 2006):

$$LMTD = \frac{(T_{H,in} - T_{cw,out}) - (T_{H,out} - T_{cw,in})}{\ln\left(\frac{T_{H,in} - T_{cw,out}}{T_{H,out} - T_{cw,in}}\right)} \tag{38}$$

Where $T_{H,in}$ and $T_{cw,in}$ are respectively the temperature of the hot working fluid inlet and of the cooling water inlet, the subscript *out* represents the outlets of those same streams temperatures.
To conclude the calculations regarding the condenser, Eq. (21) requires the temperature of the wet bulb, this value was assumed constant over the year and therefore the value used is calculated from the year average temperature and humidity at the location of the site, retrieved from (Landsvirkjun, 2002) and (US Department of Commerce, 2015).

2.4.5 Heat Exchanger

For the heat exchangers, the size that represents the comparison dimension to be able to estimate its cost is the extent of the area along which the heat transfer occurs. In this thesis, one cycle, illustrated in Figure 5 includes a heat exchanger for reheating purposes, to bring saturated steam to superheated condition. The binary cycle configuration also uses heat exchangers, shown in Figure 7, in this case the role of the complex of heat exchangers is to change a saturated liquid to superheated condition, therefore it involves a phase change. Here, to simplify, the equations of area definition will be assumed to be the same in both cases, with only difference in the heat transfer coefficient, but further analysis could be done on the diameter of tubes, their layout, the

materials used and various other elements characterizing the heat exchangers (Coulson et al., 2006). The pinch point of the heat exchangers was used equal to the condenser's and it is 5K.
The formula to be able to define the area of the heat exchanger is then calculated as follows (Hajabdollahi, Ahmadi, & Dincer, 2012):

$$A_{HX} = \frac{\dot{Q}_{HX}}{U_{HX} LMTD} \tag{39}$$

Where $\dot{Q}_{HX}$ is calculated in the same way as for the condenser in Eq. (35). Similarly, LMTD is also calculated using Eq. (38) by simply replacing the cooling water data with the data of the cold stream entering the heat exchanger, and using the hot superheated steam in reference to T_H. The constant U_{HX} is the heat transfer rate and is the only factor considered different between the heat exchangers used ($U_{HX} = 2200 W/m^{2}°C$ unless otherwise stated) (Subramanian, 2004).

2.4.6 Other components

The pumps were accounted for in a limited way. Only two pumps were considered, the cooling water pump and the reinjection pump; some remaining pumps are for example the auxiliary pumps, the pump for the wet scrubbing water, brine treatment pumps and others. The pumps sizing depends on the exergy rate that is obtained by combining Eq. (5) and Eq. (6), together with assuming a certain pump efficiency to fit the requirements (assumed 0.75 efficiency for both pumps).
The generator's size is directly defined by the work output produced by the turbine, therefore its cost can be estimated with exponential scaling by using power as the defining size and scaling exponent α=0.6 (Bejan & Tsatsaronis, 1996).
The cost of a component such as the AVR does not vary with size as per the report of Landsvirkjun. Therefore, the cost of the AVR considered is the same as the one from Theistareykir.
In order to give the total costs a realistic dimension, the spare parts were also evaluated. The spare parts from Landsvirkjun's report were based on the turbine, generator and AVR, therefore, in order to quantify the spare parts weightage in the analysis, the costs were expressed as a percentage of the sum of the cited components and then applied in same proportion to the sum of the same three components evaluated for this analysis.

2.4.7 Chemicals for wet scrubbing

The quantity of chemicals, such as NaOH, required to be added into the cold water stream needs to be estimated in order to evaluate its cost. The molar ratio of NaOH to HCl needed for complete scrubbing is 1:1, as shown by the chemical reaction in Eq. (4). Therefore, one mole of NaOH has to be supplied in order to react with one mole of HCl. The content of hydrogen chloride measured in IDDP-1 was 100ppm, therefore the equivalent molar quantity of NaOH has to be supplied to the stream (Markusson & Hauksson, 2015). The molal concentration of HCl (b_{HCl}) in the steam is:

$$b_{HCl} = \frac{C_{HCl}}{M_{HCl}} = \frac{0.1\ g/kg_{steam}}{36.45\ g/mol} = 0{,}00274\ mol/kg_{steam} \tag{40}$$

Where C_{HCl} and M_{HCl} are respectively the concentration of HCl in the steam and the molar mass of HCl.

The amount of NaOH needed is expressed as a function of the wellhead mass flow rate and the molal concentration of HCl as follows:

$$\dot{m}_{NaOH} = M_{NaoH}\, b_{HCl}\, \dot{m}_{Wellhead}\, 10^{-3} \tag{41}$$

2.5 Use of Matlab

All the elements of theory introduced before this point regarding exergy, costing and sizing are all combined into calculations in order to have results that can be defined as a thermoeconomic analysis of the cycles in question. The calculations are written in the form of Matlab codes, able to elaborate all variables introduced and combine additional ones, according to the situation. For each cycle, the analysis was reiterated as many times as the number of wellhead pressures analysed, visible in Figure 9 in the next chapter.

The codes are structured in such a way that they are able to precisely calculate, by approximation from greater and smaller value (squeeze theorem), the operating characteristics such as pressures, temperatures, mass flows, thermodynamic values and many others when varying the inputs.

3 Application

3.1 State-by-state cycle thermoeconomic balance

This chapter aims at showing the application of the concepts introduced in Chapter 2 to the cases explained in Chapter 1 with respect to cycle options proposed in literature for IDDP-1.

The thermoeconomic analysis, by definition, includes the exergetic analysis. By combining Eq. (7) and Eq. (9) that define cost rates according to exergy rates, the exergy flow analysis is included in the cost rate analysis. In order to avoid repetitiveness and save steps, the thermoeconomic analysis will be presented directly. Eq. (27) is used to define the investment cost rates.

Generally, component by component thermoeconomic analysis is done in the same direction as that of the flow of the exergy stream, that is, with the flow of the geofluid; it seems more significant to follow the stream in its course.

Furthermore, to avoid repetitions once more, the first cycle is described in more details while the following ones will be only showing the differences in comparison to the first cycle, i.e. the single flash wet scrubbing. The cooling tower streams have the same numbering in every cycle therefore the thermoeconomic analysis of the cooling tower will not be repeated. All the other components that have the same characteristics but different numbers will report only the equations with the corresponding numbers to the specific case.

3.1.1 Single flash cycle with wet scrubbing

The numbers of the state points for the analysis of the single flash cycle with wet scrubbing are in reference to Figure 4. The thermoeconomic balance is made in accordance with the direction of the stream, the following analysis is executed state by state, considering every component, starting with the well.

Well:

The well is the first component of any geothermal cycle, it is the tool that allows the extraction of the steam, and is therefore the first step of the thermoeconomic analysis. In other words, from an exergetic point of view, no fuel exists for state point 1. Only the product exists, which is in this case the superheated steam, and it comes to a cost that is in fact only generated by the well cost.

Hence, Eq. (10) will be written for state 1 as:

$$\dot{C}_1 = \dot{Z}_{well} \tag{42}$$

The investment cost of the well $\dot{Z}_{well}$ is defined by using Eq. (27) and the information in section 2.3.2 regarding the well initial cost.

By definition, the unit cost of exergy at state point 1 is (from Eq. (15)):

$$c_1 = \frac{\dot{C}_1}{\dot{E}_1} \tag{43}$$

State 7, chemicals:

This state is the inlet of the cold water mixed with chemicals in order to perform the wet scrubbing. Here, it is assumed that the cold water comes at no cost, from state point

6, for simplicity reasons. The assumption is valid due to the abundant availability of fresh water in the area. Therefore, the capital costs at state point 7 are only represented by the purchase of the chemicals, in this case NaOH. Similarly to state 1, the flow of state 7 comes directly as a product which cost is only the cost rate of NaOH. Therefore, state 7 thermoeconomic balance can be written as:

$$\dot{C}_7 = \dot{C}_{NaOH} \tag{44}$$

And

$$c_7 = \frac{\dot{C}_7}{\dot{E}_7} \tag{45}$$

Where $\dot{C}_{NaOH}$ is calculated according to Eq. (24).

State 2, mixing:
State 2 is the mixing of the superheated steam with the cool water, here, no capital investment is made, two fluxes of matter are mixed together, therefore summing the two streams is also equivalent to summing their exergy flows. Thus, for state point 2 cost rates are given as:

$$\dot{C}_2 = \dot{C}_7 + \dot{C}_1 \tag{46}$$

And

$$c_2 = \frac{c_7\dot{E}_7 + c_1\dot{E}_1}{\dot{E}_2} \tag{47}$$

Separator:
The separator has one inlet and two outlets of streams. The valuable stream that will be used for generating the power is state 3. Therefore, for this component, the cost rate of the fuel is $\dot{C}_F = \dot{C}_2 - \dot{C}_8$ and the cost rate of product is $\dot{C}_P = \dot{C}_3$. Hence, the thermoeconomic balance for state 3 is given by:

$$\dot{C}_3 = \dot{C}_2 - \dot{C}_8 + \dot{Z}_{separator} \tag{48}$$

Here, $\dot{Z}_{separator}$ is defined by combining Eq. (27) and Eq. (19), by inputting the results of Eq. (32). Consequently, the only unknown variable is $\dot{C}_8$. By applying the exergetic definition $\dot{E}_8$ can be defined, therefore one needs to define c_8, the unit cost of exergy exiting the separator. The stream at state 8 is going to the reinjection well, it is an exiting stream that needs further processing (reinjection), not to be released to the environment. This reinjection is cost-evaluated by using Eq. (18), where the capital cost rate of the process is the investment rate of the reinjection well. Therefore, c_8 can be defined as:

$$c_8 = -\frac{\dot{Z}_{reinjection}}{\dot{E}_8} \tag{49}$$

And therefore,

$$c_3 = \frac{c_2\dot{E}_2 - c_8\dot{E}_8 + \dot{Z}_{separator}}{\dot{E}_3} \tag{50}$$

All the elements necessary to analyse the next step are now known, since $\dot{Z}_{reinjection}$ is defined, as usual, by Eq. (27) together with the investment cost.

Turbine:
The turbine is the component that converts exergy of the working fluid into useful electric work. Nevertheless, the turbine does have two separate exergy outlets, the first is the work power output, and the second is that of exiting working fluid after expansion in the turbine. The first outlet is the valuable one, and the one to which one wants to attribute the costs of the component in order to be able to cost the power output. For this, the following relation as given in Bejan et al. (1996):

$$\dot{C}_{\dot{W},turb} = \dot{C}_3 - \dot{C}_4 + \dot{Z}_{turbine} \tag{51}$$

An additional relation is required in order to value $\dot{C}_4$. The explanation is given by Bejan et al. and states: "*Since the purpose of a turbine is to generate power, all costs associated with the purchase and operation of the turbine should be charged to the power. Both the exergy rate spent to generate the power and the exergy rate exiting the turbine were supplied to the working fluid in the components upstream of the turbine at the same average cost per exergy unit. This cost would change only if exergy were added to the working fluid during the turbine expansion. Therefore, the cost per unit of exergy of the working fluid remains constant."* (Bejan & Tsatsaronis, 1996) The relation is then given as:

$$c_4 = c_3 \tag{52}$$

In this way, the product stream $\dot{C}_{\dot{W},turb}$ carries the total cost of the component, together with all the previous costs upstream. The investment rate of the turbine $\dot{Z}_{turbine}$ is defined by Eq. (20) and Eq. (27).
The unit cost of the work output up to this point can be expressed by:

$$c_{\dot{W},turb} = \frac{\dot{C}_{\dot{W},turb}}{\dot{W}_{turb}} \tag{53}$$

Since the important element to cost will be the *net work output* bearing the costs of the *entire plant*, this will be calculated at last. Prior to that, it is required to cost all the streams and components of the plant, both upstream and downstream from the turbine. The stream, after exiting the turbine, continues its passing through the condenser. The condenser itself has a second inlet, from the cooling tower, that carries a cost. Therefore, in order to give the costs of the cooling tower to the condenser, the thermoeconomic analysis of the cooling tower will be presented prior to the condenser's.

Cooling tower:
The following cooling tower thermoeconomic balance is valid for every single cycle studied in this work as the same state numbers are used in every cycle.
The cooling tower uses fresh water as make up water that, like for the wet scrubbing water, will be assumed having no cost. The cooling tower has two inlets and two outlets, its role is to cool water by using ambient air. It can be considered as a heat exchanger when executing the thermoeconomic analysis, as found in the work of Bejan et al. (1996). Then, the cooling tower product and fuel cost rate are given by $\dot{C}_P = \dot{C}_{20} - \dot{C}_{22}$ and $\dot{C}_F = \dot{C}_{23} - \dot{C}_{24}$.
Therefore, the thermoeconomic balance equation of the cooling tower is:

$$\dot{C}_{20} - \dot{C}_{22} = \dot{C}_{23} - \dot{C}_{24} + \dot{Z}_{CoolingTower} \tag{54}$$

The capital investment rate associated to the cooling tower $\dot{Z}_{CoolingTower}$ is defined before in sections 2.3.2 and 2.4.3.
Stream at state point 24 is hot (and humid) air being released to the environment with no further processing, therefore it is exergy lost to which Eq. (17) can be applied. The unit cost of exergy of stream at state point 24 is then:

$$c_{24} = 0 \tag{55}$$

The air flow entering the cooling tower represented by state number 23 has to be cost-evaluated. The only cost attributable to stream at state point 23 is the cost of the work required for running the fan. Here a choice on how to deal with the cost of the fan has to be made. There are two options:
Either, one gives a defined cost to the power used for the fan by considering that cost a simple monetary cost per unit. This would be equivalent to assuming it is a stream of electricity purchased to generate the work of the fan. In this case, the work of the fan would not be considered as a parasitic load, to subtract from the turbine's power outlet, but simply a cost rate.
Or, the work of the fan can be considered as a parasitic load. In this case, when calculating the net power output of the plant, the power dedicated to the fan is subtracted from the power output of the turbine. No direct monetary cost is attributed to the work of the fan; the total cost rate of the plant then remains unaltered. Subtracting the parasitic load from the turbine output decreases the net output which automatically increases the unit cost of final power generated by the plant, which actually is the increase due to accounting for the unit cost of the fan.
Nevertheless, the object of the study is the analysis of power generating cycles, therefore, purchasing electricity while producing it, is not necessary. The plant produces electric power that contributes to running the fan of the cooling tower. Therefore, the preferred option to account for the cost of the work of the fan is the second option illustrated.
Hence, when considering subtracting the work of the fan from the work output, the unit cost of the work of the fan is:

$$c_{23} = c_{\dot{W},fan} = 0 \tag{56}$$

This option was chosen also because if the first option was chosen one would have to estimate the cost according to the electricity need and therefore market cost, which involves more uncertainties.
Successively, because the purpose of the thermoeconomic analysis is to account the costs to the main stream at the condenser outlet, stream 20 will carry all the costs of the cooling tower, as it is the one entering the condenser (after being pumped). So, the cost rate of state 20 can be expressed as:

$$\dot{C}_{20} = \dot{Z}_{CoolingTower} \tag{57}$$

The only element to evaluate is stream at state 22. In order to estimate its cost rate one needs to consider the following steps.
When adding the cooling water pump and the total piping cost of the cooling system, stream at state 21 cost rate is written as:

$$\dot{C}_{21} = \dot{C}_{20} + \dot{Z}_{CoolingPump} + \dot{Z}_{CoolingPiping} \tag{58}$$

The work input to the pump is subtracted from the total work output, like for the case of the fan, and therefore carries no cost other than its capital investment cost, in this point. The two capital investment rates of cooling pump and cooling piping are estimated according to Eq. (22) and using the data from Theistareykir, both combined with Eq. (27).
Stream at state 21 enters the condenser, there is no cost added between state 21 and state 22 as the condenser costs are accounted on the condensed stream exiting the condenser (condenser analysis explained next). However, there is an increase of exergy from state 21 to 22, before stream at state 22 returns back into the cooling tower. In the cooling tower, the stream is cooled, but the cost of the cooling cannot be evaluated by using Eq. (18) because the capital investment rate of the cooling tower has already been accounted in stream at state 20. Therefore, in order to have stream at state 20 to carry all the costs related to the cooling tower and dealing with the exergy loss of stream at state 22, the following relation can be stated:

$$c_{22} = 0 \tag{59}$$

These relations being stated, one can see that stream at state 20 carries all the costs of the cooling tower, except for the fan, accounted into the overall thermoeconomic balance.

Condenser:
The condenser also treats two inflows and two outflows. The cost rates of product and fuel for this component are respectively $\dot{C}_P = \dot{C}_5 - \dot{C}_4$ and $\dot{C}_F = \dot{C}_{21} - \dot{C}_{22}$.
The balance for the condenser is therefore:

$$\dot{C}_5 - \dot{C}_4 = \dot{C}_{21} - \dot{C}_{22} + \dot{Z}_{condenser} \tag{60}$$

The cooling water streams cost rates ($\dot{C}_{21}$ and $\dot{C}_{22}$) have been defined in the cooling tower analysis, while the cost rate of stream 4 ($\dot{C}_4$) is defined by c_4 in the turbine analysis. It is to be noticed that $\dot{C}_{22}$ is null, so by not being subtracted from the cost, it

shows how the exergy increase of the cooling water after the condenser is a lost stream of exergy and therefore an economic loss.
Now, the remaining cost flow rate required is $\dot{C}_5$ obtainable from c_5 given by equation:

$$c_5 = \frac{c_4\dot{E}_4 + c_{21}\dot{E}_{21} + \dot{Z}_{condenser}}{\dot{E}_5} \tag{61}$$

Here it is possible to notice that $\dot{C}_5$ carries the costs of both the cooling tower and the condenser.

Reinjection:
State 9 is the last state of the process of the geothermal fluid. After being condensed, the fluid is pumped to the reinjection well to return into the reservoir. The thermoeconomic balance of state 9 is shown here:

$$\dot{C}_9 = \dot{C}_5 + \dot{Z}_{DrainPump} \tag{62}$$

Here, even though the stream is being reinjected, the reinjection well cannot be accounted to stream at state 9 as it has already been accounted in stream at state 8 in Eq. (49). The two streams at states 8 and 9 join into a single stream before being reinjected.

Up to this point, every component has been considered separately and in conjunction with their respective adjacent components. The final step is to put together all the previous elements in order to have the thermoeconomic balance of the entire cycle and therefore the entire plant. In this final phase, the general costs of the plant can be added to the equation. The total cost of the plant is given as:

$$\dot{C}_{total} = \dot{C}_9 + \dot{C}_{\dot{W},turb} + \dot{C}_{other} \tag{63}$$

Where subscript *other* represents the sum of all costs, not directly appearing in the components economic balance, such as generator, AVR, electric system, spare parts, and all the listed elements in the previous chapter.
The work output is the net work, corresponding to the turbine work minus the parasitic load. These concepts can be put into formulas as follows. Then:

$$\dot{W}_{net} = \dot{W}_{turb} - \dot{W}_{ParasiticLoad} \tag{64}$$

Finally, the unit cost of output can be calculated as follows:

$$c_{\dot{W},net} = \frac{\dot{C}_{total}}{\dot{W}_{net}} \tag{65}$$

Where $c_{\dot{W},net}$ is expressed in \$/kJ.

3.1.2 Single flash cycle with wet scrubbing and heat recovery

The cycle consists of an additional heat exchanger compared to the previously studied cycle. As explained in Chapter 1, the role of the heat exchanger is to recuperate the heat lost in the wet scrubbing in order to bring the steam back to a superheated condition. The numbers of the state points for the analysis of this cycle are in reference to Figure 5. The thermoeconomic balance is made in accordance with the direction of the stream, the following analysis is executed state by state, considering every component, starting with the well.

Well:
The well's thermoeconomic analysis is defined by Eq. (42) and Eq. (43).

Heat recuperator:
The heat recuperator behaves as a counter-flow heat exchanger whose purpose is to heat up a fluid without any phase change. Hence, the thermoeconomic balance of a heat exchanger in terms of fuel and product is defined by Bejan et al. (1996) as:

$$\dot{C}_5 - \dot{C}_4 = \dot{C}_1 - \dot{C}_2 + \dot{Z}_{HX} \tag{66}$$

The investment rate of the recuperator (heat exchanger), $\dot{Z}_{HX}$ is defined according to section 2.3.2 by applying Eq. (19) then Eq. (27) after sizing the recuperator using equation (39).
According to the direction of the stream, it is preferable to give the cost to stream at state 5. In order to do so, the steps prior to stream at state 5 have to be defined.
Stream 2 is the exit of the initial stream from the recuperator, because no cost was considered to be added in between, the following relation can be applied:

$$c_2 = c_1 \tag{67}$$

Hence,

$$\dot{C}_2 = c_1 \dot{E}_2 \tag{68}$$

Then, the inflow at state 9 is the cold water for the wet scrubbing, the exergoeconomic balance is estimated as in Eq. (44):

$$\dot{C}_9 = \dot{C}_{NaOH} \tag{69}$$

The mixing of the streams was defined earlier by Eq. (46) and Eq. (47) that respectively become:

$$\dot{C}_3 = \dot{C}_9 + \dot{C}_2 \tag{70}$$

and

$$c_3 = \frac{c_9 \dot{E}_9 + c_1 \dot{E}_2}{\dot{E}_3} \tag{71}$$

The stream then undergoes the separation of phases and the equations characterising it are Eq. (48) and Eq. (49), respectively applied to this cycle as:

$$\dot{C}_4 = \dot{C}_3 - \dot{C}_{10} + \dot{Z}_{separator} \tag{72}$$

And

$$c_{10} = -\frac{\dot{Z}_{reinjection}}{\dot{E}_{10}} \tag{73}$$

Hence, the specific cost flow rate at state 4 becomes:

$$c_4 = \frac{c_3\dot{E}_3 - c_{10}\dot{E}_{10} + \dot{Z}_{separator}}{\dot{E}_4} \tag{74}$$

Eq. (66) can be solved for stream at state 5 as all the costs are now being carried by stream 4. The unit cost of exergy at state 5 is:

$$c_5 = \frac{c_4\dot{E}_4 + c_1(\dot{E}_1 - \dot{E}_2) + \dot{Z}_{HX}}{\dot{E}_5} \tag{75}$$

Hence

$$\dot{C}_5 = c_5\dot{E}_5 \tag{76}$$

Except the above mentioned heat recuperator, there is no design difference between this cycle and the wet scrubbing single flash, therefore, the thermoeconomic balance can be shown directly with little explanation.
For the turbine, Eq. (51) and Eq. (52) become:

$$\dot{C}_{\dot{W},turb} = \dot{C}_5 - \dot{C}_6 + \dot{Z}_{turbine} \tag{77}$$

And

$$c_6 = c_5 \tag{78}$$

The cooling tower equations from Eq. (54) to Eq. (59) stay the same, and Eq. (60) for the condenser becomes:

$$\dot{C}_7 - \dot{C}_6 = \dot{C}_{21} - \dot{C}_{22} + \dot{Z}_{condenser} \tag{79}$$

Similarly, Eq. (61) is applied to this cycle by writing:

$$c_7 = \frac{c_6\dot{E}_6 + c_{21}\dot{E}_{21} + \dot{Z}_{condenser}}{\dot{E}_7} \tag{80}$$

And to close the cycle, Eq. (62) relative to the drain is expressed as:

$$\dot{C}_{11} = \dot{C}_7 + \dot{Z}_{DrainPump} \tag{81}$$

Finally, the total cycle thermoeconomic balance is expressed in the same way as for the single flash with wet scrubbing, where the net work is defined as per Eq. (64) and the cost rates are added together, as per the following equation (from Eq. (63)):

$$\dot{C}_{total} = \dot{C}_{11} + \dot{C}_{\dot{W},turb} + \dot{C}_{other} \tag{82}$$

Finally, Eq. (65) can be applied to find the cost per unit of exergy of the total plant, which is the cost per unit net work output.

3.1.3 Single flash cycle with wet scrubbing and additional turbine

As explained in Chapter 1, this cycle configuration only differs from the single flash wet scrubbing by the addition of a turbine. The aim of this additional turbine is to produce work from fluid at wellhead conditions without losing the superheated condition after expansion. The numbers of the state points for the analysis of this cycle are in reference to Figure 6. The thermoeconomic balance is made in accordance with the direction of the stream, the following analysis is executed state by state, considering every component, starting with the well.

As seen previously, the thermoeconomic balance for the well is defined by Eq. (42) and Eq. (43). Then, the first turbine is treated in a similar way as in the previous cycles with change in state point notations. The first turbine's thermoeconomic balance is expressed by the following equations (as per Eq. (51) and Eq. (52)):

$$\dot{C}_{\dot{W},turb\_1} = \dot{C}_1 - \dot{C}_2 + \dot{Z}_{turbine\_1} \tag{83}$$

And

$$c_2 = c_1 \tag{84}$$

Here, a cost rate for the first work output is obtained. Then the geothermal fluid keeps its course in the cycle and becomes the same process as in the first cycle analysed. Therefore, the thermoeconomic equations are as follows:
Chemicals:

$$\dot{C}_8 = \dot{C}_{NaOH} \tag{85}$$

And

$$c_8 = \frac{\dot{C}_8}{\dot{E}_8} \tag{86}$$

For the mixing part where wet scrubbing occurs:

$$\dot{C}_3 = \dot{C}_8 + \dot{C}_2 \tag{87}$$

And

$$c_3 = \frac{c_8 \dot{E}_8 + c_2 \dot{E}_2}{\dot{E}_3} \tag{88}$$

The separator's cost rate of fuel is $\dot{C}_F = \dot{C}_3 - \dot{C}_9$ and its product cost rate is $\dot{C}_P = \dot{C}_4$. Therefore, its thermoeconomic balance is:

$$\dot{C}_4 = \dot{C}_3 - \dot{C}_9 + \dot{Z}_{separator} \tag{89}$$

Where, similarly to Eq. (49) specific cost flow rate at state point 9 is given as:

$$c_9 = -\frac{\dot{Z}_{reinjection}}{\dot{E}_9} \tag{90}$$

Then the flow enters the second turbine, here, similarly to the first one, the analysis is the same but only the state point notations change:

$$\dot{C}_{\dot{W},turb\_2} = \dot{C}_4 - \dot{C}_5 + \dot{Z}_{turbine\_2} \tag{91}$$

And

$$c_5 = c_4 \tag{92}$$

For the condenser, product and fuel cost rates are respectively $\dot{C}_P = \dot{C}_6 - \dot{C}_5$ and $\dot{C}_F = \dot{C}_{21} - \dot{C}_{22}$. Therefore, its thermoeconomic balance equation is given as:

$$\dot{C}_6 - \dot{C}_5 = \dot{C}_{21} - \dot{C}_{22} + \dot{Z}_{condenser} \tag{93}$$

Adapting Eq. (61) to this cycle results in:

$$c_6 = \frac{c_5 \dot{E}_5 + c_{21} \dot{E}_{21} + \dot{Z}_{condenser}}{\dot{E}_6} \tag{94}$$

The last state point of the cycle is then represented by the following equation:

$$\dot{C}_{10} = \dot{C}_6 + \dot{Z}_{DrainPump} \tag{95}$$

Finally, the total exergetic balance is expressed by summing the power outputs and subtracting the parasitic load for the net work output. Then Eq. (64) becomes:

$$\dot{W}_{net} = \dot{W}_{turb\_1} + \dot{W}_{turb\_2} - \dot{W}_{ParasiticLoad} \tag{96}$$

Then the total costs have to be added together according to Eq. (63) in the following equation:

$$\dot{C}_{total} = \dot{C}_{10} + \dot{C}_{\dot{W},turb\_1} + \dot{C}_{\dot{W},turb\_2} + \dot{C}_{other} \tag{97}$$

Finally Eq. (65) also applies here in its original form to determine the unit cost of exergy of the total plant, single flash cycle with additional turbine.

3.1.4 Binary Cycle

The function of the binary cycle has been described in Chapter 1. This design differs from the previous cycles analysed in terms of functioning and consequently also in terms of components. Here the geothermal fluid is only responsible for providing heat to a secondary working fluid. The working fluid is fresh water that, by mean of a series of heat exchangers, gets superheated. The major elements such as the production and reinjection wells together with the turbine and the condensing system remain present in this cycle, but the way to interpret them in this thermoeconomic analysis will differ from the previous cycles. The numbers of the state points for the analysis of this cycle are in reference to Figure 7.

As shown in Figure 7, this cycle is formed by two streams composing two separate loops (cooling water is not considered), interacting together only by heat exchange. Therefore, the thermoeconomic analysis has to be held in a different way than the previous cycles. Here follows the explanation:

The loop of the geothermal fluid carries both exergy and costs, where exergy is distributed to the binary fluid at different points, and the costs can also be accounted to the binary fluid at different points, as long as they all get accounted for. The aim of a thermoeconomic analysis is to give a cost to the product created. Here, the product is electricity, and it is generated by the turbine. The fluid that runs the turbine is the binary fluid, therefore the costs of the cycle have to be transferred to this fluid, following the direction of the exergy flow. Nevertheless, the binary fluid is a closed loop. As it is noticeable from the previous analyses of this work and the review of Chapter 2, a stream of exergy always carries a cost, unless it is released to the environment without being processed. In order to apply its thermoeconomic balance, one needs to set a starting point for accounting for the costs. Otherwise, because every cost needs to be calculated according the previous cost, for a closed loop, costs will always depend on each other and would not be defined in the absolute.

According to the other cycles analysed, state *a* of the binary cycle should carry the previous costs, this would mean it carries the costs of the condensing system (condenser + cooling tower) and the costs of stream at state *f*. But, stream at state *a* gets processed through the heat exchangers (state points *b, c,* and *d*) and reaches state point *e* with both higher exergy and higher cost rate as it now carries the costs of all the components it passes through. Once in the turbine, it generates electricity and therefore the cost of unit power can be defined, but the thermoeconomic balance of the turbine, from Bejan et al. (1996) states that there should be an auxiliary relation to cost the turbine, that is, in this case, $c_e = c_f$. Because c_e is composed by the sum of streams coming from stream at state *a*, and c_a also accounts for the cost of stream at state *f*, the relation $c_e = c_f$ cannot be verified because c_f depends on c_a, but it also defines c_a. Then, another relation to "break" the loop must be defined. This relation is given as:

$$c_f = 0 \tag{98}$$

By setting this auxiliary relation, the end point of the thermoeconomic balance is defined, which is after the turbine, it is state point f. Therefore, the starting point of this analysis can be set at state point a.

First, stream at state *a* will be studied. Here stream *a* is the exit of the condenser, the cost rates of product and fuel of the condenser are $\dot{C}_P = \dot{C}_a - \dot{C}_f$ and $\dot{C}_F = \dot{C}_{21} - \dot{C}_{22}$. Hence Eq. (60) becomes:

$$\dot{C}_a - \dot{C}_f = \dot{C}_{21} - \dot{C}_{22} + \dot{Z}_{condenser} \tag{99}$$

Combining Eq. (61) with Eq. (98) the unit cost of stream at state *a* is expressed by:

$$c_a = \frac{c_{21}\dot{E}_{21} + \dot{Z}_{condenser}}{\dot{E}_a} \tag{100}$$

Then the cost rate of stream *a* is:

$$\dot{C}_a = c_a \dot{E}_a \tag{101}$$

$\dot{C}_a$ now carries the costs of the condenser and the cooling system. After state point *a*, the stream is pumped and brought back to a higher pressure through a pump, with only one inlet and one outlet. Therefore, the thermoeconomic balance at this point is, similar to Eq. (62) given by:

$$\dot{C}_b = \dot{C}_a + \dot{Z}_{PumpBinary} \tag{102}$$

Where $\dot{Z}_{PumpBinary}$ is estimated like the other pumps in the previous cycles.
By definition, the unit cost of exergy at state b is:

$$c_b = \frac{\dot{C}_b}{\dot{E}_b} \tag{103}$$

After state point *b,* the binary fluid enters the first heat exchanger, the preheater. Here, another set of auxiliary relations is required for a complete analysis. The geothermal fluid is a separate stream, flowing in the opposite direction as the binary fluid. Therefore, components placed downstream of the geothermal fluid stream are actually upstream in the binary fluid stream. Hence, in order to obtain the cost rates upstream in the binary fluid, the cost rates downstream of the geofluid have to be defined.
The well is defined like in every previous cycle by Eq. (42); and Eq. (43) is reminded here as $c_1 = \frac{\dot{Z}_{well}}{\dot{E}_1}$. Since the choice of giving all the costs to the binary fluid was made, the geofluid does not get any added cost when going through the heat exchangers. Hence, the following relations can be made:

$$c_2 = c_1 \tag{104}$$

And

$$c_3 = c_2 \tag{105}$$

Finally, stream at state 4 also needs to be cost-evaluated. Eq. (18) can be applied to stream at state 4 as this is the case of a stream being reinjected after passing through heat exchangers. Therefore:

$$c_4 = -\frac{\dot{Z}_{well}}{\dot{E}_4} \tag{106}$$

Now that the geofluid stream has been defined in terms of unit cost of exergy, the costing of the binary fluid can be evaluated. So, after state *b,* the binary fluid enters the first heat exchanger, the preheater (PH). Here the cost rates of product and fuel of the preheater are respectively $\dot{C}_P = \dot{C}_c - \dot{C}_b$ and $\dot{C}_F = \dot{C}_3 - \dot{C}_4$.
Therefore, the thermoeconomic balance of this component is:

$$\dot{C}_c - \dot{C}_b = \dot{C}_3 - \dot{C}_4 + \dot{Z}_{PH} \tag{107}$$

And the cost per unit of exergy of state *c* is expressed as:

$$c_c = \frac{c_b\dot{E}_b + c_3\dot{E}_3 - c_4\dot{E}_4 + \dot{Z}_{PH}}{\dot{E}_c} \tag{108}$$

It is noticeable that stream at state *c* carries the costs of the reinjection well, together with everything coming prior to state *b*. It also accounts for the investment cost of the preheater, $\dot{Z}_{PH}$, calculated according to Eq. (19) then Eq. (27) after being sized according to Eq. (39). The only exception is that for the preheater, φ takes value φ = 1.10 as this component will have the tube side exposed to the chloride-induced corrosion.

Next, the working fluid enters the evaporator (EV), a second heat exchanger whose purpose is to heat the fluid up to evaporation. The cost rate of product and fuel are respectively $\dot{C}_P = \dot{C}_d - \dot{C}_c$ and $\dot{C}_F = \dot{C}_2 - \dot{C}_3$, therefore, its exergoeconomic balance is:

$$\dot{C}_d - \dot{C}_c = \dot{C}_2 - \dot{C}_3 + \dot{Z}_{EV} \tag{109}$$

And for the unit cost of exergy at this point, one can write:

$$c_d = \frac{c_c\dot{E}_c + c_2(\dot{E}_2 - \dot{E}_3) + \dot{Z}_{EV}}{\dot{E}_d} \tag{110}$$

Similarly to the case of the preheater, the investment rate of the evaporator, $\dot{Z}_{EV}$, is estimated, including the higher value of φ, φ=1.10.

The binary fluid now enters the super heater (SH), another heat exchanger, which causes the binary fluid to reach superheated condition. The thermoeconomic balance of this component follows exactly like that of the previous two heat exchangers which is then represented by the following equations:

$$\dot{C}_e - \dot{C}_d = \dot{C}_1 - \dot{C}_2 + \dot{Z}_{SH} \tag{111}$$

And

$$c_e = \frac{c_d \dot{E}_d + c_1(\dot{E}_1 - \dot{E}_2) + \dot{Z}_{SH}}{\dot{E}_e} \quad (112)$$

As previously, $\dot{Z}_{SH}$ is defined by defining the size of the super heater with Eq. (39) and its cost rate is defined by Eq. (19) then Eq. (27).

Finally, stream at state *e* enters the turbine to produce work. Eq. (51) can be applied here and the thermoeconomic balance of the turbine are given as:

$$\dot{C}_{\dot{W},turb} = \dot{C}_e - \dot{C}_f + \dot{Z}_{turbine} \quad (113)$$

And

$$c_{\dot{W},turb} = \frac{\dot{C}_{\dot{W},turb}}{\dot{W}_{turb}}$$

Now, the positive point about the proceedings of this choice of thermoeconomic analysis is that $\dot{C}_{\dot{W},turb}$ carries all the costs of the components shown in the analysis, for both the binary and the geothermal fluids. Therefore, the only costs to be added are the "other" costs, as considered already in the previous cycles.
Then, Eq. (63) can be written as:

$$\dot{C}_{total} = \dot{C}_{\dot{W},turb} + \dot{C}_{other} \quad (114)$$

Finally, by using Eq. (64), Eq. (65) can be reported here:

$$c_{\dot{W},net} = \frac{\dot{C}_{total}}{\dot{W}_{net}}$$

3.2 Application criteria

The thermoeconomic analysis of the cycles is done in various sets of configurations, for every cycle, in order to be able to find an optimum solution. The first criteria used to reiterate the analysis of the cycles was to study the cycle performance at various pressures and mass flow rates available at the wellhead conditions. The curve measurements of mass flow rates and pressures were presented in the work of Hjartarson et al. (2014). Since the values were only measured in a few points, the curve is a modelled curve from the measured points. Figure 9 below is a curve from that work, on which calculations of this work are based. It is noticeable that with the increase of the wellhead pressure the mass flow rate of the geothermal fluid decreases.

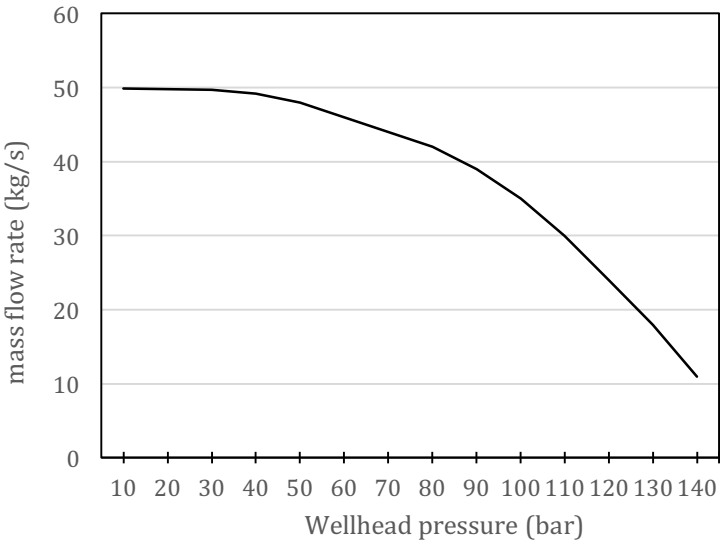

Figure 9: Productivity curve of IDDP-1

Figure 10 below shows the enthalpy of the well IDDP-1, during the last measurements available, in 2011 and 2012. The majority of evaluations from measurements, even in previous dates, showed little variation in the enthalpy as it was mainly between 3100 and 3200 kJ/kg for various wellhead pressures and mass flow rates measured (Einarsson et al., 2015).

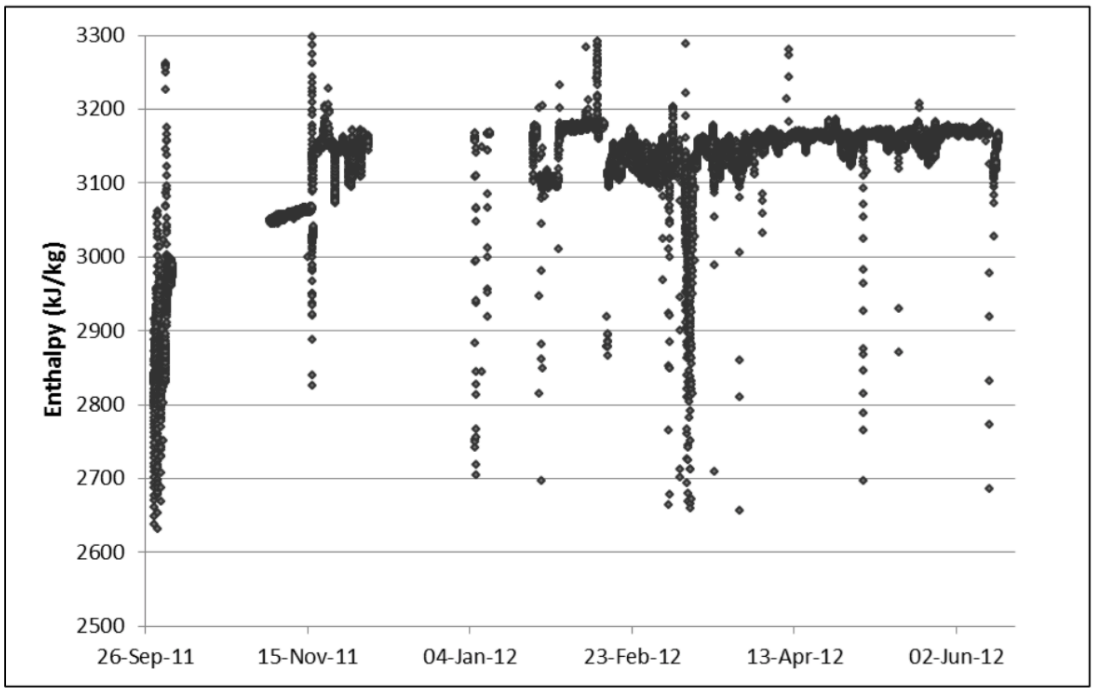

Figure 10: Enthalpy evaluated from temperature and pressure measurements (source: (Einarsson et al., 2015)

Then, the cycles were analysed by changing some parameters in order to see what effects it has on output as explained in section 2.2.4. These changes were made in the perspective of a thermoeconomic optimization, next chapter shows the results of all the thermoeconomic analyses done for the cycles.

4 Analysis and results

4.1 Thermoeconomic analysis of cycles

The thermoeconomic analyses are presented for every cycle over the entire wellhead pressure range available from the productivity curve in Figure 9. First the exergetic analysis shows some important factors taken into consideration in every cycle. Then the economic part is added to complete the analysis. In order to be able to proceed later to alternative scenarios, for practical reasons, a first analysis of the optimal wellhead pressure and mass flow rate was made once the results about optimal wellhead pressures were obtained. A comparison of the four cycles is made prior to the scenario analysis.

A few parameters have been set as a base case to run every cycle calculation. First, the life time of the plant was assumed to be 25 years and the interest rate of the project was set to 4% (Organisation for Economic Co-operation and Development, 2015). Then, the typical operation and maintenance cost was chosen to be 5% of initial investment for every component unless otherwise specified. Finally, the pumps efficiencies were set at 0.75. All costs shown are in 2014 USD.

Similarly to the previous chapter, the analysis of the cycles will be done individually for each cycle, more in detail for the first, single flash wet scrubbing, and then the relevant differences are added from cycle to cycle. The state numbers correspond to the already presented diagrams of every cycle.

Furthermore, all the exergy flow rates of each cycle can be found in Appendix A.

4.1.1 Single flash with wet scrubbing

The single flash with wet scrubbing is the only cycle that does not utilize the thermal heat from the superheated steam to generate power. Figure 11 shows the exergy rates of states 1 to 4. It is noticeable that there is a drop of exergy rate when the wet scrubbing occurs, between state 1 and state 2; this represents the exergy destroyed by cooling the stream down. The destruction reaches its lowest percentage rate, of 2.5%, at wellhead pressure of 40bar, point at which $\dot{E}_3$ is at its highest. At this point, the exergy lost in the separator is 0.5% of the entering stream. This loss is little because only low exergy saturated liquid is taken away from the stream. The exergy stream of state 4, E4 ($\dot{E}_4$), is the exergy remaining after generating electricity through the turbine. The exergy rate of state 4 also represents a (inevitable) loss for the cycle as it is exergy that did not get transferred from the stream to the generator. In the case of $\dot{E}_4$, another interesting factor to put attention on, is the gap between the curves E3 and E4. The bigger this gap, the greater the exergy transferred to the generator which is maximum at a pressure of 40bar. Hence, according to these results, a preliminary conjecture can be made, it appears that the best working condition is the one using wellhead pressure of 40bar.

The remaining exergy flows, those concerning, among other components, the condenser, the cooling tower and the reinjection, are not being discussed in this part, but for more information, their respective values can be found in Appendix A.

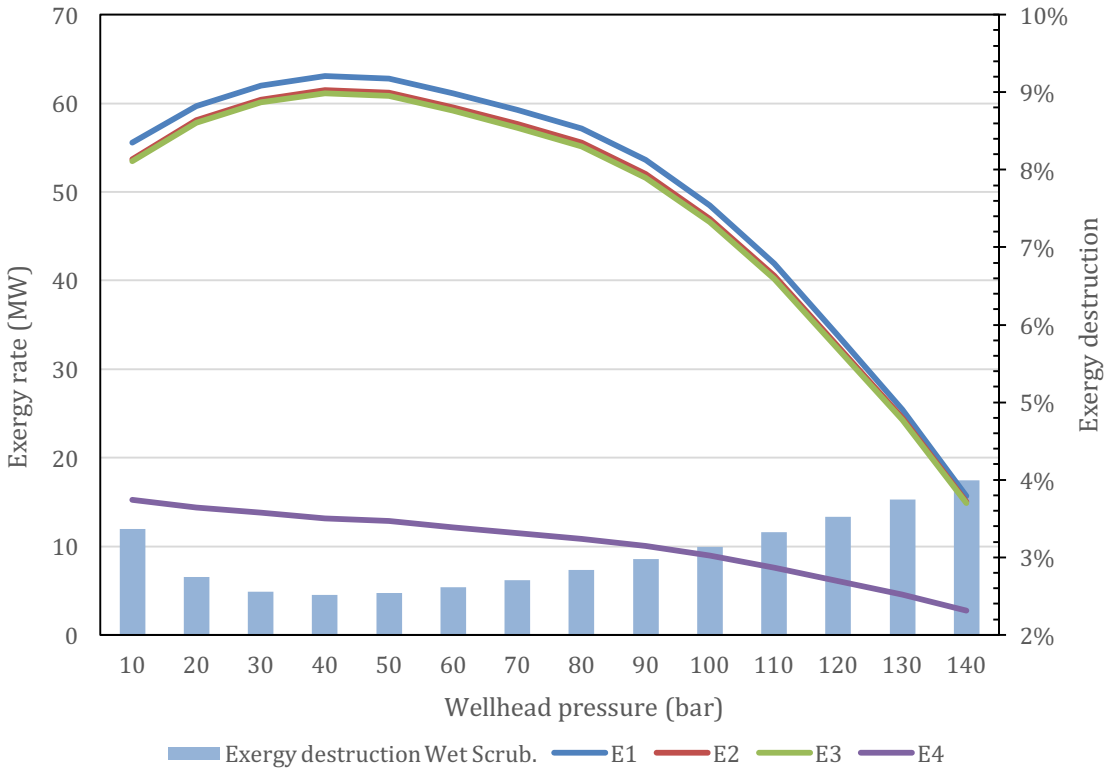

Figure 11: Exergy rates in the single flash wet scrubbing cycle

Figure 12 shows that the net work output follows a pattern almost identical to that of $\dot{E}_3$, increasing until a maximum peak value and then going down as the pressure increases. Even though the wellhead pressure constantly increases and the mass flow rate decreases, as shown in Figure 9, the maximum net work output occurs at a specific combination, that is for steam at pressure of 40bar flowing at 49.2kg/s. This means that for a similar mass flow rate, more work can be produced at higher pressure, until the mass flow rate decreases too much for the pressure to compensate. On Figure 12, the cost flow rate of the entire plant is shown as a function of well head pressure, and one can notice that, not surprisingly, it follows the same pattern as the net work output, but with lesser steepness. This minor steepness is due to the lower sensitivity of the total cost rate to the net work output. Number of factors affect the costs other than the work output and the fact that the work output decreases faster than the total cost rate causes the unit cost of exergy to follow an inverse path compared to the cost flow rate. As can be seen in Figure 13, the unit cost of exergy decreases to a minimum value, reached at wellhead pressure of 40bar to then go up together with the increasing wellhead pressure.

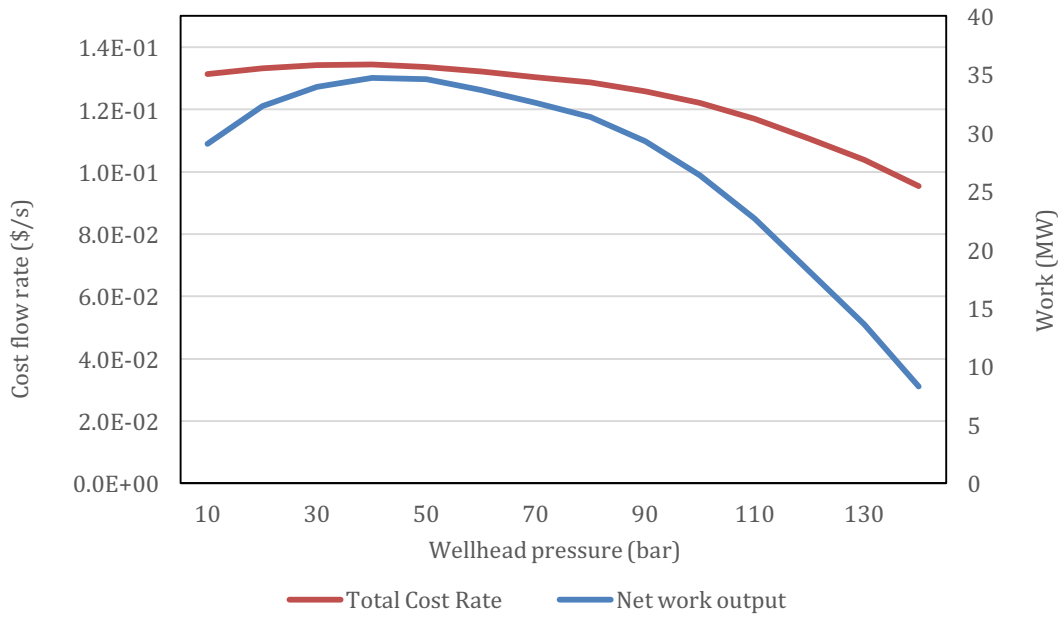

Figure 12: Total cost flow rate for single flash cycle

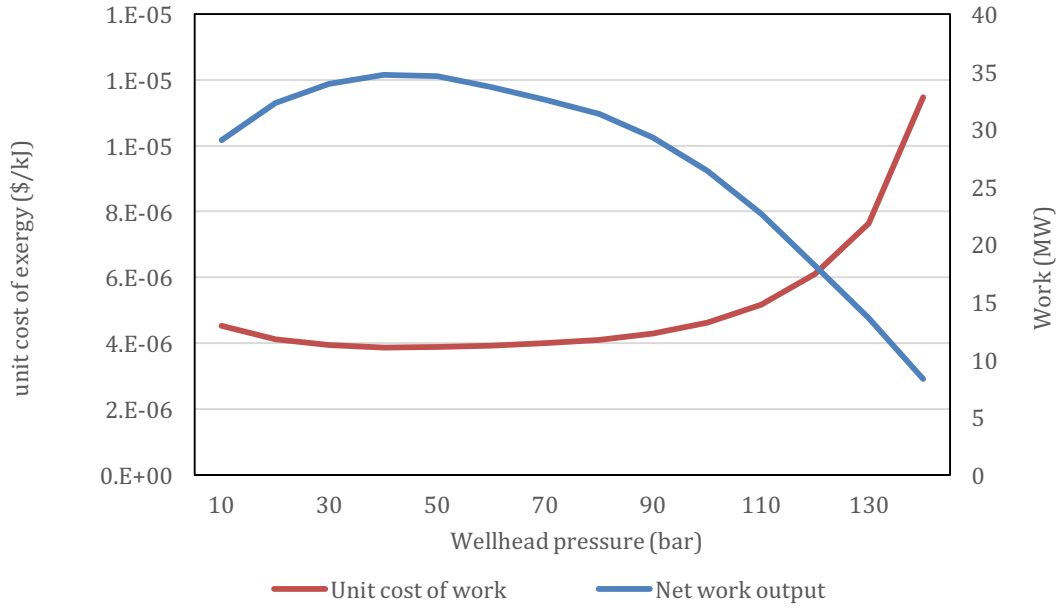

Figure 13: Unit cost of work for single flash cycle

For single flash wet scrubbing, the maximum net work output obtained is 34.7MW and it is produced at a unit cost of 3.87×10^{-6} \$/kJ. With the initial conditions stated before, there is no higher net work output possible as well as there is no lower unit cost of exergy reachable. Therefore, it appears that the optimum condition to run this cycle confirms the previous conjecture and corresponds to the highest net work produced at the lowest unit cost of exergy. This condition was only verified for wellhead pressure of 40bar.

Figure 14, shows the detail of the cost rates of the major components of the cycle. It is noticeable that the well, C1 (equivalent of $\dot{C}_1$), represents a third of the costs for the lower pressure configurations. Since its value does not depend on the power output, it is constant, therefore its portion increases with pressure as the other costs decrease. The cost of the well is not depending on the wellhead pressure. The cost flow rate of the

chemicals for the wet scrubbing, C7 ($\dot{C}_7$) , also decreases with the increase of the wellhead pressure, therefore with the decreasing mass flow rate. Its slice shows that even though it is a cost that occurs constantly throughout the entire production time, it is a very low contribution to the total costs. The intermediary costs adding to the previous, prior to the turbine are represented by C3-C2. Even though the detailed costs cannot be shown for these components, these intermediary costs are plotted nevertheless to show that they are of a similar order of magnitude than $\dot{C}_7$; these intermediary costs follow a slowly decreasing pattern mainly because of the decreasing wellhead mass flow. Then, the investment rate of the turbine, Zturbine ($\dot{Z}_{turb}$), follows the general pattern of the work it produces, as the work is a defining variable of its value. $\dot{Z}_{turb}$ reaches its maximum at wellhead pressure of 40bar; but because the cost of the turbine also depends on other factors, as per equation (20), the pattern is of a much lower steepness than the one of the work.

C9 ($\dot{C}_9$) represents all the costs after the turbine. Here it is important to notice that even though the work has been produced already, this cost is of significant magnitude. Since the costs of both the cooling tower and the condenser vary directly with the mass flow rate, and because these components are responsible for the major part of the costs of $\dot{C}_9$, it appears obvious that the value of this cost rate decreases with the decreasing of the wellhead mass flow rate.

Finally, C other ($\dot{C}_{other}$), as explained in Chapter 3, is the remaining part of the costs considered but not shown explicitly. The main reason for its slowly decreasing pattern is that it includes the costs of the generator, depending on the work output, and of the spare parts, depending on the capital cost of both the generator and the turbine, that decrease with the increase of pressure.

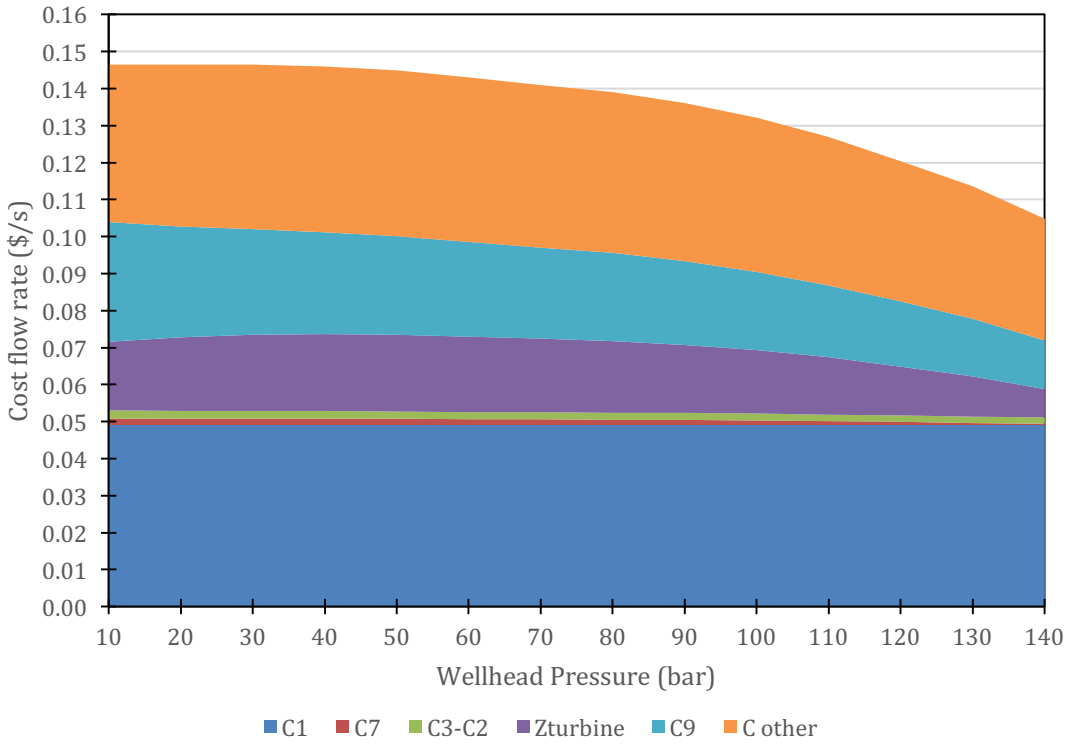

Figure 14: Cost flow rates of components of the single flash cycle with wet scrubbing

Finally, for more clarity and to facilitate the interpretation, the cost per unit of exergy can be expressed, as per Table 1, in terms of US Dollars per kWh ($/kWh).

Table 1: Cost per unit of kWh produced by single flash cycle

Pressure (bar)	10	20	30	40	50	60	70
Unit cost ($/kWh)	0.01629	0.01486	0.01423	0.01392	0.01396	0.01413	0.01442

Pressure (bar)	80	90	100	110	120	130	140
Unit cost ($/kWh)	0.01478	0.01548	0.01665	0.01858	0.02194	0.02747	0.04128

4.1.2 Wet scrubbing and heat recuperator

The addition of the recuperation system to single flash wet scrubbing has significant effects on the overall cycle performance. Figure 15 shows the exergy rates of streams at states 1, 5 and 6. The first thing that should be noted is that the exergy destroyed between the exit of the well and the entrance of the turbine is much smaller compared to the previous cycle with no reheat, both in absolute and percentage value. This is due to the heat recuperator that by recovering heat actually recovers exergy. Here, the pattern of the exergy destruction, between $\dot{E}_1$ and $\dot{E}_5$, expressed in percentage of $\dot{E}_1$, increases as the wellhead mass flow rate decreases. In this cycle the highest value of $\dot{E}_5$ is reached for wellhead pressure of 40bar, but the biggest gap between $\dot{E}_5$ and $\dot{E}_6$ is reached for wellhead pressure of 50bar. Nevertheless, this gap at 50bar is only 0.04% larger than at 40bar. Similarly to the simple wet scrubbing cycle, the optimum condition for running this cycle from an exergetic point of view seems to be between 40 and 50bar of wellhead pressure. Because the exergy destruction rate is smaller for wellhead pressure of 40bar and the exergy rate entering the turbine is greater, the condition of 40bar could be preferred over 50bar.

The effects of the heat recuperation can be clearly observed by comparing the exergy at the inlet of the heat exchanger $\dot{E}_4$ and at the outlet $\dot{E}_5$; while the exergy lost in the form of liquid separated is practically null as can be observed from the curve of $\dot{E}_{10}$.

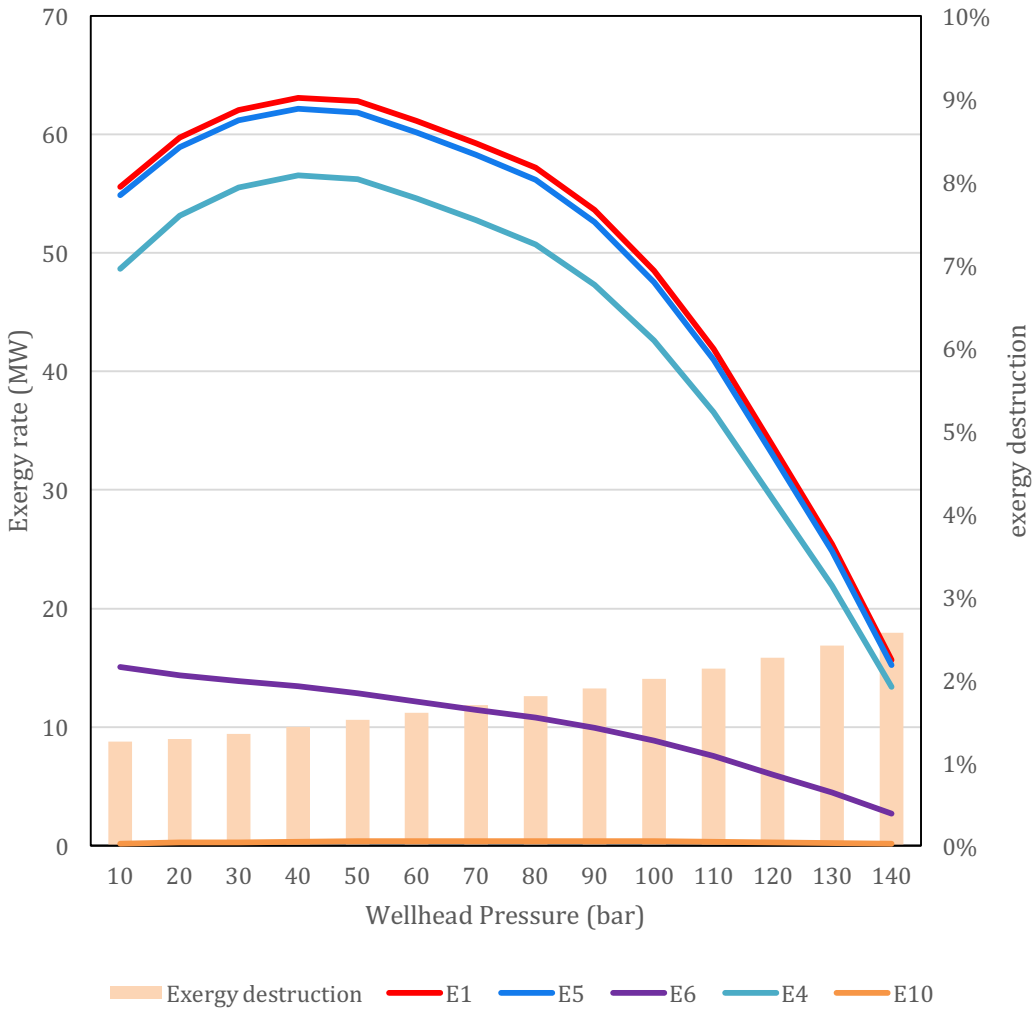

Figure 15: Exergy rates in the heat recovery cycle

A thermoeconomic summary of the whole cycle is illustrated in Figure 16. Here the curves are very similar again to the previous cycle, and again, the best option is for wellhead pressure of 40bar, as the net work output reaches its peak at this pressure and totals 39.15MW. At the same wellhead pressure also corresponds the lowest cost per unit of exergy reached, and its value is 3.47×10^{-6} \$/kJ. Hence, because the unit cost of exergy is the lowest, and the net work output is the highest, the condition of wellhead pressure 40bar is the optimal condition for this cycle.

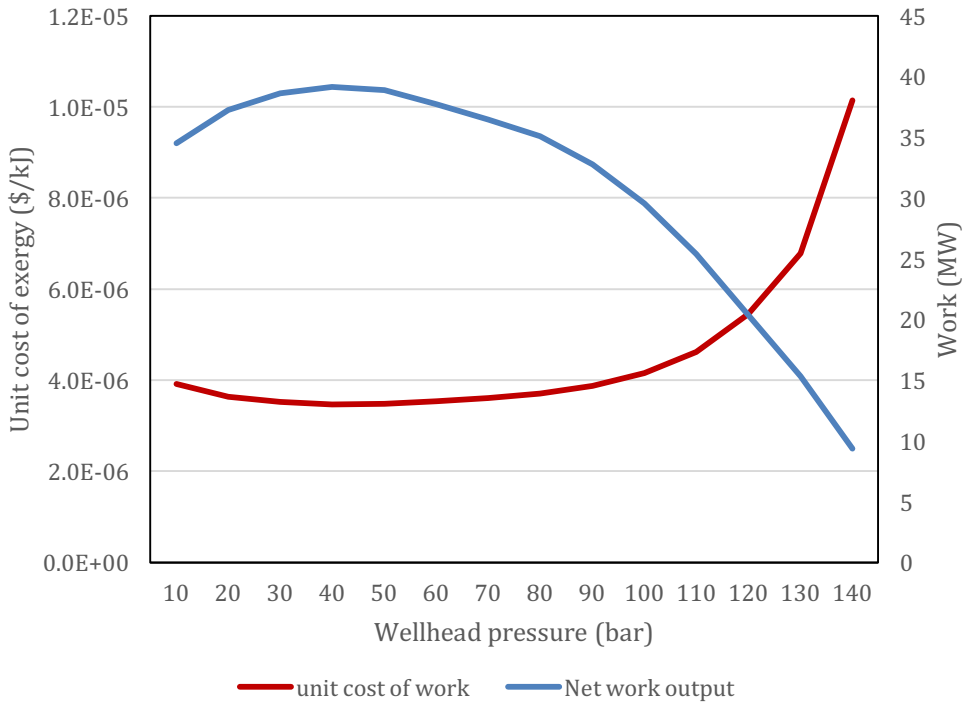

Figure 16: Unit cost of work of the heat recovery cycle

Then, the cost flow rate of the heat recuperating cycle is almost identical to the simple wet scrubbing with the only addition of the heat recuperator's cost. Comparing the additional cost to the entire plant cost would not make sense as the total plant cost is of order of magnitude 10^3 times the cost of heat exchanger. For this, only the detail of the heat exchanger's cost will be analysed and the unit cost of exergy entering the turbine will be compared to its corresponding value in the simple wet scrubbing cycle. As shown in Figure 17 the investment cost rate of the heat exchanger ZHX ($\dot{Z}_{HX}$) follows a decreasing pattern as the wellhead pressure increases. Even though the heat rate of the condenser decreases as the mass flow decreases, the LMTD increases faster, therefore reducing the heat exchange area and therefore its cost rate. The cost per unit of exergy entering the turbine of both the single flash cycle (SF) and the heat recovery cycle (HR) appear to be almost identical, with HR:c5 slightly lower than its equivalent in SF (SF:c3). Even though costs have been added to stream 5 in the HR, the unit cost of its exergy is slightly lower than the entering stream of the SF because the exergy rate of this same stream is higher for the HR. The increase in exergy rate brought by the heat exchanger is able to compensate its (low) investment cost rate.

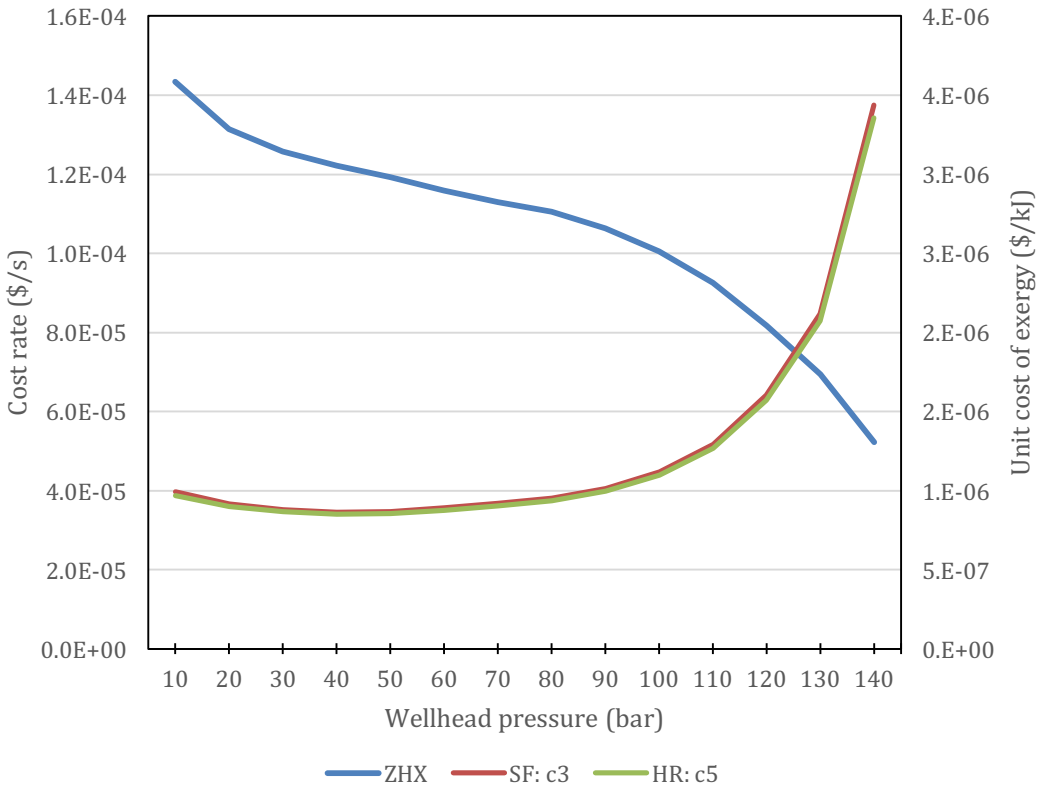

Figure 17: Heat exchanger cost rate and comparison of unit cost of exergy entering the turbine between SF and HR

This cycle performs better than the SF, therefore its cost per kWh will be lower, Table 2 illustrates the cost of the electricity produced by this configuration of power cycle.

Table 2: Cost per unit of kWh produced by heat recovery cycle

Pressure (bar)	10	20	30	40	50	60	70
Unit cost ($/kWh)	0.01408	0.01310	0.01268	0.01250	0.01251	0.01273	0.01300

Pressure (bar)	80	90	100	110	120	130	140
Unit cost ($/kWh)	0.01332	0.01394	0.01496	0.01665	0.01960	0.02444	0.03650

4.1.3 Wet scrubbing and additional turbine

The analysis of the cycle with wet scrubbing and additional turbine was done similarly to the cycle with heat recovery. This cycle is identical to the SF with the addition of a turbine right at the outlet of the well. Consequently, it produces work in two distinct times that will bring costs in these two points and exergy will vary accordingly. Stream at state 1 is directly entering the turbine to produce work without phase change of the fluid that leaves the stream exiting the turbine with a significant content of exergy ($\dot{E}_2$). Between states 2 and 4 the wet scrubbing occurs and destroys part of the exergy. As visible in Figure 18, the exergy destroyed between $\dot{E}_2$ and $\dot{E}_4$ is always contained in a range between 1.0% and 1.5% of $\dot{E}_2$; it is so far the most exergy-efficient cycle. As the curves E2 and E4 have less than 1.5% difference, when one considers the total exergy that is transferred to the generators by looking at the difference between the exergy

rates of $\dot{E}_1$ and $\dot{E}_5$, the gap between E2 and E4 seems of little interest. Therefore, the patterns of $\dot{E}_1$ and $\dot{E}_5$ resemble a lot to the previous cycles' equivalents and the largest result for $(\dot{E}_1 - \dot{E}_2) + (\dot{E}_4 - \dot{E}_5)$ is at wellhead pressure of 50bar, only 0.6% higher than the same gap at 40bar generating the maximum value for $\dot{E}_1$. Based on this graph, the best performances seem to be reached between 40 and 50 bar.

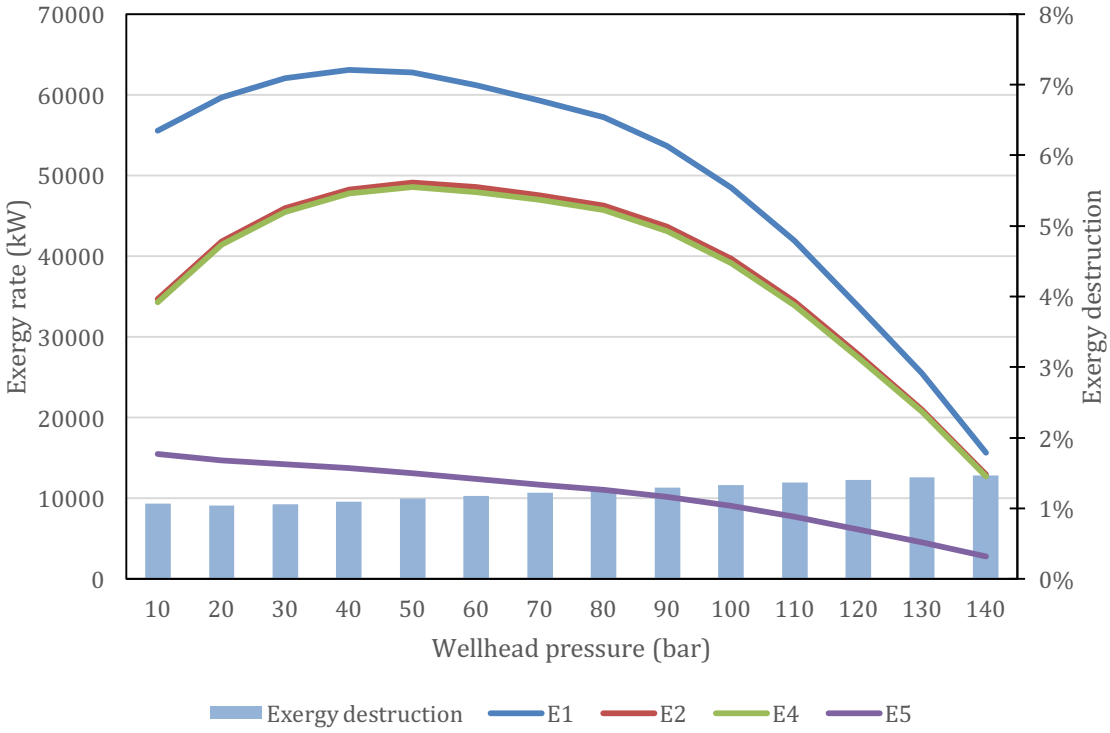

Figure 18: Exergy rates in the additional turbine cycle

When looking at the overall work produced by the cycle and the unit cost of product exergy, the optimal condition should be found. Once again, the patterns of the net work output and of the unit cost of work follow the same in this cycle too, as shown in Figure 19. The only difference is that in this case the lowest unit cost of exergy occurs at pressure 50bar while the highest net work production occurs at pressure 40bar. Both the unit cost of exergy and the net work output are 0.3% higher for pressure 40bar than for pressure 50bar. If a choice were to be made, on the economic point of view one should go for the cheapest in terms of cost per unit, therefore the best solution appears to be for wellhead pressure 50bar.

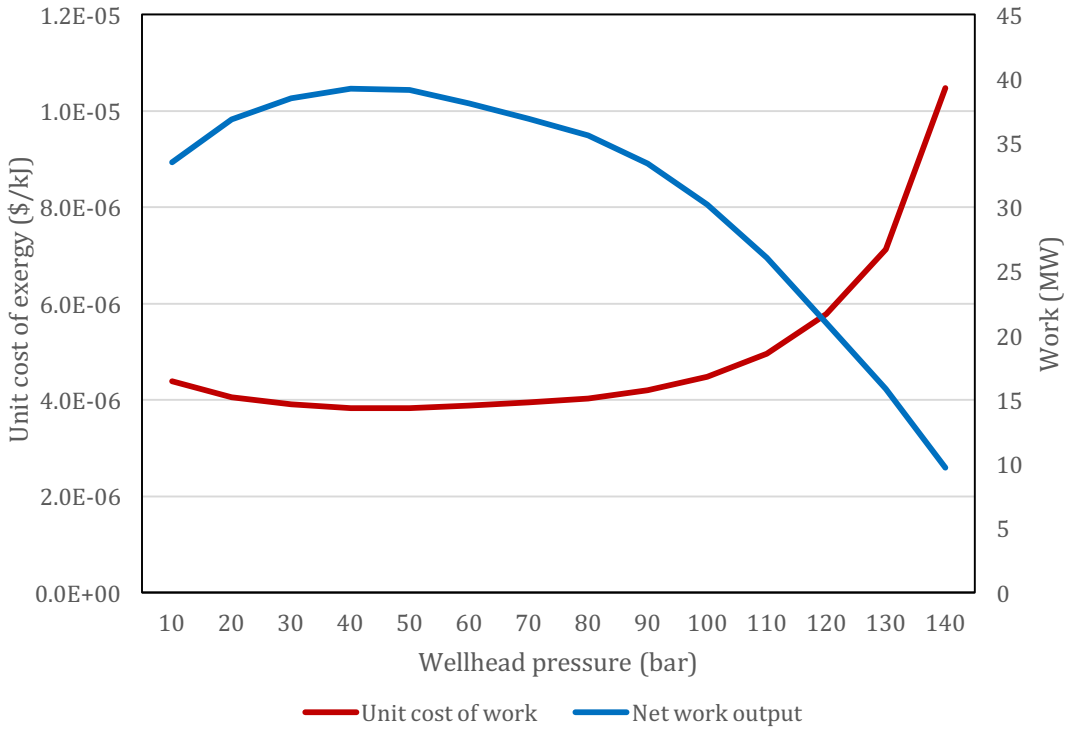

Figure 19: Unit cost of work of the additional turbine cycle

In the case of the cycle with additional turbine, costs added have to be estimated according to the variations compared to the other cycles. The cycle has two turbines but each one is of smaller size than turbines for the cycles explained before, therefore less expensive individually. Figure 20 shows the comparison between one turbine of the HR and the sum of the two turbines in the AT. The choice of the HR turbine was made as a comparison because it interacts with superheated steam while the SF turbine does not as it only deals with saturated vapour. The investment rate of first turbine of the AT is represented by the curve Zturbine1, in which only a dry expansion occurs and the cost rate follows a decreasing pattern from lower to higher wellhead pressure. The second turbine's curve, Zturbine2 has the same pattern as the turbine of the HR. The area in green represents the sum of the cost rates of the two turbines of the AT. It shows that for a similar total work output of the turbines of both cycles, the cost rate of the turbines of AT is considerably higher than the cost rate of the only turbine of HR.

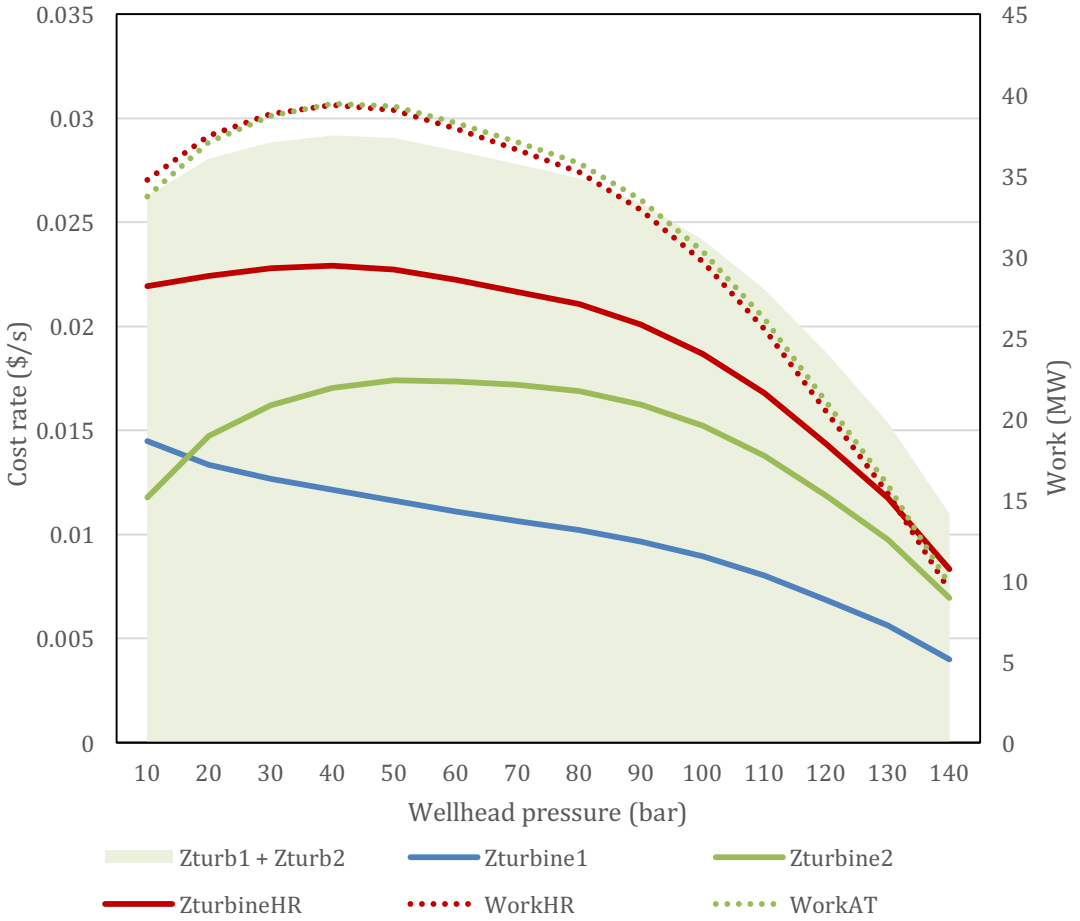

Figure 20: Turbines investment rates comparison

To have a more concrete idea of the unit cost of energy production, the results are compared here in Table 3.

Table 3: Cost per unit of kWh produced by additional turbine cycle

Pressure (bar)	10	20	30	40	50	60	70
Unit cost ($/kWh)	0.01580	0.01461	0.01407	0.01381	0.01377	0.01396	0.01421

Pressure (bar)	80	90	100	110	120	130	140
Unit cost ($/kWh)	0.01451	0.01512	0.01614	0.01784	0.02081	0.02566	0.03769

4.1.4 Binary cycle

The last cycle of the series is the binary cycle. This cycle does not have any wet scrubbing; therefore, no exergy destruction occurs by cooling the stream. Here, an interesting comparison is between the two exergy rates of state 1 and state e, one being the well exit and the other the turbine inlet. The exergy rates are plotted in the graph shown in Figure 21. This cycle, even though it does not destroy exergy through wet scrubbing, results in a cycle with the highest exergy destruction rate. At the maximum

exergy flow rate from the well, $\dot{E}_1$, occurring at pressure 40bar, 4.17% of this is destroyed in the cycle before entering the turbine as $\dot{E}_e$. The exergy destruction, nevertheless, decreases significantly as the wellhead pressure increases in the lower pressures, enough to make $\dot{E}_e$, at pressure 50bar, greater by 0.17% than at 40bar while $\dot{E}_1$ decreased by 0.46% over this same pressure range. Hence, the highest inlet pressure of the turbine $\dot{E}_e$ is obtained for wellhead pressure of 50bar with an exergy destruction from $\dot{E}_1$ of 3.57%.

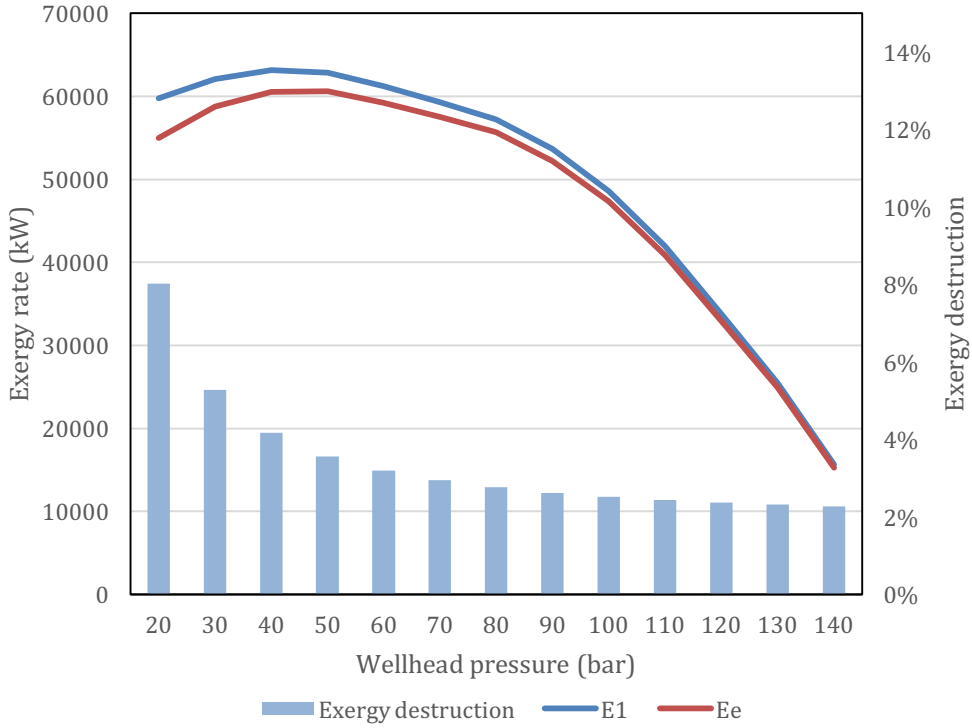

Figure 21: Exergy rates of binary cycle

As for the previous cycles analyses, the net work output is compared to its total unit cost. This comparison is shown in Figure 22, where the economic analysis confirms the exergetic one, as both the highest net work output and the lowest cost per unit of exergy are obtained for wellhead pressure of 50bar. This optimal condition is verified with a net work output of 38.32MW at a cost of 4.73×10^{-6} \$/kJ.

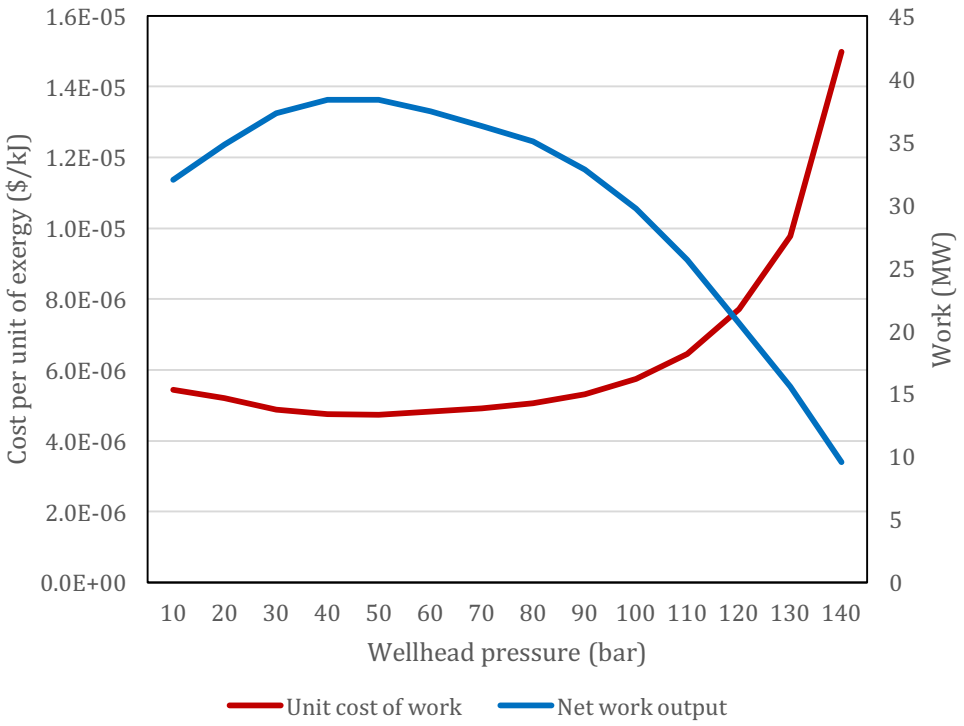

Figure 22: Unit cost of work of the binary cycle

The binary cycle consists of a series of heat exchangers (the design could also only feature a major single one) that bring new costs. Even though this cycle does not have to account for any cost relative to wet scrubbing and separation, the costs, illustrated in Figure 23 are still comparable with the previous cycles. The stacked areas represent the three heat exchangers investment cost rates, to be read on the left axis. The curves represent the total cost rates of the two cycles appearing, binary cycle and single flash and to be read on the right axis. The total cost rate difference between the two cycles starts with the BC cost rate being 36% higher than the total cost rate of the SF at lowest pressure and reaches a maximum of 50% higher than the total cost rate of the SF. The comparison is made with the SF as the purpose is to show the impact of adding the heat exchangers and removing the separator and wet scrubbing, affecting the total cost rate.

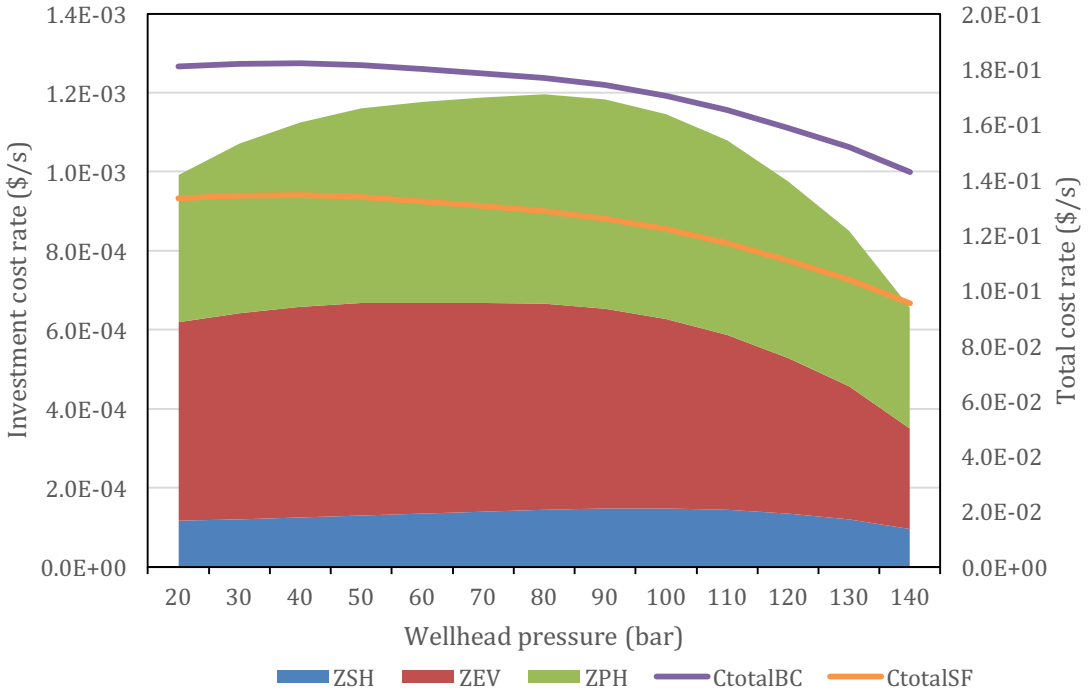

Figure 23: Investment rates of heat exchangers

To conclude the individual cycle analyses, the unit cost per kWh of electricity produced is given in Table 4 below.

Table 4: Cost per unit of kWh produced by binary cycle

Pressure (bar)	10	20	30	40	50	60	70
Unit cost ($/kWh)	0.01958	0.01874	0.01756	0.01710	0.01705	0.01733	0.01772

Pressure (bar)	80	90	100	110	120	130	140
Unit cost ($/kWh)	0.01819	0.01911	0.02066	0.02323	0.02775	0.03520	0.05393

4.1.5 Cycles comparison

The cycles were analysed in terms of thermoeconomic aspect and the net work output of every cycle can be viewed in Figure 24, together with the respective unit cost of exergy. Here, one can easily note that the single flash cycle configuration with only wet scrubbing and no means of utilizing superheated steam is the lowest power generator. A clear gap separates its work output from the work output of the other three cycles. Of these three cycles utilizing superheated steam, the binary cycle is the one that performs the worst, especially at lower wellhead pressures (under 50bar). The heat recovery cycle is the one performing best in terms of work output in the lower pressure range, up to a wellhead pressure of 50bar, after which it meets the same power output as the binary cycle and the two curves overlap until the highest pressure reaches 140bar. Finally, the cycle with additional turbine gives a slightly lower output than the heat recovery at 10bar but meets it and even overtakes it at pressures higher than 60bar but its curve only stays slightly above both the binary cycle and the heat recuperating cycle. After

wellhead pressure of 50bar, at equal wellhead pressure, the net work output difference between the three cycles is never greater than 700kW.

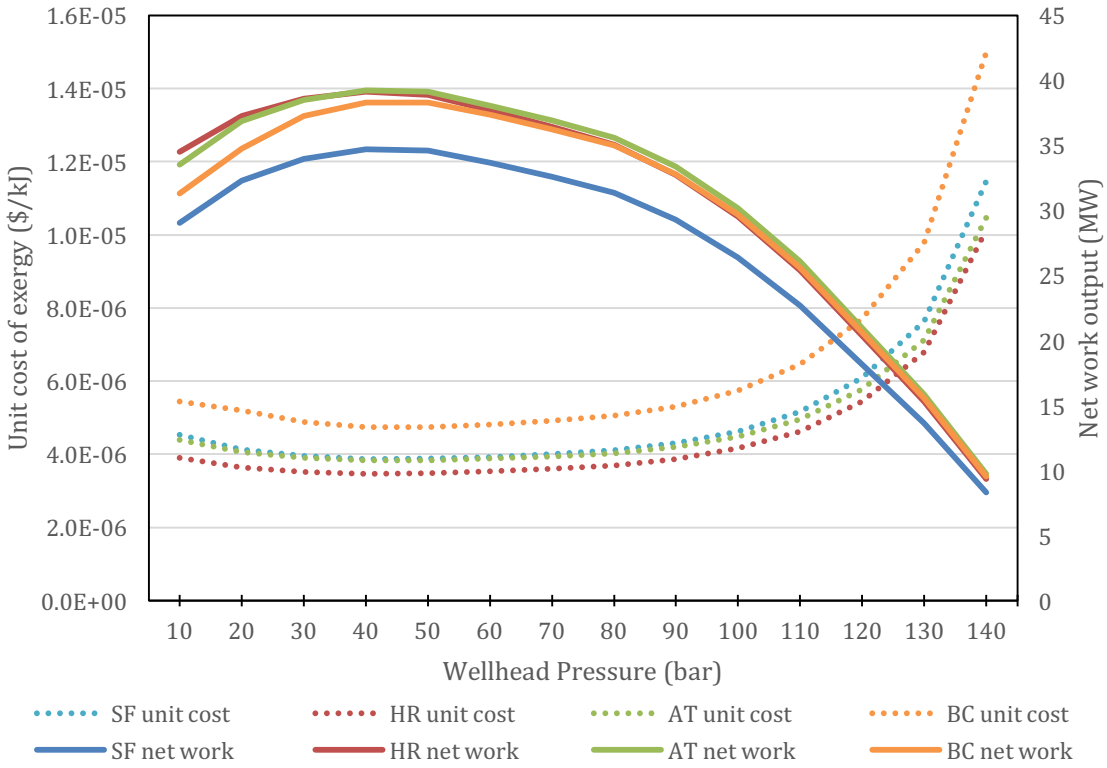

Figure 24: Net work output and unit cost of exergy of studied cycles

The common point between all the cycles plotted in Figure 24 is that the highest net work output for each cycle is obtained at the same wellhead pressure of 40bar. Nevertheless, only the heat recovery cycle and the single flash have their lowest unit cost of exergy at wellhead pressure of 40bar; the two other cycles see their lowest unit cost of exergy at 50bar well output.
As visible on the graph, the cycle with the highest unit cost of exergy is the binary cycle. A net gap separates the binary cycle's curve from both the single flash and additional turbine curves, that practically overlap. The lowest of all is the heat recovery cycle.
Graphically, it is even easier to define the heat recovery cycle as the best option for this well, IDDP-1, as its unit cost of exergy is clearly the lowest and its total net work output is the one reaching the highest value of all and is the highest in low pressure conditions and second highest, by little difference, elsewhere.

The thermoeconomic examination made up to here served a great purpose in defining the best working wellhead pressure for every cycle and the best performing cycle overall. This optimal pressure framing represents the first criteria for the optimization as it narrows the field down a lot by limiting the further analyses to a single pressure value. An optimal point has been found for each cycle, therefore all changes following are applied only to the optimal wellhead pressure case.

4.2 Optimization through scenarios

In order to further analyse the thermoeconomics of the cycles, some scenarios have been imagined and emulated in the following sections. Most of the changes are of economic nature, trying to identify which criterion drives the cost in which direction and to what extent. The following analyses are explained only by comparing the single flash wet scrubbing cycle to the heat recovery cycle, as the changes affect the other cycles in very similar ways. Nevertheless, for more details, all the results are reported in the tables of Appendix B.

4.2.1 Well cost

As mentioned before, IDDP-1 had a drilling cost much higher than a regular well, because of the incidents and the great depth. A scenario has been imagined by assuming that the well would be drilled at a regular cost, with no issues such as encountering magma 3 times, therefore, the well is considered a common production well. IDDP-1 nevertheless, is not a regular well as it is a very deep well, even though the expected depth was not reached, the newly set cost of the well results being 8 Million USD, instead of 20 Million USD. This scenario tries to simulate the situation where the incidents are assumed not to happen. The table below shows the results of changing the cost of the well over the total cycle's significant data. All variables are displayed in their absolute value while the cost flow rate is also shown as a percentage change from the original base case.

Table 5: Effects of a cheaper well

Well cost 8MUSD	$\dot{W}_{net}$	$\dot{C}_{total}$		Cost of electricity
	(kW)	($/s)	(Δ%)	USD/kWh
Single flash	34709	0.10497	-21.9%	0.01089
Heat recuperator	39157	0.10652	-21.6%	0.00979

On Table 5 shown above, it is noticeable that by decreasing the investment cost of the well by 60% it affects the total cost rate, and the cost per unit of decreases by 22%. The net work output does not change as this is only an investment cost change. It can be affirmed that the well cost of IDDP-1 being so high, substantially affects the cost rate of the plant, and should be kept in mind in a broader analysis or for future projects.

4.2.2 Pumps efficiencies variation

The pumps are components that are present in every thermal cycle, they consume work, and their efficiency influences their cost. The efficiency of a pump is measured by comparing its product to its fuel. Greater efficiency grants greater exergy of product at the same work input, or lower input for the same exergy output provided. The cost of a pump grows exponentially as the efficiency increases as visible in Figure 25.

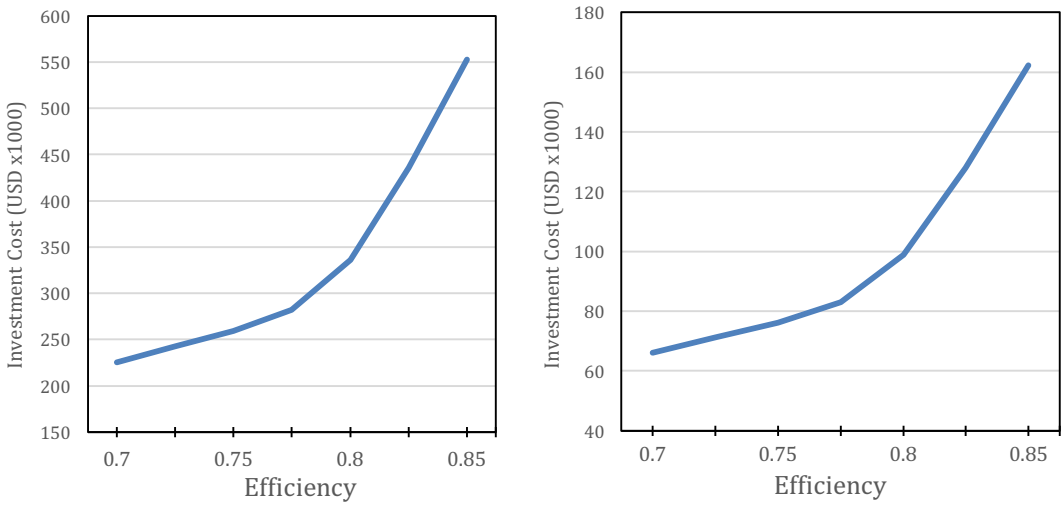

Figure 25: Investment cost of cooling water pump (left) and drain pump (right) according to efficiency

Using the same formula for both pumps' costs, shown in Eq. (22), it appears clear that the cooling water pump is remarkably more expensive than the drain pump, more than 3 times as expensive for the same nominal efficiency. This is due to the fact that the pump investment cost is also a function of the exergy of the output stream, which in case of the cooling water, is much greater than the exergy of the drain water (roughly 5.6 times greater). In this situation, the scenario has been changed to a condition where the pumps were set to a higher efficiency, without looking for exaggeration. Table 6 shown below reports the values for a 10 percentage point increase (from 75% to 85%) in both the pumps used in the cycles. The efficiency change in this case only slightly affects the total cost rate as it has been kept reasonably low, resulting in less than 1% increase in the costs of every cycle. Because the difference is so little, the efficiency of the pump will not be of concern in the following steps within this work.

Table 6: Effects of more efficient pumps

Pumps η=0.85	$\dot{W}_{net}$	$\dot{C}_{total}$		Cost of electricity
	(kW)	($/s)	(Δ%)	USD/kWh
Single flash	34709	0.13533	0.7%	0.01404
Heat recuperator	39159	0.13664	0.5%	0.01256

4.2.3 Price of chemicals' influence

The wet scrubbing technology is a system that relies on the addition of an external agent to the stream, NaOH in this case. The addition happens at a rate directly related to the steam mass flow rate and therefore related to the production of electricity. Even though NaOH is a chemical that is found in abundance on the planet and on the market, nothing guarantees that its cost will stay the same over time and not increase (or why not, decrease). This scenario analyses the possibility of paying for NaOH (or another chemical substance) a cost rate 3 times larger that the cost used in the original case, that is, for NaOH at 1$/kg. Table 7 below illustrates the results obtained.

Table 7: Effects of a higher cost for chemicals

NaOH @ 1$/kg	$\dot{W}_{net}$	$\dot{C}_{total}$		Cost of electricity
	(kW)	($/s)	(Δ%)	USD/kWh
Single flash	34709	0.13800	2.7%	0.01431
Heat recuperator	39158	0.13954	2.7%	0.01283
Binary cycle (not affected)	38314	0.18434	0%	0.01732

It is noticeable that with a 200% increase in NaOH unit cost, the influence is limited to less than 3% higher total cost rate of the plant, even though this is a cost that occurs together with production. The binary cycle is obviously not affected by such a condition, but nevertheless, the effect of the higher price of chemicals yet does not make the binary cycle cheaper than the other cycles.
Also in this case, the effects of the change in price of the chemical NaOH will be considered marginal and not analysed in the next steps.

4.2.4 Life time of plant

When considering a project over a long time-period, its true lifetime is not always strictly defined or known. The lifetime of a project has to be estimated. Components will have different lifetimes, and a project's life can vary because of many reasons. In theory, a geothermal power plant could last for decades, mechanically speaking. Unfortunately, the technology progresses make a power plant obsolete after a much lower number of years. For this study, 25year lifetime was chosen, that is a generally accepted life duration of a geothermal power plant. Nevertheless, to realise how much the lifetime of a project influences its cost rate, the alternative scenario considers a 30year lifetime of plant. This is not an excessive duration for an entire power plant, even though it may be excessive for single components. Anyway, the results of having a lifetime of 30 years are presented in Table 8 below.

Table 8: Effects of a longer lifetime of plant

30 years lifetime	$\dot{W}_{net}$	$\dot{C}_{total}$		Cost of electricity
	(kW)	($/s)	(Δ%)	USD/kWh
Single flash	34709	0.12157	-9.5%	0.01261
Heat recuperator	39158	0.12297	-9.5%	0.01131

Here, the effects of a 5 years longer lifetime (+20%) result in a decrease of almost 10% of the total cost rate and therefore of the unit cost of electricity. As 25year lifetime is generally the minimum lifespan of a geothermal power plant, it does not seem far-fetched to apply 30 years as a condition. The prolonged lifetime will be an important factor in the combined scenarios analyses, as it seems to bring sensitive results.

4.2.5 Interest rate variation

The interest rate of a project is a delicate aspect of the financial part of the planning. According to various estimations and local conditions as well as sector averages, the interest rate can be more or less precisely set. The interest rate represents the risk of a project, showing how much a project should be bringing in returns over its lifetime. The longer the expected lifetime, the higher the risk. The risks are for example external risks, they correspond to the financial situation of the country itself, as well as the

geopolitical condition, these also define the availability of funds from banks. Internal risks are for example risks linked to the financial solidity of the company owning the project, the bigger the company the lower the risk, therefore the lower the interest rate. The interest rate is also determined by the track record of the company itself, influenced according to the experience and the results in the past of the company. There are also risks that belong to the project. Project risk is the risk that the project may not work, partially or totally; it is possible to include for example the risks due to unsuccessful drillings, depending on the maturity of the project. The insurance risk also plays a role, insurance can insure for many risks and this depends from project to project, bankruptcy or failure risks can also be included into this type of risk. Finally, the market risk is a factor that is both internal and external as it collocates the ability of making profits of the project into the market situation, the bigger the margin of the company compared to the market, the better the performance, the lower the risk. The initial interest rate was set to 4%, as according to the OECD a minimum of 3.54% is required for projects in USD of at least 18 years lifetime (Organisation for Economic Co-operation and Development, 2015).

For the interest rate influence, two different scenarios have been imagined. The first utilises 8% interest rate, as this could happen in other situations or in economically unstable times. The effects of this scenario are exposed in Table 9 below.

Table 9: Effects of a higher interest rate (8%)

8% interest rate	$\dot{W}_{net}$	$\dot{C}_{total}$		Cost of electricity
	(kW)	($/s)	(Δ%)	USD/kWh
Single flash	34709	0.19583	45.7%	0.02031
Heat recuperator	39158	0.19809	45.7%	0.01821

Here, by doubling the interest rate, bringing it to 8%, one can note a rough 46% increase in the total cost rate for every cycle. This illustrates high sensitivity of the costs to the interest rate. To go even further, as many variables of the previously listed or financial crises could affect the future over the following 25 years of a plant, a scenario where the interest rate is as high as 12% has been emulated. In this case, as per Table 10, one can notice that by tripling the interest rate of the project, the total cost rate practically doubles, reaching 98% increase. This confirms that the selection of the interest rate is not to be neglected and therefore this will be brought in the following section too.

Table 10: Effects of a higher interest rate (12%)

12% interest rate	$\dot{W}_{net}$	$\dot{C}_{total}$		Cost of electricity
	(kW)	($/s)	(Δ%)	USD/kWh
Single flash	34709	0.26589	97.9%	0.02758
Heat recuperator	39158	0.26896	97.9%	0.02473

4.2.6 O&M costs

Finally, the last choice of variable to change was oriented towards the O&M costs. These costs are usually easier to estimate, as they typically have very similar values according to the sector the plant is built in. In this case, IDDP-1 is subject to various minerals and gases that are generally only bringing problems (corrosion, scaling…) into plants. This work only brought the problem of chloride mitigation and already accounted for higher O&M costs in the parts exposed to chloride-induced corrosion. Nevertheless, Table 11 shows a scenario where O&M costs are much higher (triple) and their influence results in being lower than what could be expected. In this case, a 200% increase in the O&M costs results in slightly more than 9% increase in the total plant cost rate, for every cycle.

Table 11: Effects of higher O&M costs

O&M 15%	$\dot{W}_{net}$	$\dot{C}_{total}$		Cost of electricity
	(kW)	($/s)	(Δ%)	USD/kWh
Single flash	34709	0.14701	9.4%	0.01525
Heat recuperator	39158	0.14870	9.4%	0.01367

4.2.7 Scenario combinations

Once the most interesting scenarios were identified, a few of them have been combined into multi-criteria scenarios. Figure 26 shows the different scenarios combinations for the heat recovery cycle, as it resulted in being the most interesting cycle throughout the entire analysis. Here the results are shown as a ratio of the original case for the HR cycle, that is 0.01250$/kWh at 40bar wellhead pressure. All the cycles´ multi-criteria scenarios can be found in the Appendix C in the form of tables, with more data outputs.

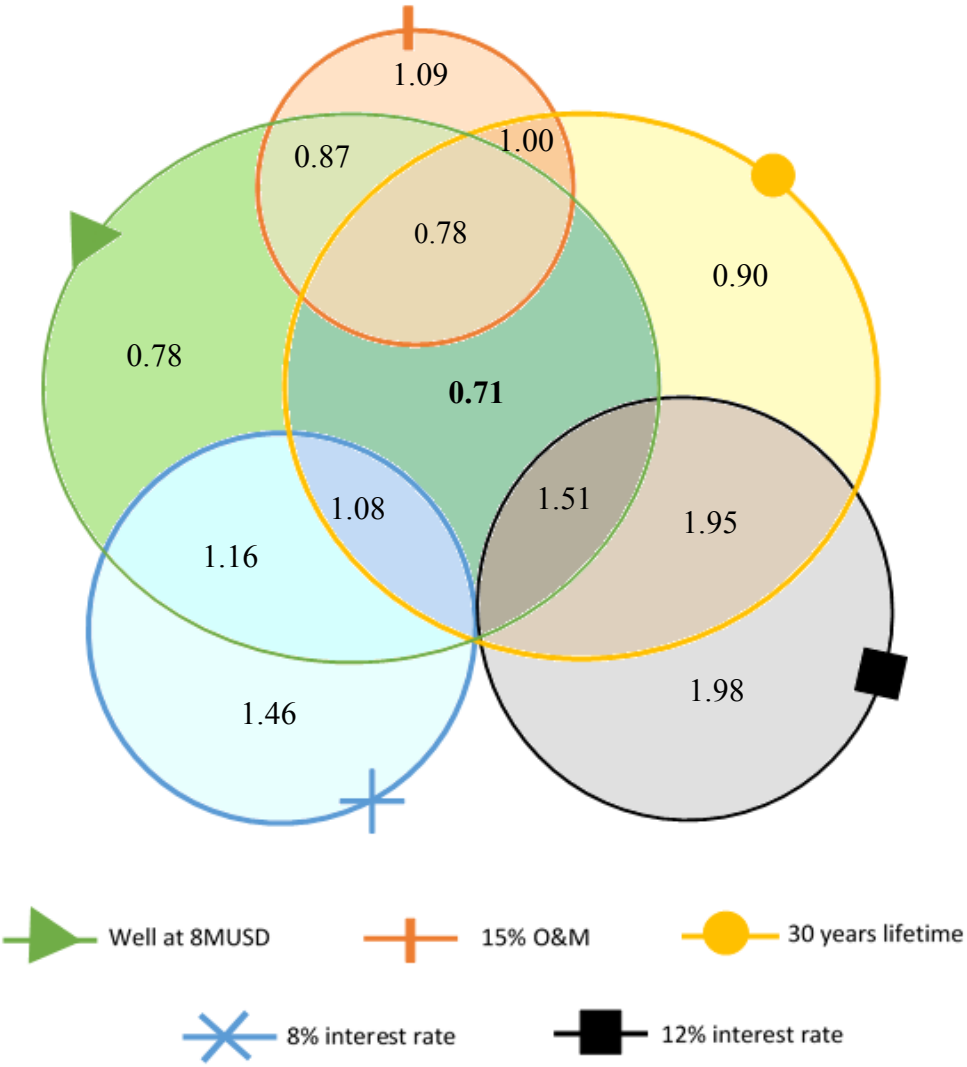

Figure 26: Multi-criteria scenario combination of heat recovery cycle

From the above figure, one can note that, not surprisingly, the lowest cost of electricity is reached when combining the two scenarios that were driving costs down; these were the longer lifetime and the lower cost of the well. On the other hand, the most expensive scenario is the one having 12% interest rate and no other conditions, as it was not calculated together with the increased O&M.
The lowest cost reached can serve as a reference point as it considers variables more suitable to plants with regular costs of drilling while a 30years lifetime is not an exaggeration.
As mentioned before, this analysis only gives results that are low estimations of real costs. Nevertheless, the results obtained are much lower (3 times lower for the 5 lowest scenarios results) than other power plants in the world. This does not prove much as the costs considered are only portions of the real costs, but this could be a motivation for further study of this project.

5 Conclusions

A thermoeconomic analysis of a full geothermal cycle is composed of an exergetic analysis and of an economic analysis, both executed for every component singularly. The more accurate the details in both the analyses the more precise the outcome. In this work, the analyses were based on important data such as mass flow rates and wellhead pressures that have margin of uncertainty as they come from tests and conjectures. Nevertheless, when it comes to geothermal energy, knowing with precision the behaviour of the fluid located underground is limited as it can only be approximated by making calculated guesses through measurements and modelling. In this study, four cycles have been analysed, and their design was based solely on the chloride mitigation matter.

The results of the thermoeconomic analyses of all the cycles aiming at the chloride mitigation in IDDP-1 came to the conclusion that the best cycle to use for this purpose is the single flash with heat recovery. This cycle is able to produce the greatest amount of power among all cycles, and the wellhead pressure at which it produces the said highest output is also the situation in which the electricity output costs less on a per unit basis. This combination could not come handier as, under a thermoeconomic point of view, it allows to perform in the best possible way.

Furthermore, not only the heat recovery cycle is thermoeconomically the best, but also from a point of view of design structure and corrosion resistance it does better than the others. In fact, the positive aspect of having a non-moving heat exchanger is that corrosion and fatigue will affect it less than for example an additional turbine. The scaling in the heat exchanger is easier to mitigate than in various other components. Furthermore, the corrosive fluid only passes through the tubes of the heat exchanger while the shell remains safe as the steam going through it is clean. This contributes to keeping the maintenance and the capital costs to the lowest possible. Comparing the heat recuperating cycle to the binary cycle, under a design point of view, the binary cycle does not seem to be a functional or realistic idea, as for such a heat exchange rate, a far too large heat exchange area, therefore structure, would be needed. In any case, the cycles with more feasibility limits resulted in being less performing.

This work is limited in the research of costs; deeper studies would bring more precise results. For the companies, it is a substantial work to make more detailed estimations for a specific plant, plus, because of the competitive market, they do not let such information outside of the directly concerned parties very easily. Luckily the generous collaboration of Landsvirkjun allowed to execute a rather precise economic estimation, but because the exact results could not be displayed, the economic analysis loses precision. Since the technique used to cost each cycle is the same for each one, the comparative analysis held in this work still maintains its full validity. The scenarios studied can be analysed in broader terms and with more criteria. It would also be of great interest to execute a component by component thermoeconomic optimization for which literature contains various methods and applications.

It is important to consider the fact that these cycles are focused only on the chloride mitigation, not on other elements present in the geothermal fluid, such as for example, silica, responsible for scaling. These cycles could not be achieved according to their design because many thermodynamic limitations would incur. The cycle that seems applicable to the situation is the heat recuperating cycle and therefore could need further analysis and work considering more aspects of the circumstances. Even though the cycles studied may not be constructible, their analysis still represents a useful and

important work for the purpose of thermoeconomic analysis of geothermal power plants.

Bibliography

Ahmadi, P., & Dincer, I. (2011). Thermodynamic analysis and thermoeconomic optimization of a dual pressure combined cycle power plant with a supplementary firing unit. *Energy Conversion and Management*, *52*(5), 2296–2308. http://doi.org/10.1016/j.enconman.2010.12.023

Ármannsson, H., Fridriksson, T., Gudfinnsson, G. H., Ólafsson, M., Óskarsson, F., & Thorbjörnsson, D. (2014). IDDP—The chemistry of the IDDP-01 well fluids in relation to the geochemistry of the Krafla geothermal system. *Geothermics*, *49*, 66–75. http://doi.org/10.1016/j.geothermics.2013.08.005

Árnadóttir, T., Geirsson, H., & Jiang, W. (2008). Crustal deformation in Iceland: Plate spreading and earthquake deformation. *Jokull*, (58), 59–74.

Bejan, A., & Tsatsaronis, G. (1996). *Thermal Design and Optimization*. John Wiley & Sons.

Cengel, Y. A., & Design, D. (2005). *ThermodynamicsAn Engineering Approach 5th Edition By Yunus A Cengel: ThermodynamicsAn Engineering Approach*. Digital Designs.

Chauhan, V. (2014). *Combined Cycle for Cold Storage and Power Generation Using Low Temperature Renewable Heat Resource*. SCHOOL OF ENGINEERING INDIAN INSTITUTE OF TECHNOLOGY MANDI, Mandi, India.

Coulson, J. M., Richardson, & Sinnot. (2006). *Chemical engineering design* (4. ed., reprinted). Amsterdam: Elsevier, Butterworth-Heinemann.

Dincer, I., & Rosen, M. A. (2012). *EXERGY: Energy, Environment and Sustainable Development*. Newnes.

DiPippo, R. (2012). *Geothermal power plants: principles, applications, case studies and environmental impact*. Butterworth-Heinemann. Retrieved from

http://books.google.com/books?hl=en&lr=&id=Ea2osquPZwUC&oi=fnd&pg=PP1&dq=%22in+improving+the+standard+of+living+for+all+peoples.+It+must+then+find%22+%22to+the+environmental+effects+of+geothermal+power+generation,+but%22+%22problems+have+been+and+continue+to+be+addressed+with+effective%22+&ots=CK5pAOO1hI&sig=t2LJPjGoNp-Bs6iLFKn56Pq-WK0

Economic Indicators: CEPCI - Chemical Engineering. (2015). Retrieved from http://www.chemengonline.com/economic-indicators-cepci/?printmode=1

Einarsson, Sveinsson, Ingason, K., Kristjansson, & Holmgeirsson. (2015). Discharge Testing of Magma Well IDDP-1.

El-Sayed, & Tribus. (1983). Strategic use of thermoeconomics for system improvement. In *Efficiency and costing*.

Frangopoulos, C. A. (1987). Thermo-economic functional analysis and optimization. *Energy*, *12*(7), 563–571.

Frangopoulos, C. A. (1991). Comparison of thermoeconomic and thermodynamic optimal design of a combined cycle plant. Presented at the International conference on the analysis of thermal and energy systems, Athens, Greece.

Friðleifsson, G. Ó., Elders, W. A., & Albertsson, A. (2014). The concept of the Iceland deep drilling project. *Geothermics*, *49*, 2–8. http://doi.org/10.1016/j.geothermics.2013.03.004

Fridleifsson, G. Ó., Pálsson, B., Albertsson, A., Stefánsson, B., Gunnlaugsson, E., Ketilsson, J., & Gíslason, Þ. (2015). IDDP-1 drilled into magma–world's first magma-EGS system created. In *Proceeding, World Geothermal Congress, Melbourne, Australia*. Retrieved from https://pangea.stanford.edu/ERE/db/WGC/papers/WGC/2015/37001.pdf

Fridleifsson, G. ó., Elders, W. A., & Bignall, G. (2013). A plan for a 5 km-deep borehole at Reykjanes, Iceland, into the root zone of a black smoker on land. *Scientific Drilling*, *16*, 73–79. http://doi.org/10.5194/sd-16-73-2013

Green, D. W., & Perry. (2008). *Perry's chemical engineers' handbook* (Vol. 796). McGraw-hill New York. Retrieved from http://daniyalomidghaemi.persiangig.com/perey/Perrys%20Chemical%20Engineers%20Handbook,%208th%20Edition0001.doc

Hajabdollahi, H., Ahmadi, P., & Dincer, I. (2012). Exergetic Optimization of Shell-and-Tube Heat Exchangers Using NSGA-II. *Heat Transfer Engineering*, *33*(7), 618–628. http://doi.org/10.1080/01457632.2012.630266

Harvey, W. S. (2015). *Special Topics in Engineering*. Lecture, Reykjavik University, Iceland.

Hirtz, P., Buck, C., & Kunzman, R. (1991). Current techniques in acid-chloride corrosion control and monitoring at The Geysers. In *Sixteenth Workshop on Geothermal Reservoir Engineering* (pp. 83–95). Retrieved from http://pangea.stanford.edu/ERE/pdf/IGAstandard/SGW/1991/Hirtz.pdf

Hjartarson, S., Sævarsdóttir, G., Ingason, K., Pálsson, B., Harvey, W. S., & Pálsson, H. (2014). Utilization of the chloride bearing, superheated steam from IDDP-1. *Geothermics*, *49*, 83–89. http://doi.org/10.1016/j.geothermics.2013.08.008

Ingvarsson, O. G. (2015). *Forhönnun gufuskilju (forskilju) út frá gefnum vinnuskilyrðum*.

Landsvirkjun. (2002). RANNSÓKNABORANIR Á VESTURSVÆÐI við Kröflu í Skútustaðahreppi Mat á umhverfisáhrifum.

Markusson, S. H., & Hauksson, T. (2015). Utilization of the Hottest Well in the World, IDDP-1 in Krafla. In *Proceedings World Geothermal Congress*. Retrieved from https://pangea.stanford.edu/ERE/db/WGC/papers/WGC/2015/37009.pdf

Marshall and Swift. (2015). Marshall and Swift Equipment Cost Index (Q12015). *Cost Indexes*. Retrieved from http://scholars.unh.edu/cost/6

Moghaddam, A. R. (2006). *A conceptual design of a geothermal combined cycle and comparison with a single-flash power plant for well NWS-4, Sabalan, Iran*. Retrieved from http://hdl.handle.net/10802/7154

Muangnoi, T., Asvapoositkul, W., & Wongwises, S. (2007). An exergy analysis on the performance of a counterflow wet cooling tower. *Applied Thermal Engineering*, *27*(5-6), 910–917. http://doi.org/10.1016/j.applthermaleng.2006.08.012

Organisation for Economic Co-operation and Development. (2015). *Changes in Minimum Commercial Interest Reference Rates (CIRRs)*. Retrieved from http://www.oecd.org/tad/xcred/renewable-en.pdf

Orkustofnun (National Energy Authority). (2015). *Energy Statistics in Iceland 2014*.

Saemundsson, K. (1979). Outline of the geology of Iceland. *Jokull*, (29), 11–28.

Saemundsson, K. (1991). Jarðfræði Kröflukerfisins. In *Náttúra Mývatns* (Garðarsson, A. et al., pp. 24–95).

Simonson, J. M., & Palmer, D. A. (1994). *PRODUCTION AND MITIGATION OF ACID CHLORIDES IN GEOTHERMAL STEAM*.

Sodium Hydroxide Naoh Alkali Price. (2015). Retrieved 1 December 2015, from http://www.alibaba.com/product-detail/sodium-hydroxide-naoh-alkali-price-for_60134176111.html

Souders, M., & Brown, G. G. (1934). Design of Fractionating Columns I. Entrainment and Capacity. *Industrial & Engineering Chemistry*, *26*(1), 98–103. http://doi.org/10.1021/ie50289a025

Stefánsson, A. (2014). *Geochemical assessment of the utilization of IDDP#1, Krafla*.

Subramanian, S. (2004). Shell and Tube Heat Exchangers.

Tsatsaronis, G., & Pisa, J. (1994). Exergoeconomic Evaluation And Optimization of Energy Systems - Application to The CGAM Problem. *Energy*, *19*(3), 287–321.

Tsatsaronis, G., & Winhold, M. (1985). Exergoeconomic Analysis And Evaluation of Energy-Conversion Plants -I. A New General Methodology. *Energy*, *10*(1), 69–80.

US Department of Commerce, N. (2015). Dewpoint and Wet-bulb from Relative Humidity. Retrieved 25 November 2015, from http://www.srh.noaa.gov/epz/?n=wxcalc_rh

Valdimarsson, P. (2015). *Electricity generation from low-temperature geothermal resources*.

Valero, A., Lozano, M. A., Serra, L., & Torres, C. (1994). Application of The Exergetic Cost theory To The CGAM Problem. *Energy*, *19*(3), 365–381.

Zarrouk, S. J., & Purnanto, M. H. (2015). Geothermal steam-water separators: Design overview. *Geothermics*, *53*, 236–254. http://doi.org/10.1016/j.geothermics.2014.05.009

Þeistareykir. (2015). Retrieved 20 November 2015, from http://www.landsvirkjun.is/rannsoknirogthroun/virkjunarkostir/theistareykir/

Appendix A

Exergy rates for single flash wet scrubbing (kW), from Figure 11 :

Pressure (bar)	10	20	30	40	50	60	70	80	90	100	110	120	130	140
E1	55549.76	59700.61	62017.11	63076.11	62791.15	61139.69	59249.06	57183.81	53606.8	48508.57	41887.7	33733.56	25451.75	15638.66
E2	53677.89	58061.1	60432.52	61491.18	61194.92	59543.11	57644.2	55563.57	52010.14	46986.57	40496.25	32544.01	24497.74	15014.08
E3	53481.39	57798.39	60120.72	61141.01	60817.07	59148.86	57237.92	55148.95	51600.81	46597.59	40144.34	32247.56	24264.01	14864.05
E4	15245.33	14393.11	13790.96	13177.98	12864.9	12152.76	11489.67	10863.21	10008.53	8924.71	7610.492	6063.995	4534.541	2765.715
E5	711.7819	704.0756	700.9127	694.0791	678.4924	652.2703	626.4472	600.8722	561.0574	506.6605	437.2963	352.5218	266.6319	164.4704
E7	21.39434	26.08777	31.60824	37.4804	43.27711	48.59931	54.03009	59.54088	63.47403	65.09872	63.5279	57.69046	49.00868	33.87806
E8	196.4975	262.7027	311.7967	350.1645	377.8523	394.246	406.2779	414.6183	409.3225	388.9744	351.9091	296.4433	233.7339	150.0227
E9	718.2911	710.5143	707.3224	700.4263	684.6971	658.2352	632.176	606.367	566.1882	511.2938	441.2953	355.7456	269.0702	165.9744
E20	3834.153	3699.388	3623.234	3541.711	3423.481	3257.621	3098.611	2944.596	2724.493	2438.077	2085.088	1665.218	1247.38	761.7023
E21	3834.153	3699.388	3623.234	3541.711	3423.481	3257.621	3098.611	2944.596	2724.493	2438.077	2085.088	1665.218	1247.38	761.7023
E22	13375.65	12905.52	12639.85	12355.45	11943	11364.39	10809.67	10272.39	9504.543	8505.367	7273.944	5809.205	4351.552	2657.24

Exergy rates for single flash heat recovery (kW), from Figure 15:

pressure (bar)	10	20	30	40	50	60	70	80	90	100	110	120	130	140
E1	55550.36	59698.74	62017.75	63076.77	62790.49	61139.04	59248.42	57184.43	53605.03	48509.11	41889.12	33733.17	25452.04	15639.2
E2	49026.14	53625.12	56082.81	57182.51	56935.98	55371.71	53541.33	51519.42	48121.41	43366.37	37274.42	29867.27	22413.7	13693.29
E3	48835.27	53375.23	55785.55	56844.64	56565.57	54977.34	53125.36	51083.67	47679.1	42932.48	36868.21	29511.73	22121.51	13497.31
E4	48656.15	53134.01	55498.49	56521.15	56217.17	54613.84	52750.85	50701.72	47304.59	42577.1	36548.37	29242.44	21910.05	13363.94
E5	54855.31	58931.76	61181.15	62176.78	61839.22	60163.18	58247.19	56157.03	52591.15	47534.05	40996.73	32970.79	24839.67	15238.3

E6	15086.44	14333.44	13868.35	13415.64	12848.71	12129.9	11453.44	10812.14	9944.082	8849.378	7527.259	5981.975	4460.196	2712.356
E7	647.563	647.2561	647.0247	641.634	627.1746	602.2599	577.3379	552.4176	514.3445	462.9452	398.125	319.6707	240.7648	147.8717
E9	5.374875	7.38607	9.579776	11.8854	14.14452	16.2465	18.37786	20.53858	22.13692	22.96785	22.66188	20.84278	17.95009	12.58625
E10	179.113	241.2211	287.0628	323.4863	348.4042	363.4967	374.5138	381.95	374.5046	355.3841	319.8428	269.284	211.4583	133.3666
E11	653.4849	653.1751	652.9417	647.5016	632.91	607.7675	582.6176	557.4694	519.0481	467.1788	401.7658	322.594	242.9665	149.2239
E21	3689.277	3570.837	3503.764	3428.147	3314.946	3154.876	3000.312	2850.225	2636.164	2357.88	2015.148	1608.334	1204.004	734.9208
E20	3689.277	3570.837	3503.764	3428.147	3314.946	3154.876	3000.312	2850.225	2636.164	2357.88	2015.148	1608.334	1204.004	734.9208
E22	12870.24	12457.06	12223.07	11959.28	11564.37	11005.96	10466.75	9943.167	9196.403	8225.592	7029.955	5610.761	4200.234	2563.811

Exergy rates of single flash additional turbine (kW), from Figure 18:

Pressure (bar)	10	20	30	40	50	60	70	80	90	100	110	120	130	140
E1	55550.51	59699.52	62018.24	63076.61	62790.00	61138.87	59249.54	57183.65	53606.06	48510.06	41888.29	33733.27	25451.82	15639.06
E2	34651.53	41842.72	45918.08	48260.16	49098.49	48532.12	47561.83	46276.92	43652.20	39679.62	34387.77	27767.15	20989.64	12916.07
E3	34557.23	41710.26	45755.19	48072.84	48893.10	48316.16	47337.63	46047.88	43426.05	39465.83	34195.01	27605.83	20863.81	12836.17
E4	34281.10	41409.11	45430.98	47730.50	48540.01	47961.04	46982.89	45695.87	43087.37	39151.92	33917.65	27377.66	20688.32	12726.28
E5	15475.90	14685.88	14203.21	13727.34	13133.36	12395.34	11696.78	11037.58	10145.46	9023.32	7671.37	6093.55	4539.52	2757.35
E6	647.59	646.24	645.11	638.87	623.58	597.86	572.18	546.43	507.66	455.79	390.88	312.86	234.75	143.52
E8	3.80	4.18	4.70	5.27	5.81	6.24	6.66	7.01	7.15	6.97	6.48	5.58	4.48	2.92
E9	65.42	107.95	141.23	167.89	187.78	200.35	209.55	215.67	213.85	203.23	183.52	153.80	120.20	76.35
E10	653.52	652.15	651.01	644.72	629.28	603.33	577.41	551.42	512.30	459.96	394.45	315.72	236.89	144.84
E21	3741.44	3604.80	3529.64	3447.49	3328.52	3164.70	3006.37	2853.13	2635.85	2354.77	2010.10	1602.29	1197.56	729.56
E20	3741.44	3604.80	3529.64	3447.49	3328.52	3164.70	3006.37	2853.13	2635.85	2354.77	2010.10	1602.29	1197.56	729.56
E22	13052.21	12575.55	12313.33	12026.75	11611.72	11040.23	10487.88	9953.31	9195.31	8214.74	7012.35	5589.68	4177.75	2545.09

Exergy rates for binary cycle (kW), from Figure 21:

Pressure (bar)	20	30	40	50	60	70	80	90	100	110	120	130	140
E1	59751	62067.97	63125.08	62836.53	61182.94	59291.28	57223.15	53642.46	48542.51	41915.94	33755.26	25468.23	15649.05
E2	52913.53	55486.43	56553.36	56227.75	54572.63	52641.09	50513.14	47034.82	42240.05	36165.34	28852.52	21546.28	13089.86
E3	9882.231	12838.1	14910.72	16338.45	17166.51	17729.38	18081.52	17802.28	16841.81	15149.81	12674.57	9912.969	6303.215
E4	1051.232	1098.174	1135.665	1155.302	1152.508	1145.754	1135.041	1092.362	1014.769	899.3128	743.0492	574.9788	362.1832
Ea	642.1186	640.8292	634.3822	618.9095	593.1216	567.3337	541.5458	502.8639	451.2882	386.8184	309.4547	232.091	141.8334
Eb	697.3336	748.6603	793.3011	824.8293	839.1968	849.3056	855.1589	835.3405	786.6808	706.0123	590.1707	461.6406	293.7276
Ec	9007.014	11898.73	13946.41	15377.04	16232.74	16828.72	17217.7	16998.28	16120.26	14532.29	12181.76	9544.73	6079.22
Ed	48581.75	52573.3	54247.39	54287.1	52900.2	51165.76	49192.83	45872.43	41242.89	35343.77	28218.01	21085.09	12816.24
Ee	54958.91	58786.92	60492.83	60594.55	59228.37	57546.86	55642.96	52233.88	47318.88	40893.94	32954.91	24878.63	15293.95
Ef	14841.24	14171.62	13623.92	13000.01	12242.04	11543.68	10882.75	9997.006	8884.165	7550.493	5995.542	4465.174	2711.195
E21	3684.806	3576.671	3481.984	3356.49	3187.133	3026.082	2870.113	2650.388	2366.594	2019.616	1609.453	1202.663	732.4679
E20	3684.806	3576.671	3481.984	3356.49	3187.133	3026.082	2870.113	2650.388	2366.594	2019.616	1609.453	1202.663	732.4679
E22	12751.06	12376.86	12049.21	11614.94	11028.89	10471.58	9931.861	9171.514	8189.462	6988.764	5569.42	4161.747	2534.663

Appendix B

Influence of a cheaper well, from Table 5:

Well cost 8MUSD	$\dot{W}_{net}$	$\dot{C}_{total}$		Cost of electricity
	(kW)	($/s)	(Δ%)	USD/kWh
Single flash	34709	0.10497	-21.9%	0.01089
Heat recuperator	39157	0.10652	-21.6%	0.00979
Additional turbine	39243	0.12113	-19.5%	0.01111
Binary cycle	38314	0.12553	-31.9%	0.01179

Influence of higher pumps efficiencies, from Table 6:

Pumps η=0.85	$\dot{W}_{net}$	$\dot{C}_{total}$		Cost of electricity
	(kW)	($/s)	(Δ%)	USD/kWh
Single flash	34709	0.13533	0.7%	0.01404
Heat recuperator	39159	0.13664	0.5%	0.01256
Additional turbine	39244	0.15147	0.6%	0.0138
Binary cycle	38314	0.18532	0.5%	0.01741

Influence of higher price of chemicals (NaOH), from Table 7:

NaOH @ 1$/kg	$\dot{W}_{net}$	$\dot{C}_{total}$		Cost of electricity
	(kW)	($/s)	(Δ%)	USD/kWh
Single flash	34709	0.13800	2.7%	0.01431
Heat recuperator	39158	0.13954	2.7%	0.01283
Additional turbine	39243	0.15416	2.4%	0.01414
Binary cycle (not affected)	*38314*	*0.18434*	*0%*	*0.01732*

Influence of a longer lifetime of plant, from Table 8:

Lifetime of 30 years	$\dot{W}_{net}$	$\dot{C}_{total}$		Cost of electricity
	(kW)	($/s)	(Δ%)	USD/kWh
Single flash	34709	0.12157	-9.5%	0.01261
Heat recuperator	39158	0.12297	-9.5%	0.01131
Additional turbine	39243	0.13617	-9.5%	0.01249
Binary cycle	38314	0.16654	-9.7%	0.01565

Influence of higher interest rate, from Table 10:

12% interest rate	$\dot{W}_{net}$	$\dot{C}_{total}$		Cost of electricity
	(kW)	($/s)	(Δ%)	USD/kWh
Single flash	34709	0.26589	97.9%	0.02758
Heat recuperator	39158	0.26896	97.9%	0.02473
Additional turbine	39243	0.29808	98.0%	0.02734
Binary cycle	38314	0.36717	99.2%	0.03450

Influence of higher interest rate, from Table 9:

8% interest rate	$\dot{W}_{net}$	$\dot{C}_{total}$		Cost of electricity
	(kW)	($/s)	(Δ%)	USD/kWh
Single flash	34709	0.19583	45.7%	0.02031
Heat recuperator	39158	0.19809	45.7%	0.01821
Additional turbine	39243	0.21948	45.8%	0.02013
Binary cycle	38314	0.26898	45.9%	0.02527

Influence of higher O&M costs, from Table 11:

O&M 15%	$\dot{W}_{net}$	$\dot{C}_{total}$		Cost of electricity
	(kW)	($/s)	(Δ%)	USD/kWh
Single flash	34709	0.14701	9.4%	0.01525
Heat recuperator	39158	0.14870	9.4%	0.01367
Additional turbine	39243	0.16471	9.4%	0.01511
Binary cycle	38314	0.20130	9.2%	0.01891

Appendix C

For the following tables, the combinations of scenarios are represented by combinations of letters, each letter being attributed to a single scenario. The correspondence is:

A: Base case
B: Well cost 8MUSD
C: Pumps η=0.85
D: NaOH @ 1$/kg
E: Lifetime 30years
F: Interest rate 12%
G: Interest rate 8%
H: O&M 15%

Single flash multi-criteria scenarios:

Scenarios	B+E	B+E+F	B+E+G	B+E+H
Net Work (kW)	34709	34709	34709	34709
C total ($/s)	0.09501	0.20191	0.14498	0.10389
c total ($/kJ)	2.74E-06	5.82E-06	4.18E-06	2.99E-06
Cost electricity (USD/kWh)	0.00985	0.02094	0.01504	0.01078

Heat recuperator multi-criteria scenarios:

Scenarios	B+E+F	B+E+G	B+E+H	B+G	B+H	E+H	E+F
Net Work (kW)	39158	39158	39158	39158	39158	39158	39158
C total ($/s)	0.20490	0.14712	0.10541	0.15751	0.11833	0.13617	0.26518
c total ($/kJ)	5.2.E-06	3.8.E-06	2.7.E-06	4.0.E-06	3.0.E-06	3.5.E-06	6.8.E-06
Cost electricity (USD/kWh)	0.01884	0.01353	0.00969	0.01448	0.01088	0.01252	0.02438

Additional turbine multi-criteria scenarios:

Scenarios	B+E	B+E+F	B+E+G	B+E+H
Net Work (kW)	39243	39243	39243	39243
C total ($/s)	0.10961	0.23325	0.16740	0.11988
c total ($/kJ)	2.79E-06	5.94E-06	4.27E-06	3.05E-06
cost electricity (USD/kWh)	0.01006	0.02140	0.01536	0.01100

Binary cycle multi-criteria scenarios:

Scenarios	B+E	B+E+F	B+E+G	B+E+H
Net Work (kW)	38314	38314	38314	38314
C total ($/s)	0.11292	0.24345	0.17419	0.12421
c total ($/kJ)	2.95E-06	6.35E-06	4.55E-06	3.24E-06
cost electricity (USD/kWh)	0.01061	0.02287	0.01637	0.01167

School of Science and Engineering
Reykjavík University
Menntavegur 1
101 Reykjavík, Iceland
Tel. +354 599 6200
Fax +354 599 6201
www.ru.is